Patient-Specific Induced Pluripotent Stem Cell Models of Parkinson's Disease

Dissertation

for the award of the degree

"Doctor rerum naturalium" (Dr. rer. nat.)

of Georg-August-Universität Göttingen

at the Faculty of Biology

of the Georg-August University School of Science (GAUSS)

submitted by

Mei-Chih Liao

from Taichung, Taiwan

Göttingen, 2013

<u>Thesis Committee</u>:

Prof. Dr. Ahmed Mansouri
Molecular Cell Differentiation Group, Max Planck Institute for Biophysical Chemistry, Göttingen

Prof. Dr. Ernst Wimmer
Department of Developmental Biology, Georg-August-Universität Göttingen

<u>Members of the Examination Board</u>:

Prof. Dr. Ahmed Mansouri
Molecular Cell Differentiation Group, Max Planck Institute for Biophysical Chemistry, Göttingen

Prof. Dr. Ernst Wimmer
Department of Developmental Biology, Georg-August-Universität Göttingen

<u>Further Members of the Examination Board</u>:
Prof. Dr. Andreas Wodarz
Department of Anatomy and Cell Biology, Georg-August-Universität Göttingen

Dr. Roland Dosch
Department of Developmental Biochemistry, Georg-August-Universität Göttingen

Prof. Dr. Walter Paulus
Department of Clinical Neurophysiology, Universitätsmedizin Göttingen

Prof. Dr. Reinhard Schuh
Department of Molecular Developmental Biology, Max Planck Institute for Biophysical Chemistry, Göttingen

Date of oral examination: October 21, 2013

Declaration

I hereby declare that this thesis "Patient-Specific Induced Pluripotent Stem Cell Models of Parkinson's Disease" has been written independently, with no other aids than those cited.

Mei-Chih Liao
Göttingen, August 2013

Acknowledgements

When it comes to convey my acknowledgements for completion of this doctoral dissertation, I have lots of words and thoughts in my mind. However, I would apologize that I could not write them down word by word.

I would like to express my sincere appreciation towards Prof. Ahmed Mnsouri. Under his supervision, I got the opportunity to work in this quite interesting field of stem cell biology and continuous support. Although almost everything was new to me, I was encouraged to face challenges.

I also would love to thank Prof. Ernst Wimmer. As the other thesis supervisor, his advice and suggestions led me on the right way of doing the research.

In this work, many people contributed their efforts to it. Prof. Claudia Trenkwalder and Dr. Brit Mollenhauer, they were very kind to recruit PD patients for conducting the starting material for the project. I am very grateful to Prof. Ralf Dressel for the evaluation of teratoma formation. His patience and support gave me a lot of flexibility for doing work. Patrick Probst and Sigurd-Günter Hille, they helped me for those MolBio cloning and sequencing. Prof. Stefan Jakobs and Dr. Susann Kummer, I very appreciated them joining this project and devoting their aspirations. In particular, Susann she did a great work for phenotypic assay of mDA neurons. She also inspired and encouraged me to move forward to the further work.

During these 4 years as a doctoral student, I was very appreciated that I worked in the Molecular Cell Differentiation group and Department of Molecular Cell Biology. Thomas Schulz and Sharif Mahsur, they provided me many supports on cell culture. Since I spent most of time on cell culture, they are indeed important to me!! Dr. Christian Krug and Dr. Tamara Rabe, they are much more knowledgeable about the development of dopaminergic neurons. They are always nice to give me advice and help when I was lost in the maze of complicated brain. Dr. Zeeshan Ahmad, Farnaz Shamsi, and Dr. Hélène Foussard, I am very grateful to work with you, sharing the experience and life moments. Especially, they are patient to my occasional hyper. XD Thanks to all former and current members in the department for the inspiring and nice working environment.

And, but not the end, my father & mother are my biggest support and always stand there for me. I wish them always keep healthy and happy.

Contents

List of Figures

List of Tables

Abbreviations

ATP	adenosine triphosphate
BDNF	brain-derived neurotrophic factor
bFGF	basic Fibroblast growth factor
BSA	bovine serum albumin
cAMP	cyclic adenosine monophosphate
CCCP	carbonyl cyanide m-chlorophenyl hydrazone
cDNA	complementary deoxyribonucleic acid
CNS	central nervous system
DA	dopaminergic
DAPI	4',6-Diamidino-2-phenylindole
DMEM	Dulbecco's modified Eagle's medium
DMSO	dimethyl sulfoxide
DNA	deoxyribonucleic acid
dNTP	deoxyribonucleotide triphosphate
EB	embryoid body
EDTA	Ethylenediaminetetraacetic acid
EPSC	excitatory postsynaptic current
ERK	extracellular signal-regulated protein kinases
ESC	embryonic stem cell
FACS	fluorescence-activated cell sorting
FCS	foetal calf serum
FGF2	fibroblast growth factor 2
FGF20	fibroblast growth factor 20
FGF8	fibroblast growth factor 8
FP	floor plate
GDNF	glial cell-derived neurotrophic factor
GO	gene ontology
h	hour
HBSS	Hank's buffered saline solution
hESC	human embryonic stem cell

hiPSC	human induced pluripotent stem cell
iPSC	Induced pluripotent stem cell
IRES	internal ribosome entry site
KO	knockout
KRS	knockout serum replacement media
LRRK2	Leucine-rich repeat kinase 2
LTR	long terminal repeat
MAPK	mitogen-activated protein kinase
mDA	midbrain dopaminergic
MEF	mouse embryonic fibroblast
MEF-CM	MEF conditioned media
min	minute
mRNA	messenger ribonucleic acid
Na butyrate	sodium butyrate
P/S	penicillin/streptomycin
PBS	Phosphate buffered saline
PCR	Polymerase chain reaction
PD	Parkinson's disease
PDL	poly-D-lysine
PFA	paraformaldehyde
PNS	peripheral nervous system
PSC	pluripotent stem cell
qRT-PCR	quantitative reverse transcriptase PCR
RNA	ribonucleic acid
ROCK	rho-associated protein kinase
ROS	reactive oxygen species
RPM	revolutions per minute
rt	room temperature
RT-PCR	reverse transcriptase PCR
SCNT	somatic cell nuclear transfer
SD	standard deviation

SDS	sodium dodecyl sulfate
SNpc	substantia nigra pars compacta
SSEA	stage specific embryonic antigen
SV40	simian virus 40 derived polyadenylation site
TGFβ3	transforming growth factor 3
TH	Tyrosine hydroxylase
TRA	tumor rejection antigen
WPRE	woodchuck hepatitis virus posttranscriptional regulatory element
wt	wild-type

Abstract

Parkinson's disease (PD) is one of the common neurodegenerative diseases. In particular, it affects the elderly and associates with the movement disorder. The hallmarks of PD are progressive loss of midbrain dopaminergic neurons and the appearance of Lewy bodies in the affected neurons. At present, the etiology of PD is not well understood and may reflect the interactions of environmental and genetic factors. The main hurdle in studying PD pathogenesis is the inaccessibility to the brain tissues from PD patients. Recent advances in cellular reprogramming now allow an alternative approach for investigating PD. PD patients' dermal fibroblasts can be converted to the pluripotent state, and further differentiated to the disease relevant cell type, dopaminergic neurons. Such PD affected neurons in culture represent a promising departure point for exploring the pathogenic factors of PD.

Here, we have generated disease specific human induced pluripotent stem cells (hiPSCs) from 3 individual idiopathic PD patients and 2 healthy persons' fibroblast. We applied a single lentiviral vector (hSTEMCCA-loxP) encoding OCT4, KLF4, SOX2, and c-MYC, and subsequently were able to generate the transgene-free hiPSCs using Cre-loxP recombination. The genomic constitutions of PD-hiPSCs were found identical to their parental fibroblasts by DNA fingerprinting. The characteristics of PD-hiPSCs resembled human embryonic stem cells (hESCs) displaying the expression of pluripotency marker genes, and the capability of differentiating into the three germ layers. Neural precursors were derived from PD-hiPSCs, and then examined by transcriptome analysis. Our results revealed some differentially expressed genes involved in axon guidance and neuron differentiation. Among those candidates, FGF20 was down regulated in PD patients. By Directed differentiation of floor-plate (FP) derived midbrain dopaminergic (mDA) neurons from hiPSCs, large population of specific midbrain dopaminergic neurons could be achieved. We exposed these control and PD specific hiPSCs derived mDA neurons to mitochondrial stress. PD-hiPSC derived mDA neurons were susceptible to CCCP treatments. Interestingly, FGF20 was able to counteract these cellular stresses. FGF20, therefore, might hold the capacity for dopaminergic neuroprotection.

1 Introduction

1.1 Parkinson's Disease

Parkinson's disease (PD) is one of the most prevalent neurodegenerative disorders worldwide. It is a lifelong and progressive disease that mainly causes complicated cardinal motor symptoms. More than 1 % of the population over 65 years of age is affected, and its prevalence is increased in individuals by aging (Bekris, Mata, & Zabetian, 2010).

1.1.1 Clinical Aspects

In 1817, the clinical features of PD were first depicted in the monograph of "*An Essay on the Shaking Palsy*" published by James Parkinson. He described the presence of primary motor signs including resting tremor, rigidity, and bradykinesia as characteristics of PD, and the way that the disease progresses over time. Therefore, this neurological disease was named as Parkinson's disease in honor of his contribution (Lees, 2007). Those typical features affect PD patients' voluntary motor movements. Tremor (resting tremor) is the most apparent and notable PD symptom. It can be easily noticed on PD patient's shaking hand when they are at rest. Another characteristic feature of PD, bradykinesia (slowed movement), leads PD patients to make simple tasks difficult and time-consuming due to reduction of speed and amplitude of movements. Muscle rigidity limited PD patients' the range of motion and cause body pain (Jankovic, 2008). However, non-motor symptoms can develop during PD, as well. Cognitive impairment, sleep disturbance, depression, and abnormal behavior, such neuropsychiatric symptoms are common to observe in PD patients. They might be caused by the disease itself or accompanied by disability and inconvenience of daily life. By all means, the patient with PD would be affected by motor dysfunction, but also reduced quality of life.

1.1.2 PD Pathology

According to post-mortem studies of PD patients, a lot of cell death of dopaminergic (DA) neurons was observed in the Substantia Nigra pars compacta (SNpc), a region of the midbrain (Figure 1.1). Approximately 60% of the SN DA neurons were already lost at the onset of PD symptoms. Moreover, the axonal projections of the SN dopaminergic neurons to the striatum are reduced, and near 80% DA transmitter is depleted. Therefore, it is believed that the loss of SN DA neurons results in the loss of dopaminergic transmission in the

striatum, leading to the majority of classic motor symptoms of PD. In the past decades, the major emphasis of PD research has been focused to the degeneration of midbrain DA neurons that have been consistently identified as the most severely damaged circuit. However, what causes massive SN DA neuronal death is still not fully understood.
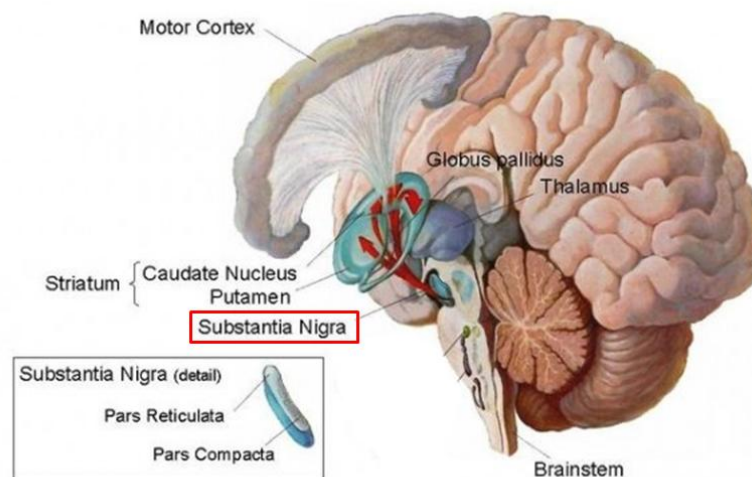
Figure 1.1: Brain Regions Affected by Parkinosn's disease.

The major aspect of PD pathological anatomy is the disappearance of pigmented dopaminergic neurons in the ubstantia nigra (pars compacta), resulting in loss of neuronal projection into the putamen. The image was taken from http://www.doctortipster.com/.

Another PD pathological hallmark is Lewy Bodies (LB). (Figure 1.2) LBs are intraneuronal cytoplasmic inclusions, frequently found in PD patients' brain tissues at autopsy. LBs contain a variety of proteins, neurofilaments, ubiquitin and α-synuclein. Among these components, misfolded α-synuclein is the predominant constituent of LBs, suggesting that it play a central role in the pathogenesis of PD (Spillantini et al., 1997). Heiko Braak and his colleagues proposed a theory (Braak's theory) for the progression of PD based on LB pathology progression (Braak & Braak, 2000). However, recent studies have shown that 7-8 % of PD patients did not present medullary LBs (Kalaitzakis, Graeber, Gentleman, & Pearce, 2008). Therefore; the cause of PD seems to be more related to the degree of dopaminergic cell loss than to the severity of Lewy pathology.

Normal aging induces neurodegeneration of DA neurons of SN at a rate of approximately 5% per decade, in PD patients the neurodegeneration rate is about 10 fold faster (Fearnley & Lees, 1991). The severity and progression of PD might tightly link to aging induced neurodegeneration.
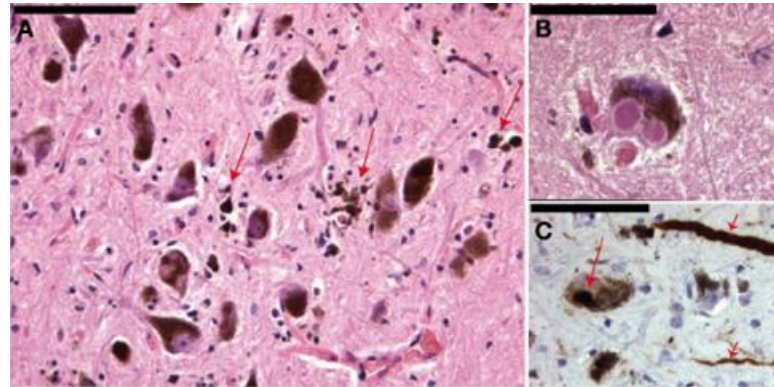
Figure 1.2: Micrographs of mesencephalon Parkinson's disease.

(A) Shows neuronal degeneration in the substantia nigra (arrows) by HE staining. (B) Shows a neuron with two classical Lewy bodies. (C) Shows α-synuclein staining with positive staining of a Lewy body (long arrow) and Lewy neurites (short arrows). The image was modified from (den Dunnen, 2013)

1.1.3 PD Etiology and Environmental Contribution

Parkinson's disease is a multifactorial neurological disease. Most cases of PD are sporadic: idiopathic disorder may arise from the combinations of environmental and genetic vulnerabilities. The rest of PD (~5%) is the result of genetic defects. Although the familial PDs, genetic inheritance, are rare, they share the pathological, biochemical, and clinical features with idiopathic PD. Therefore, researchers have tried to explore the possible mechanisms of PD underlying the Mendelian PD mutations in the past years. A number of genes associated with PD have been identified, either autosomal dominant (α-synuclein, LRRK2, UCHL1) or autosomal recessive (Parkin, DJ-1, PINK1, ATP13A2) (Thomas & Beal, 2007) (Bekris, et al., 2010). Most of the loci are involved in the impairment of ubiquitin-proteasome system or mitochondrial dysfunctions. Studying those genetic defects provides an insight into PD pathogenesis. Besides, they provide some supportive causes for idiopathic PD (Corti, Lesage, & Brice, 2011).

Environmental factors have been suspected to be the critical cause of PD since 1918's influenza pandemic. Infectious agents in the environment affected many individuals leading to the development of Post-encephalitic Parkinsonism (Poskanzer & Schwab, 1963). The environmental hypothesis was further reinforced by N-methyl-4-phenyl-1, 2, 3, 6-tetrahydropyridine (MPTP) as drug abuse in 1980s (Langston, Ballard, Tetrud, & Irwin, 1983). Rural pesticides, such as rotenone or paraqua (Ossowska et al., 2006), also have similar adverse effects leading to DA neuron degeneration (Freire & Koifman, 2012). All of these toxins were subsequently identified to inhibit the activity of mitochondrial complex I, enhance the intracellular reactive oxygen species (ROS), and result in cell death eventually. To this point, by applying these toxins, such as MPTP, animal models can be established for studying PD *in vivo* (Jackson-Lewis & Przedborski, 2007).

Investigation the monogenetic defects might shed light on the cellular mechanisms of PD. Nevertheless, the interplay of aging and environmental risks is more likely to contribute to the development of Parkinson's disease.

1.1.4 PD Causative Hypothesis

Loss of midbrain dopaminergic neurons and the formation of Lewy Bodies (LBs) are typical characteristics of PD. However, mechanisms underlying this neurodegeneration are not very clear yet. Different hypotheses have been proposed to contribute to neuronal cell death of PD: (1) abnormalities in mitochondrial function and (2) increased level of oxidative stress, (3) defects in protein metabolism through ubiquitin proteasome system (UPS), and (4) autophagy (Schapira & Jenner, 2011). Besides, the assumption of multifactorial genesis was linked to the interaction of environmental susceptibility and genetic vulnerability. Therefore, the hypotheses mentioned above might be interconnected to each other, resulting in PD pathogenesis.

1.1.4.1 Mitochondrial Dysfunction and Oxidative Stress in PD

Neurons are ATP demanding cells because of the need of energy for impulse transmission. For this reason, mitochondria are enriched in the neuronal cells. Intracellular ATP production is via oxidative phosphorylation and electron transport by five multisubunit complexes (complex I–V) in the mitochondria. During ATP production high amounts of reactive oxygen

species (ROS) (e.g. superoxide anion (O_2^-), hydrogen peroxide (H_2O_2) and hydroxyl radicals (•OH)) can be produced. However, if ROS is generated within a physiological level, those superoxides can be eventually converted to H_2O by the intracellular antioxidant enzymes (ex. superoxide dismutase, catalase, glutathione peroxidase and glutathione S-transferase, etc.). If the electron transport is blocked (e.g. inhibition of complex I) or mitochondrial function is abnormal (ex. inability of cytochrome c or antioxidant enzyme), it would accumulate excessive ROS and cause serious destruction to the cellular functions, leading to cell death (Fukui & Moraes, 2008) (Ciccone, Maiani, Bellusci, Diederich, & Gonfloni, 2013). Therefore, mitochondrial dysfunction and excessive ROS production are common seen in neurodegenerative disorders.

Abundant evidence from PD post-mortem studies supported that oxidative stress induced cell degeneration in the Substantia Nigra. Increased amounts of oxidative damaged lipids, proteins, and DNA were found in sporadic PD patients' affected tissues. ROS detoxification systems were altered, like decreased amount of glutathione (GSH), reduced activity of mitochondrial complex I (Jenner, 2003). In particular, DA neurons are more likely susceptible to oxidative stress due to highly oxidative intracellular environment (Lotharius & Brundin, 2002). The turnover of the neurotransmitter dopamine (DA) within the cell is processed by monoamine oxidase (MAO), catechol-O-methyltransferase (COMT) or autooxidation. (Figure 1.3) The process of oxidation of DA would result in the production of H_2O_2. PD patients have a reduced H_2O_2 clearance capacity, suggesting that the incidence of oxidative stress and lesion of antioxidant system might be the cause of PD pathogenesis.
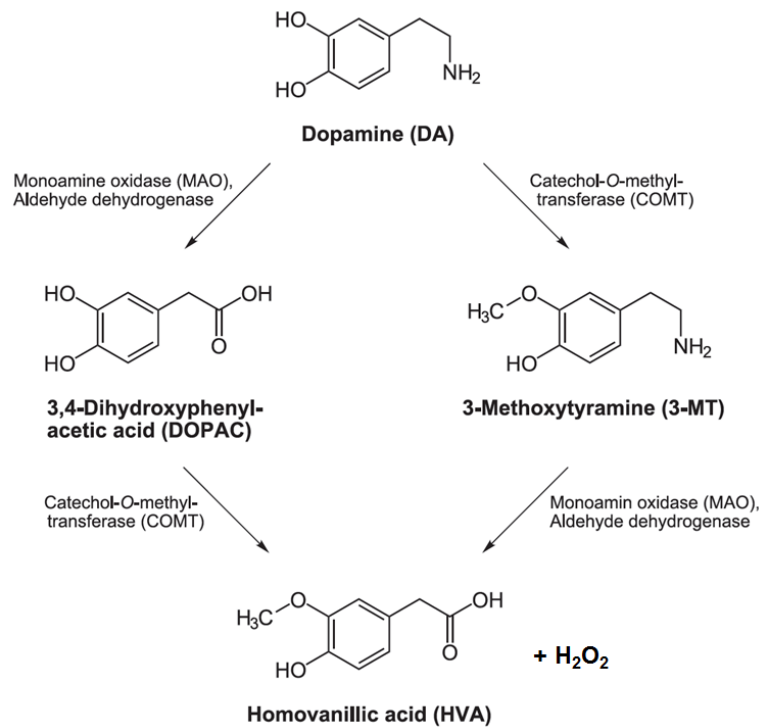
Figure 1.3: Dopamine Degradation.

Dopamine is converted to inactive metabolites by MAO and COMT, accompanied by the production of H_2O_2. H_2O_2 is subsequently broken down to free radicals ($\bullet$OH & OH$^-$). The cellular antioxidant system would eliminate free radicals and turn into H_2O eventually. The image was modified from http://en.wikipedia.org/wiki/Dopamine

1.1.4.2 Impairment of ubiquitin proteasome system in PD

The other pathological characteristic of PD is Lewy Bodies (LBs). LB formation is ascribed to the abuse of ubiquitin-mediated protein degradation, resulting in aberrant or misfolded protein aggregations and intracellular presence of proteinaceous deposits. Parkin acts as an E3 ubiquitin ligase, primarily involved in the targeting of aggregation-prone substrates for degradation by the UPS. Genetic evidence showed that defective parkin in PD affected tissues would hamper the protein metabolism, protein aggregations accumulated (Shimura et al., 2000). Especially α-synuclein, the major component of LBs, was often found overexpressed or mutant form in either sporadic PD or familiar PD. An impairment of UPS function is one of contributive factors to the proteolytic stress due to fibrilization and aggregation of excess or mutant α-synuclein in the cytosol (Bennett et al., 1999) (Tofaris, Layfield, & Spillantini, 2001).

As a matter of fact, these cellular pathways might be interconnected. For example, α-synuclein is not only involved in the LB formation. The N-terminal membrane-binding domain of α-synuclein specifically binds to the mitochondrial membrane and causes mitochondrial fragmentation. The amount of α-synuclein localized into mitochondria of SN neurons increases dramatically in PD (Nakamura et al., 2011). PINK1 plays a role of mitochondrial quality control. When the mitochondria is damage, interrupting membrane potential, PINK1 would recruit cytoplasmic parkin to the mitochondria and initiate the autophagic degradation of damaged mitochondria. Both parkin and PINK1 exert functions of ubiquitination and mitochondrial integrity, and implicate these cellular interactions in the PD disease progression (Matsuda et al., 2010). Besides, oxidative damage is also known to disturb ubiquitination and proteasome activity (Jenner, 2007). Thus, combination of oxidative stress, mitochondrial dysfunction, and impairment of UPS are likely to contribute to multifactorial vulnerability of DA neurons degeneration in PD.

1.1.5 Current Therapeutic Approaches of PD

Till now there is no cure for Parkinson's disease, but a few of medical treatments could alleviate PD symptoms. 1-3, 4-dihydroxyphenylalanine (L-DOPA), a precursor of dopamine, is a typical first-line drug administration for PD patients. Initially it provides an excellent effect for reducing the motor symptoms. As the progression of the disease, PD patients would experience severe side effects, such as motor fluctuations and dyskinesias (Lang & Lozano, 1998). Moreover, there are alternative therapeutic options including dopamine agonists, anticholinergic agents, and monoamine oxidase-B (MAO-B) inhibitors (Samii, Nutt, & Ransom, 2004). Besides, the surgery of deep brain stimulation (DBS) can benefit some population of severe PD patients. By placing the brain pacemaker in PD patient's body and sending electrical impulses to specific parts of the brain, it can help manage some of the PD symptoms and subsequently improve the patient's quality of life (Kleiner-Fisman et al., 2006). In 2006, DBS has been approved for PD treatments by the Food and Drug Administration in United States. Nevertheless, it still carries the risk factors based on the invasion therapy. Some small molecules, ex GDNF or Neurturin, have been proposed to delay or arrest neurodegeneration in PD, but their potential of neuroprotection has not been conclusively approved yet (Obeso et al., 2010).

Transplantation of fetal mesencephalic tissue in PD patients has been applied in clinical uses. The grafted dopaminergic neurons can restore regulated dopamine release, and provide significant symptomatic relief. In the most successful cases, patients were able to resume an independent life after transplantation. However, the limited source of fetal tissues, occurrence of adverse effects: dystonia, immune rejection, and variability of functional outcome restrict its applications (Lindvall & Bjorklund, 2004).

Advanced development in stem cell research has provided a new therapeutic approach for Parkinson's disease. Stem cells have the capability of self-renewal and plasticity to generate multilineage cells. Thus, they are a suitable source of various kinds of cells needed for cell therapy. To date, generating dopaminergic neurons from different stem cells have been succeeded. Those include mesenchymal stem cells (MSCs), human embryonic stem cells (hESCs), and induced pluripotent stem cells. However, the cell identity, purity, and quality control of differentiated DA neurons for transplantation should be considered crucially (Pawitan, 2011). In whatever manner, stem cell approaches still hold enormous competence either in cell therapy or modeling diseases.

1.1.6 Research Models of PD

Parkinson's disease (PD) is a neurodegenerative disease characterized by the cell death of midbrain Dopamine (DA) neurons and the ensuing locomotor symptoms. Over the past two decades, identification of genetic defects has shed insights into the molecular pathogenesis of PD (Klein & Schlossmacher, 2007). However, the greatest obstacle for PD research is inaccessible to live PD patients' brain, and lack of patient-specific midbrain DA neurons for mechanistic research and drug discovery. Therefore, in an attempt to mimic the PD neurodegenerative and motor phenotypes different animal models have been created. Administration of neurotoxins (MPTP or 6OHDA) to the striatum area of rats' brain would cause selective dopaminergic neuron death and produce motor deficits. They lead to acute cell death but not fulfill the slow progression of neurodegeneration observed in PD patients. In the other way, PD related genetic studies have been applied to animals, either transgenic or knockout models, even to non-vertebrate systems (e.g. Drosophila, Zebrafish) (Blandini & Armentero, 2012). Despite the animal models show significant motor phenotype and are useful for unraveling the genetic roles on cellular pathways and mechanism of midbrain DA

neuron degeneration, there are still some drawbacks, like short life span, less complex brain structure and different physiological states. Furthermore, they could not interpret precisely the authentic features of PD disease in human. A model system that directly reflects the nature of genetics and physiology of the human condition is still urgently demanded (Pu, Jiang, Zhang, & Feng, 2012). Thanks to the advance of stem cell biology, pluripotent stem cell seems to overcome the intractable problem and transfers PD research in many prospects.

1.2 Pluripotent Stem Cells

Human pluripotent stem cell (hPSC) has the capability of giving rise to almost all of the cell types of body. Therefore, they hold great promise for both scientific research and medical use. To date, a few of methods were established for the generation of hPSC: human embryonic stem cell (hESC) from the inner cell mass of preimplantation embryos, conversion of somatic cells into human induced pluripotent stem cell (hiPSC), and cloned human embryonic stem cell.

1.2.1 Human Embryonic Stem Cell

The first human embryonic stem cell line (hESC) was derived from the inner cell masses of blastocysts in 1998 by James Thomson's group (Thomson et al., 1998). They reported that the derived hESC cell lines with normal karyotypes expressed high levels of telomerase activity and presented ES cell specific surface markers. Besides, those hESC cell lines were able to *in vivo* differentiate to all three germ layers (ectoderm, mesoderm, and endoderm), showing the capacity of pluripotency.

Similar to mouse ES cells, Oct4, Sox2 and Nanog play critical roles in human ES cells. The functions of those master regulators: Oct4, Sox2, and Nanog were subsequently identified to control self-renewal and pluripotency and maintain hESC in the undifferentiated state (Nichols et al., 1998) (Avilion et al., 2003) (I. Chambers et al., 2003) (Hart, Hartley, Ibrahim, & Robb, 2004) (Boyer et al., 2005). Moreover, unraveling the mechanisms of the lineage commitments allowed hESC to directly differentiate to different types of cells in a dish either for developmental research or clinical purposes (Figure 1.4) (Han, Williams, & Eggan, 2011) (Kadzik & Morrisey, 2012) (Spence et al., 2011) (Murry & Keller, 2008).
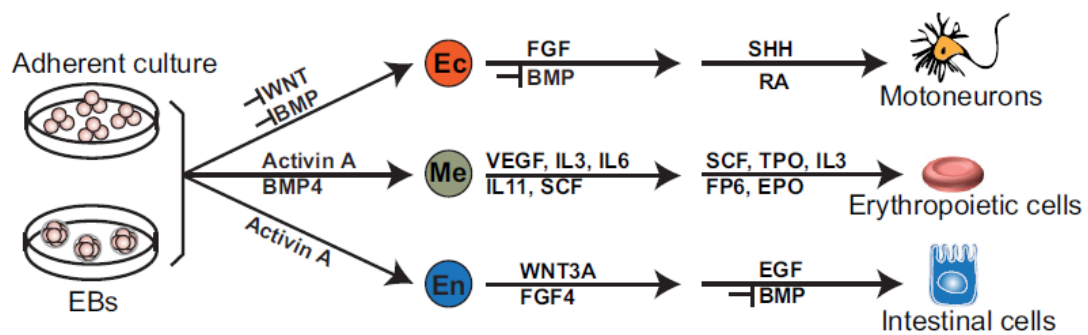
Figure 1.4: Direct Differentiation of hPSCs.

in vitro differentiation of hPSCs can be carried out either by adherent culture or Embryonic bodies (EBs) culture. The presence of growth factors and small molecules activate or inhibit various signaling pathways in a stepwise manner by mimicking embryonic development. Herein three specific examples are illustrated: motorneurons from the ectoderm (Ec), erythropoietic cells from the mesoderm (Me) and intestinal cells from the endoderm (En). The image was taken from (Zhu & Huangfu, 2013)

hESCs provide power tools for studying human embryogenesis (confirming and distinguishing the finding from mouse genetics), and the potential for clinical use (drug test or differentiated cell for cell replacements) In spite of the fact that isolation of hESCs brought the great expectations, a few of issues should be concerned. One is ethical debate that is about the destruction of human preimplantation embryos for the purpose of generating hESCs. The other one is transplanted non-autologous hESCs might cause immune rejection.

1.2.2 Human Induced Pluripotent Stem Cell

Following the breakthrough of 2006's generation of mouse induced pluripotent stem cell (Takahashi & Yamanaka, 2006), reprogramming human somatic cells to pluripotent state was achieved (Takahashi et al., 2007) (Yu et al., 2007) (Park, Zhao, et al., 2008). By introducing four defined transcription factors: Oct4, Sox2, Klf4, and c-Myc, human somatic cells are allowed to convert to human ES-like cells. These human ES-like cells were similar to ES cells in morphology and cellular characteristics. When transplanted into immunodeficient mice, they grew teratomas including a variety of tissues from three germ cell lineages, showing

their pluripotency. Thus, they were termed "human induced pluripotent stem cells" (hiPSCs). Those defined factors were also called "Yamanaka factors" for generation of iPSCs. Despite other combinations, including Nanog (Yu, et al., 2007) or hTert (Park, Zhao, et al., 2008), could generate iPSCs, most researchers adopted Yamanaka factors.

To date, iPS technology develops vigorously and attracts extensive attention. Not only that it circumvent the ethical issues concerned in hESCs, the generation of individual hiPSC could also provide the possibility of autologous transplantation, avoiding the risk of immune rejection. Besides, these specific hiPSC cell lines could be used for drug discovery, disease modeling, and the development of cellular transplantation therapies (Bellin, Marchetto, Gage, & Mummery, 2012). (Figure 1.5)

With the advance of iPS technology, various methods of hiPSC generation developed as well. The initial strategies were retro- or lenti-viral delivery approaches, trying to reach the maximum amount of transduced cells expressing reprogramming factors (Takahashi, et al., 2007) (Yu, et al., 2007). Regarding the transgenic integration and genomic instability, nonviral and nonintegrating methods have been explored. Besides, different sources (ex. skin biopsies, urine (Zhou et al., 2012) or amniotic fluid (Li et al., 2009)) or cell types (ex. fibroblasts, keratinocytes (Aasen et al., 2008) or dental pulp cells (Tamaoki et al., 2010)) have been applied. Table 1.1 lists some distinct and reproducible methods for hiPSC generation. In general, the viral methods are mostly reproducible and highly efficient.

Although iPS technology holds great promise for future medicine, it still keeps some drawbacks. If the transgenic vectors integrate to the host genome, hiPSC might be risky for exogenous reactivation and harmful for further applications, like differentiation or transplantation. Despite hiPSC resembles hESCs in many respects, hiPSC might retain epigenetic memory from the origin of somatic cells, making it more difficult to differentiate to specific cell types. Depending on different approaches of hiPSC generation, cell line−to−cell line differences make it challenging to compare the outcomes either from research or translational medicine (Bellin, et al., 2012). Therefore, iPS technology has been focused on elaborating more efficient & reproducible nonintegrating delivery methods, establishing standards for cellular characterizations and safety in use. Even if some advanced techniques were established, allowing somatic cells to convert directly to specific cell types (Caiazzo et al., 2011) (Kurian et al., 2013). hiPSC possess the flexibility and unlimited cell source for various cell lineage differentiations, pre-clinical and clinical applications.
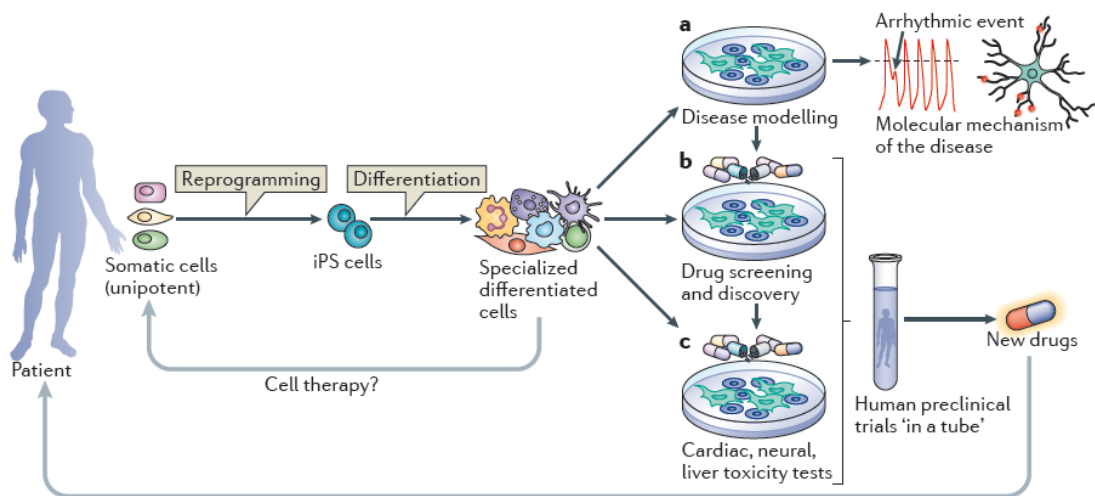
Figure 1.5: hiPSC Derivation, Differentiation, and Application.

Somatic cells from Individuals can be converted to hiPSCs. After direct differentiation, hiPSC derived specialized cells could be used for several applications: (a) disease modeling underlying disease phenotypes, (b) drug screening and discovery, and (c) cellular toxicity tests. hiPSCs provide the potential of autologous cell therapy. The image was taken from (Bellin, et al., 2012)

1.2.3 Cloned Human Embryonic Stem Cell

Since the initial discovery in Xenopus (Gurdon, 1962), somatic cell nuclear transfer (SCNT) enable to transplant a nucleus from a mature cell to an enucleated egg and give rise to a living organism. The first cloned mammal, Dolly the sheep and later others (e.g. monkeys) have been created using SCNT (Campbell, McWhir, Ritchie, & Wilmut, 1996) (Byrne et al., 2007). However, it failed to produce human cloned ES cell in last years. After a long wait, Mitalipov and colleagues have succeeded for the first time in deriving human ES cells by nuclear transfer of human somatic cells to human oocytes (Tachibana et al., 2013). They optimized the SCNT conditions used in monkeys, added extra factors (caffeine) to prevent the premature oocyte activation, and then significantly increased development of human SCNT embryos, cloned human ESC obtained. Cloned hESC displayed normal genome constitutions and received nuclear genome exclusively from parental somatic cells. Gene expression and differentiation profiles in cloned hESC were similar to embryo-derived ESCs. This breakthrough approach will give much hope and another opportunity to prepare

reprogrammed pluripotent cells for therapeutic cloning and autologous cell transplant. However, the oocytes for use are not easy to acquire legally. The technique for SCNT is not simple to achieve universally. Besides, it is imperative to compare the quality of cloned ES cells and iPS cells in many aspects.

Table 1.1: hiPSC reprogramming methods

Methods	Factors	Starting Human cell types	Reprogramming Efficiemcy	Reference
Integrating Viral methods				
Retrovirus	Oct4, Sox2, Klf4, c-Myc	adult dermal fibroblasts	~0.02%	(Takahashi et al., 2007)
		fetal fibroblasts	~0.1%	(Park, Arora, et al., 2008)
	Oct4, Sox2, Klf4, c-Myc, hTERT, SV 40 large T antigen	adult dermal fibroblasts	~0.25%	(Park, Zhao, et al., 2008)
Lentivirus	Oct4, Sox2, Nanog, Lin28	fetal and neonatal fibroblasts	0.01–0.05%	(Yu et al., 2007)
Single lentiviral vector (Cre-loxP)	Oct4, Sox2, Klf4, c-Myc	adult dermal fibroblasts	0.5-1.5%	(Soldner et al., 2009) (Somers et al., 2010)
Nonintegrating virual Methods				
Adenovirus	Oct4, Sox2, Klf4, c-Myc	fetal fibroblasts	0.000002%	(Zhou & Freed, 2009)
Sendai Virus	Oct4, Sox2, Klf4, c-Myc	neonatal and adult fibroblasts, blood cells	0.1-1%	(Seki et al., 2010) (Ban et al., 2011)
Nonviral Methods				
Protein	Oct4, Sox2, Klf4, c-Myc	neonatal fibroblasts	0.001%	(Kim et al.,, 2009)
mRNA Transfection	Oct4, Sox2, Klf4, c-Myc, Lin28	fetal and neonatal fibroblasts	~1.4%	(Warren et al., 2010)
PiggyBac	Oct4, Sox2, Klf4, c-Myc (, Lin28)	fetal fibroblasts, mesenchymal stem cells	~0.2% (w/Na butyrate)	(Woltjen et al., 2009) (Kaji et al., 2009) (Mali et al. 2010)
Minicircle Vectors	Oct4, Sox2, Nanog, Lin28	adipose stromal cells, neonatal fibroblasts	0.005%	(Narsinh et al., 2011)
Episomal Plasmids	Oct4, Sox2, SV40 large T antigen, c-myc, Lin28	foreskin fibroblasts, cord blood cells	0.0003-0.0006% (~0.035 % w/thiazovivin)	(Yu et al., 2009) (Hu et al., 2011)

1.3 Derivation of Dopaminergic Neurons from Human Pluripotent Stem Cell

Since human ESC was first isolated in 1998, the applications of human pluripotent stem cells (hPSCs) have proposed an extensive scope of possibilities for future regenerative medicine. hPSCs offer a nearly unlimited cell source and are capable of generating therapeutically relevant cell types. Especially, patient specific iPSCs make it possible to model human disease and autologous cell transplantation. In particular, the derivation of DA neurons from hPSCs has drawn an attractive attention either for increasing the knowledge of development and specification of mDA neurons or for understanding the pathogenesis of PD.

Midbrain DA (mDA) neurons play central roles in not only motor control but also motivational, rewarded and cognitive conducts. In virtue of remarkable headway of mouse genetics and mouse ESC, directed differentiation of mDA neurons has been developed in several ways. Then they were successfully applied in human ESC. Neural lineage was induced from PSCs either by suspension culture of embryoid bodies (EBs) (S. H. Lee, Lumelsky, Studer, Auerbach, & McKay, 2000) (S. C. Zhang, Wernig, Duncan, Brustle, & Thomson, 2001) or coculture on stromal feeder layers (PA6 or MS5) (Kawasaki et al., 2000) (Vazin, Chen, Lee, Amable, & Freed, 2008). Moreover, TGF-β/SMAD inhibitors (Noggin, SB431542, LDN193189 or Dorsomorphin) were employed to accelerate and to dedicate hPSCs to neural lineages (S. M. Chambers et al., 2009). Then neural stem cell/ precursors were isolated and expanded independently. Alternatively subsequent cell fate of mDA neurons was specified by patterning factors, Shh & FGF8 and undergone for maturation. Then differentiated mDA neurons were characterized by expression of specific markers, like Tyrosine Hydroxylase (TH), engrailed-1 (EN1), or PITX3...etc. Furthermore, detection of dopamine release by HPLC (Studer et al., 1996) and specific physiological properties by electrophysiological assays (Kim et al., 2002) were utilized to determine the functional properties of mDA neurons. Even *in vivo* engraftment of PSC-derived mDA neurons to adult rodent model approved that they were functional integrated to the brain tissues and restored the behavioral deficits.

The various protocols for increasing the high population of specific mDA neurons have been developed. Forced expression of midbrain-specific markers (e.g. Lmx1a or Nurr1) during neural induction was also used for differentiation of mDA neuron (Andersson et al., 2006). However, the studies of successful engraftment and long-term survival of differentiated mDA neurons were generally poor (Ferrari, Sanchez-Pernaute, Lee, Studer, & Isacson, 2006) (H.

Kim et al., 2011). Therefore, an alternative strategy was explored using floor plate-based dopamine neuron differentiation. mDA neurons are believed to originate from floor plate during brain development. Thus, early Shh exposure of hPSC during neural induction would commit high induction of floor plate precursor (Fasano, Chambers, Lee, Tomishima, & Studer, 2010). Then interplay of Shh and canonical Wnt signaling result in the robust derivation of mDA progenitor coexpressing Foxa2/Lmx1a. Maturation and maintenance of mDA Neuron were subsequently promoted under a set of neurotrophic factors (e.g. GDNF, BDNF, Ascorbic Acid, TGF-β3, cAMP). Most importantly, these floor plated-based differentiated mDA neurons show great effects on high amounts of survival cells and rescue motor function after a long time of *in vivo* engraftment (Kriks et al., 2011). The floor plate-based strategy has been adopted by different groups, modified and optimized to increase mDA neuron specification and application (Xi et al., 2012) (Denham et al., 2012) (Kirkeby et al., 2012)

1.4 Parkinson's Disease and Human Induced Pluripotent Stem Cell

PD patient specific iPSC can be generated from their skin fibroblasts, and further differentiated to disease relevant cell type: midbrain dopaminergic neurons. Besides, iPSCs hold a renewable, unlimited cell source and flexibility for PD research in a dish. In recent years, different monogenic PD-iPS cell lines have been established, like SNCA triplication, LRRK2 (G2019S), PINK1 & Parkin mutants. (Table 1.2) They observed PD phenotypes in PD-iPSC derived DA neurons and revealed possible mechanisms resulting in PD. The increased expression level of α-synuclein was found not only in SNCA mutant DA neurons, but also in LRRK2 (G2019S) mutant DA neurons. Moreover, it was often observed that the PD-iPSC derived DA neurons were sensitive to oxidative stress and ROS as evaluated from the analysis of responsive gene transcripts (e.g. cellular stress, antioxidant & apoptotic genes) were also elevated in affected DA neurons. Mitochondrial damage and impaired clearances of mitochondria (mitophagy) & aggregated protein were also evident in those PD-iPSC derived DA neuron models. The inhibitions of ERK activity or Drp1 were even proposed to improve the viability of DA neurons (Reinhardt et al., 2013) (Su & Qi, 2013). Although monogenic forms of PD only take up for a small population of PD cases, it is critically important for understanding the degeneration of DA neurons underlying these

genetic mutants. It might be a common way to cause PD no matter in familial or idiopathic PD.

Nevertheless the majority of PD cases are idiopathic. Complex interactions between environmental and genetic factors are likely to contribute to the main cause of idiopathic PD. Therefore, DA neurons generated from idiopathic PD patient specific iPSC allow us to compare the genetic compositions and disease phenotypes to discover the vulnerable circumstance. Transplantation of DA neurons derived from idiopathic PD-iPSC into the adult rodent striatum showed that transplanted cells survived and behaved functionally to reduce motor deficits (Hargus et al., 2010). The long-term survival cell rate of transplanted DA neurons was more improved with the floor plate-based differentiation protocol (Kriks, et al., 2011). These transplantation studies provide the practicable prototypes and foundations for the future cell therapy of autologous transplantation.

Table 1.2: Monogenic PD patients derived hiPSC and DA neurons

Gene	Protein	Mutation	Reference	Donors	Starting cell types	Reprogramming factors	Affected DA Neuron Phenotype	Perspective
Autosomal dominant								
LRRK2	LRRK2	G2019S	(Nguyen et al., 2011)	1 60 yr f-patient & 1 46 yr f-CTL	dermal fibroblast	Retro- OSK	Increased expression of key oxidative stress-response genes & α-synuclein protein, sensitive to caspase-3 activation and cell death caused by exposure to stress agents	
		G2019S (vs idiopathic PD)	(Sanchez-Danes et al., 2012)	4 LRRK2 (G2019S) patients, 7 idiopathic patient & 4 CTLs	dermal keratinocytes & dermal fibroblast	Retro- OSK	LRRK2 PD: increased α-synuclein accumulation in cytosol. LRRK2/ iPD: reduced numbers of neurites & neurite arborization, accumulation of autophagic vacuoles over long-time culture	
		G2019S	(Reinhardt et al., 2013)	2 55yr, 82 yr f-patients & 4 CTLS	dermal fibroblast	Retro- OSKM	Reduced neurite outgrowth & increased sensitivity to stress, increased levels of α-synuclein, increased MAPK ERK1/2 activity	Inhibition of ERK activity rescued mDA neurons as possible targets for new therapeutics
		G2019S	(Su & Qi, 2013)	1 patient & 1 CTL	dermal fibroblast	Retro- OSKM	Fewer and shorter neurites, altered mitochondrial morphology, loss of MMP, increased ROS, decreased ATP, lysosome hyperactivity	P110, a selective peptide inhibitor of Drp1, improved the viability of affected DA neurons
SNCA	α-synuclein	SNCA triplication	(Devine et al., 2011)	1 f-patient & 1 CTL (first-degree relative)	dermal fibroblast	Retro- OSKM	Evaluated SNCA expression in RNA & protein levels, increased α-synuclein secreted from cells	
		SNCA triplication	(Byers et al., 2011)	1 42yr m-patient & 1 CTL (46yr unfeccted sister)	dermal fibroblast	Retro- OSKM	Accumulation of α-synuclein, inherent overexpression of markers of oxidative stress, sensitivity to peroxide induced oxidative stress.	

Note: Donors--f: female, m: male, yr: age, CTL: control. Reprogrammimg factors--Retro: retrovirus delivery method, Lenti: lentivirus delivery method, O: Oct4, S: Sox2, K: Klf4, M: c-Myc, N: Nanog.

Table 1.2, cont.

Gene	Protein	Mutation	Reference	Donors	Starting cell types	Reprogramming factors	Affected DA Neuron Phenotype	Perspective
Autosomal recessive								
PARK6	PINK1	Q456X (nonsense) & V170G (missense)	(Seibler et al., 2011)	1 53 yr patient & 1 CTL (healthy family member)	dermal fibroblast	Retro- OSKM	Reduction of 80-90 % PINK1 mRNA level, mitochondrial depolarization showed impaired recruitment of overexpressed Parkin to mitochondria, increased	
		V170G ([Seibler, 2011 #357])	(Rakovic et al., 2013)	1 patient & 1 CTL	dermal fibroblast	Retro- OSKM	Ubiquitination of endogenous Parkin attenuates mitophagy	Disease relevant cell types are faithful in physiological condition
PARK2	Parkin	PARK2 exon deletions	(Imaizumi et al., 2012)	2 72yr f-, 50yr m-patient & 2 CTLs	dermal fibroblast	Retro- OSKM	Increased oxidative stress and enhanced activity of Nrf2 pathway, exhibited abnormal mitochondrial morphology &	
		PARK2 exon deletions	(Jiang et al., 2012)	2 patients & 2 CTLS	dermal fibroblast	Lenti- OSKN	Increased spontaneous DA release, reduced DA uptake and DAT-binding sites, elevated ROS by increasing MAO transcripts	Parkin controls dopamine utilization in human midbrain DA neurons

1.5 Aim of this Study

Parkinson's disease (PD) is a multifactorial neurodegenerative disease. The past decades PD research has drawn numerous attentions, trying to explore the disease mechanism and the medical therapies. A few sets of genetic mutants found in familial PD were identified, and their roles have been linked to mitochondrial dysfunction and impairment of UPS, given the insights of degeneration of mDA neuron, the central cause of PD. Although many efforts have been done in the animal models, the authentic PD patients' affected mDA neuron model is still imminently demanded. Despite the inaccessibility of PD patients' live brain tissue, we are able to generate PD patient specific iPSC from skin fibroblasts and further differentiate to mDA neurons.

In this study, we followed the workflow (Figure 1.6). We attempted to recruit PD patients from different kindred. Together with healthy persons, PD patient specific iPSC would be generated and characterized their states of pluripotency. Neural precursors would be then derived from these control and PD-iPSCs and applied for transcriptome analysis. By gene expression profiles between control and PD patients' neural precursors, differential cellular networks and novel molecular players might be perceived. More importantly, the phenotypes of mDA neurons derived from control and PD-iPSC would be examined using external stress stimulations, like mitochondrial damage and oxidative stress. By establishing the PD patient specific hiPS cell models, we expect to obtain the new perception for understanding Parkinson's disease.

PD patients'/ healthy person Dermal fibroblasts

Reprogramming

Control/ PD-hiPSC

Direct Neural Differentiation

Control/ PD-hiPSC derived Neural Precursors

Transcriptome Analysis

Phenotype Assay of Contrl/PD-hiPSC derived DA neurons
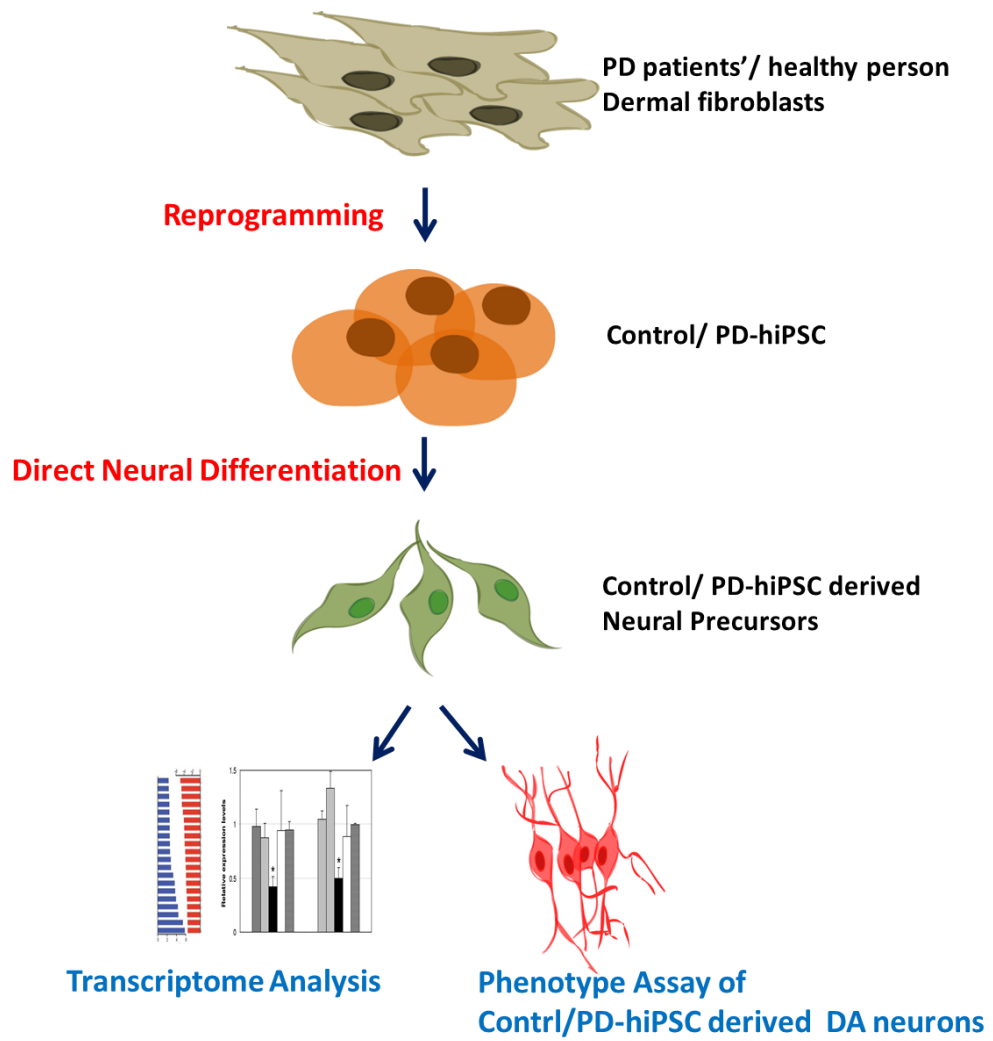
Figure 1.6: Work Flow of the Study

2 Material & Methods

2.1 Methods

2.1.1 *in vitro* Cell Cultures

2.1.1.1 Isolation of Mouse Embryonic Fibroblasts (MEFs)

The Procedure was performed by following the protocol (Mansouri, Fukumitsu, Schindehuette, & Krieglstein, 2009) which was published from our lab. Briefly, mouse embryos were removed from E13.5 CD1 pregnant mice. Their heads, limbs, tails, and viscera were cut off. The rest of the body was minced into small pieces, and incubated with Trypsin for 30 min at 37°C. Then the cell pellet was centrifuged down for 15 min at 1000 rpm, and plated on gelatinized 14.5-cm dishes. The plated MEFs were fed with MEF medium at 37°C. When newly prepared MEFs reached up to 90% confluence, the cells were either frozen as P0 or subculture for expansions. In general, MEFs can be passaged up to 4 passages for the use of feeder layers.

Mitotic Inactivation of MEFs

80-90% confluent MEFs were treated with Mitomycin C (10 µg/mL) for 2.5 h at 37°C, and either directly replated to 0.2% gelatinized plates as feeder layers or frozen for future uses.

2.1.1.2 Culture of Human Pluripotent Stem Cells (PSCs)

Human pluripotent stem cells (hPSCs), like human embryonic stem cells (H1 and H9) and human induced pluripotent stem cells (hiPSCs), were grown and maintained on a layer of mitotically inactivated MEFs (iMEFs). One day before plating PSCs, iMEFs were plated on gelatinized 3.5-cm dishes (20000 cells/cm^2). When hPSCs colonies were grown big enough, hPSCs were passaged by treatments of Collagenase IV (1 mg/ml) to lift the edges of cell colonies and manual splitting using cell scrapers. The hPSCs colonies were collected in a 15 ml Falcon tube and pulled down to the bottom by gravity in a few minutes. hPSCs colonies were washed by hPSCs medium, and the suspension containing iMEFs and Collagenase IV was removed. Washing step was repeated twice. Then hPSCs colonies were carefully broken into smaller pieces by pipetting and replated to new iMEF feeder dishes at the ratio of 1:3~1:5. hPSCs were fed with hPSC medium supplemented with bFGF (10 ng/ml) at 37°C. The medium was changed daily. hPSCs were passage about every 5~7 days. Working with

human ES cells (H1, H9) imported from WiCell (Madison, Wisconsin) was approved by the Robert-Koch Institute in Berlin (AZ. 1710-79-1-4-5) according to the German law.

2.1.1.3 Generation of Human Induced Pluripotent Stem cells (hiPSCs)

For production of lentivirus, 2nd generation Packaging System was applied in this work. To produce virus, a single packaging plasmid (psPAX2), an envelope plasmid (pMD2.G), and the transfer vector (hSTEMCCA-loxP) were included. Prior to transfection, HEK293T/T17 (ATCC, CRL-11268) (293T) were grown to 80-90% confluence in a gelatinized T75 flask. By the time transfection mixtures were first prepared as following:

(hSTEMCCA: psPAX2: pMD2.G = 10:2:1) 15 µg total plasmid/ 500 µl DMEM

<div align="center">45 µl Lipofetamine 2000/ 500 µl DMEM</div>

, mixed gently and incubated at room temperature (rt) for 20 min according to the manufacturer's instruction (Lipofetamine 2000, Invitrogen, 11668-019). Meanwhile, 293T cells were fed with fresh 9 ml 293T medium. Then the 1ml transfection mixture were slowly added to the 293T cells and incubated at 37˚C, 5% CO_2. Supernatant was carefully collected at 24 h and 36 h after transfection, and filtered through a 45 µm filter (Sartorius) to get rid of cell debris. The remaining supernatant was centrifuged for 1.5 h at 48960g in an ultracentrifuge. The viral pellets were resuspended in 100 µl PBS at 4°C overnight. The volume of 10µl for each aliquot was made and stored at -80°C.

Lentiviral Infection and Human iPSC Generation

1x10^{5} fibroblasts derived from patients or controls were infected with concentrated lentivirus in hFB medium supplemented with 5 µg/ml polybrene. The next day, the infectious medium was replaced by the fresh hFB medium. On day 3, the infected cells were transferred onto iMEF feeder plates. After 24 h, the medium was switched to hPSC medium containing 10 ng/ml bFGF and Sodium Butyrate (0.5 mM). The medium was changed every other day. On day 10, the cells were fed with hPSC medium supplemented with 10 ng/ml bFGF. About 20 days later, the ES-like colonies started to appear. Then hPSC medium was fed every day. One month after infection, the ES-like colonies were about to grow big enough. The ES-like colonies were manually picked at stereomicroscope, transferred onto fresh iMEF feeder plates, and expanded under the standard hPSC culture conditions. hiPSC colonies,

some were frozen in liquid nitrogen when expanded to passage 4-5, and some were grown for further application.

Excision of hSTEMCCA

The excision of hSTEMCCA vector from the hiPSC colonies was based on Cre/loxP recombination by transient overexpression of Cre recombinase in the cells. Delivery of Cre expression vector (pHAGE2-Cre-IRES-PuroR) into the cells was followed the procedure of reverse transfection using Lipofetamine 2000 Transfection Reagent (Invitrogen, 11668-019). One day before transfection, puromycin antibiotic resistant iMEFs (Cell Biolabs, CBA-312) were plated on gelatinized 3.5-cm dishes. hiPSCs were fed with hPSC medium containing 10 µM Y27632, additionally. At the time of transfection, transfection mixtures were first prepared as following:

2 µg Cre plasmid/ 50 µl KO-DMEM

10 µl Lipofetamine 2000/ 50 µl KO-DMEM

, incubated for 5 min at room temperature (rt). Then those two were mixed by gently pipetting, and incubated for another 30 min (maximum 50 min) at rt. Meanwhile, hiPSC colonies were dissociated into single cells by using Accutase. 800,000 hiPSCs were counted and suspended in 100 µl hPSC medium (10 µM Y27632). Transfection mixtures were added into suspended hiPSC gently for additional 15 min incubation, then plated on puromycin resistant iMEFs feeder dishes. The next morning, hPSC medium (10 µM Y27632) was freshly replaced. By the evening, puromycin selection (1.2 µg/ml) was begun 24 h following the initial transfection and lasted for 48 h. The transfected hiPSC cells were kept on feeding hPSC medium (10 µM Y27632 (ROCK inhibitor)) for one week, then MEF-conditioned hPSC medium (10 ng/ml bFGF) were replaced. The re-emergence of hiPSC colonies was noted within 1-2 week, and 5-7 colonies from each dish were picked on day 11–14 for passaging. PCR of gDNA extracted from each subclone was performed to screen for excision of the hSTEMCCA vector using the STEM_SPM primers (Table 2.3), 95°C for 3 m; followed by 33 cycles of 94°C for 30 sec, 60°C for 30 sec, and 72°C for 1 m; followed by a single cycle of 72°C for 5 m. PCR products were analyzed by running on 2% agarose gels. Furthermore, vector excision was confirmed by Southern blotting. The vector free hiPSC cells were either frozen in liquid nitrogen or kept on growing for further study.

MEF-Conditioned hPSC Medium

About 6.6 million mitotic inactive MEFs were plated on T75 flask in MEF medium and incubated overnight at 37˚C, 5%CO$_2$. The medium was switched to 15ml hPSC medium containing 5 ng/ml bFGF, and kept incubated at 37˚C, 5% CO$_2$. The MEF-Conditioned hPSC medium was collected and replaced by fresh medium onto MEFs daily for 7 days. The collected MEF-Conditioned hPSC medium was filtered through 0.22 µM filter and stored at -80˚C in aliquots. Before use, additional 10 ng/ml bFGF was added freshly into MEF-Conditioned hPSC medium.

2.1.1.4 *in vitro* Differentiation

Embryoid body (EB) formation is one of the easiest procedures for in vitro differentiation of PSCs. PSCs were dissociated into small pieces by using Collagenase IV (1 mg/ml) and manual splitting. The small clumps of cells were washed twice with hPSC medium to remove MEFs, and cultured in suspension. After 4-5 days, embryonic bodies (EBs) were formed. EBs were transferred to gelatinized plates or coverslips to grow for additionally 7 days for further differentiation. During the course of the differentiation, cells were fed with differentiation medium in the absence of bFGF. The differentiated cells were examined by immunocytochemistry for differentiation markers: Tuj1 for Ectoderm layer, AFP for Endoderm layer, and Brachyury for Mesoderm layer.

2.1.1.5 *in vivo* Differentiation

The *in vivo* differentiation experiments (teratoma formation) were performed by Prof. Dr. Ralf Dressel in the Institute of Human Genetics, University of Göttingen. At least 2 million hiPSC cells were harvested by Accutase and suspended in hPSC medium containing 10 µM Y27632 and 30% matrigel. The cells were injected into SCID or RAG-/- mice. The mice were carefully monitored for the appearance of tumors. If tumors were formed, the mice were sacrificed. Tumors were collected for histological analysis by paraffin embedding and hematoxylin and eosin (HE) staining.

2.1.1.6 Derivation and Maintenance of Human Neural Precursors

hiPSCs were harvested by 1 mg/ml Collagenase IV and plated on PA6 stromal feeder dishes (400,000 PA6 cells/3.5-cm dish). hiPSCs were fed with Neural Induction medium which contained BMP inhibitors (noggin 200 ng/ml or Dorsomorphin 2 μM) every second day. After 1~2 weeks, neural rosette structures started to appear with hiPSC colonies. By manually dissecting under the stereomicroscope, neural rosettes were transferred to poly-D-Lysine (PDL)-coated plates, and fed with NP medium supplemented with bFGF 20 ng/ml and EGF 20 ng/ml.

Maintenance of Neural Precursor Cells

After some days of incubation, NPs outgrew from neural rosette structure. Following Accutase treatments, the cells became round in shape, then the cells were collected, centrifuged, suspended in NP medium, and plated to new plates. Then neural precursor cells (NPs) were grown as monolayers on NP medium (bFGF & EGF) at 37°C and 5% CO_2. Media were changed daily or every other day. Cells were passaged every 5~7 days. Cells can be frozen with NP medium containing 10% DMSO in liquid nitrogen. So far, neural precursors can be maintained up to passage 25.

Neuronal Differentiation

50-75 x 10^4 NPs were seeded on matrigel (BD Bioscience, 356230) coated 3.5-cm culture dishes or glass coverslips. The minimal supportive medium for differentiating neural cells into neurons is neural differentiation medium containing BDNF 10 ng/ mL and 200 μM Ascorbic Acid. Differentiations are usually carried out for 1~2 weeks with media changes every two to three days.

To enrich for dopaminergic neurons, the NPs were first fed with neural differentiation medium supplemented with 100 ng/ml FGF8 & 100 ng/ml Shh (or 2 μM Purmorphamine) for neuron patterning. The medium was changed every other day. After 2 weeks, for neuron maturation, the cells were fed with neural differentiation medium containing 10 ng/ml GDNF, 10 ng/ml BDNF, 1 ng/ml TGF-β3, 200 μM Ascorbic Acid and 0.5 mM dbcAMP for subsequent weeks. Cells were analyzed after day 30 following the onset of differentiation procedure.

Culture of PA6 Stromal Cells

PA6 cells (RIKEN Bio Resource Center Cell Bank), bone-marrow derived stromal cells, were maintained in PA6 medium. Upon passage, PA6 cells were split by the ratio of 1:5. For inactivation, cells were treated with Mitomycin C (10 µg/mL) for 1 h at 37°C, and either directly replated to 0.2% gelatinized plates as feeder layers or frozen for future uses.

2.1.1.7 Differentiation of Floor-Plate Derived Dopaminergic Neurons

Midbrain dopaminergic neurons are believed to originate from the midbrain floor plate (FP) during the brain development. Herein, the differentiation protocol was modified from (Xi, et al., 2012). hiPSCs were plated on PA6 stromal feeder dishes. The next day, hiPSC were fed with FP induction medium in the presence of 10 µM SB431542, 0.1 µM LDN193189, 2 µM purmorphamine (pur), and 0.5 µM CHIR99021 (CHIR). The medium was changed every second day. In addition, Shh (C24II) 100 ng/ml was added for the first four days. On day 9, SB431542 and LDN193189 were removed. The cells were fed with FP medium (Pur & CHIR) till day 11~13. On day 11, the cells were replated on Laminin (5 µg/ml)/ Fibronectin (5 µg/ml) or on matrigel coated coverslips for immunostaining. Cells were continuously maintained on neural differentiation medium containing 10 ng/ml GDNF, 10 ng/ml BDNF, 1 ng/ml TGF-β3, 200 µM Ascorbic Acid, 0.5 mM dbcAMP, and DAPT 5µM. About day 23~25, the differentiated cells were replated on either coverslips or new dishes for future studies. After one month of differentiation, or even longer (till 40~45 days), the differentiated cells were harvested for molecular and functional analysis.

2.1.2 Biochemistry & Molecular Biology Methods

2.1.2.1 Alkaline Phosphatase Assay

hiPSC colonies were washed with PBS once, and fixed by 3.7% Formaldehyde for 20 min at room temperature (rt). Followed 3 times of PBS-washes, fixed cells were washed 3 × 10 min in NTMT solution to equilibrate to alkaline pH (9.0–9.5). Then the cells were exposed to NBT/BCIP (Roche, 11 681 451 001) diluted NTMT (200 µl/ 10 ml NTMT) in the dark with gentle shaking. If color developed, the reaction was stopped by removing NBT/BCIP, and washed by PBS.

2.1.2.2 Fluorescent Immunocytochemistry

To detect the expression of proteins by immunocytochemical methods, the cells were grown on either matrigel or PDL/laminin/fibronectin coated coverslips. At the time of assays, cells were rinsed with PBS once and fixed by 3.7% Formaldehyde for 20 min at rt. The fixed cells were washed with PBS and permeabilized by 0.5% Triton in PBS for 10 min. The cells were washed again and blocked in the blocking solution (5% BSA and 0.1% Triton in PBS) for 1 h at rt. Primary antibodies were diluted in blocking solutions, and incubated with cells either overnight at 4°C or 2 h at rt. After that, cells were washed 3 times with PBST (0.1% Tween-20 in PBS), 10 min each. Diluted fluorescent secondary antibodies were applied for conjugation of respective primary antibodies, and they were incubated for 1 h in the dark. Then the coverslips were washed 3 times with PBST. Nuclear staining was counterstained by DAPI (Vector Labs). The coverslips were sealed by nail polish and stored at 4°C in the dark.

The fluorescent images were acquired by using Leica SP5 Confocal microscope and Olympus BX60 fluorescent microscope. The processed images were done by Adobe Photoshop CS2 and arranged by Adobe Illustrator CS3. Used primary and secondary antibodies are listed in Table 2.1 & 2.2.

2.1.2.3 Isolation of total RNA

Total RNA was isolated with the RNeasy Mini Kit (Qiagen, 74104) according to the manufacturer's instructions. Briefly, collected cells were lysed and RNA was purified using silica-membrane RNeasy spin columns. DNA removal was carried by on-column DNase treatment. The concentration and quality of purified RNA were determined by the NanoDrop (Peqlab).

2.1.2.4 cDNA synthesis

0.5-1 µg total RNA was subjected to cDNA synthesis with QuantiTect Reverse Transcription Kit (Qiagen, 205311) following the manufacturer's instructions. The RNA template was annealed by a unique RT Primer Mix and transcribed into cDNA by QuantiTect Reverse Transcriptase. The final volume was equal for each sample (e.g. 20 µl). The synthesized cDNA was stored at -20°C or optimized for use in conventional PCR or QRT-PCR.

2.1.2.5 Quantitative Real-Time-PCR (QRT-PCR)

To quantify the relative expression of specific genes was relied on QRT-PCR. Target genes were amplified by their own specific primer set and normalized by housekeeping genes (GAPDH or Actin). For each reaction mix was total 10 µl:

Forward / reverse primer mix (5 µM each) 1 µl

2X SYBR Green PCR Master Mix (KAPA SYBR FAST Universal) 5 µl

ddH$_2$O 2 µl

cDNA diluent (1:2-1:5) 2 µl

The PCR was performed on the Mastercycler realplex system (Eppendorf).

2.1.2.6 Isolation of genomic DNA

Collected cell pellets were lysed in 500 µl DNA lysis buffer and 50 µl Proteinase K (10 mg/ml) at 56°C overnight. The next day, 500 µl Isopropanol was added to precipitate the genomic DNA. After 10 min of centrifugation (13.000 rpm), the supernatant was discarded, and 1 ml 70% ethanol was added to wash the cell pellets. Samples were centrifuged again for 5 min (13.000 rpm) and the supernatant was discarded. The pellets were air-dried for 5 min and dissolved in 10-50 µl TE buffer, depending on the concentration needed. The concentration and quality of resulting genomic DNA were measured by using NanoDrop.

2.1.2.7 Fingerprinting

The method was referred by (Park, Arora, et al., 2008). 50 ng of genomic DNA was used to amplify genomic regions containing highly variable numbers of tandem repeats (VNTR) in order to verify the genetic relatedness of iPS cell lines relative to their parent fibroblasts. The sequences of each primer set: D10S1214, D17S1290, D7S796 and D21S2055 were listed in Table 2.4. PCR conditions were: 94°C for 10 min followed by 35 cycles of 94°C for 1 min, 55°C for 1 min and 72°C for 1 min, with a final extension step of 72°C for 5 min. PCR products were analyzed by running on 2.5% agarose gels.

2.1.2.8 Bisulfite sequencing

The EpiTect Bisulfite Kit (Qiagen, 59104) was used for bisulfite conversion of genomic DNA, unmethylated Cytosine nucleotides (C) to Uracil nucleotides (U). The procedure was

conducted as the manufacturer's instructions. The promoter region of OCT4 were amplified by the subsequent PCR using primers (Table 2.6) previously described ((Freberg, Dahl, Timoskainen, & Collas, 2007) primer pair 4 for OCT4). The resulting amplified products were cloned into pTZ57R/T Cloning Vector (Fermentas, K1214), amplified in DH5α cells. The cloned plasmids were purified by the QIAprep Spin Miniprep Kit (Qiagen, 27106) and sequenced by ABI PRISM® 3100 Genetic Analyzer (Applied Biosystems).

2.1.2.9 Southern Blot

After overnight digestion with BamHI, 10 μg genomic DNA fragments were resolved on 0.8% agarose gel with low voltage (25 V) over 16 hours. The gel was soaked in 0.25 M HCl for 15-20 min with gentle shaking. This step is necessary for the optimal transfer of DNA fragments >4kb to the blotting membrane. Two 20 min-denaturation washes followed in denaturing buffer. Then the other two 20 min-neutralization washes were conducted. During the neutralization, the transfer stuff was started to set up, including Whatman paper, tissue paper, a big glass, a baking dish with 10X SSC buffer, and blotting membrane. The gel was rinsed with 10X SSC buffer for a while, then set to transfer DNA to blotting membrane overnight with gravity. After the DNA transfer is done, the membrane was rinsed by 2X SSC buffer to remove some residual gel, and placed on Whatman paper for a while for drying. The membrane was then UV crosslinked by Stratalinker "autocross link" setting (STRATAGENE).

The UV crosslinked membrane was set into a hybridization tube with Hybrid Mix buffer, and placed in a hybridization oven at 65°C for at least 30 min. Meanwhile, radioactive WPRE probes were generated from 50 ng PCR products using the Rediprime™ II DNA Labeling System (GE Healthcare) and [a-32P]-dCTP (PerkinElmer), according the manufacturers' protocols. Radio-labeled WPRE probes were purified using the ProbeQuant G-50 Micro Columns (Amersham Pharmacia Biotech, 27-5335-01) and heat-denatured (99°C, 5 min followed by 5 min on ice). Hybridization was performed at 65°C overnight in Hybrid Mix with slow rotation. The following day, the membrane was washed 3x in 10X SSC buffer at 65°C, wrapped with Saran Wrap and exposed to film (Kodak) for several days at -80°C.

2.1.2.10 Transcriptome Analysis

The gene expression filing of hiPSC derived neural precursors was carried out by the Transkriptomanalyselabor (TAL) -Microarray and Deep-Sequencing Facility- in University of Göttingen. Neural precursors were collected by Accutase, suspended in TRIzol® Reagent (Life Technologies, 15596-026), and frozen at -80˚C. The total RNA was isolated and assessed RNA quality by the Agilent RNA 6000 Nano Kit (Agilent, 5067-1511). Following the standard procedure, the resulting gene expression data was obtained using Human GE 4x44K v2 Microarray (Agilent, G2519F-026652).

2.1.3 Functional Assays

2.1.3.1 Electrophysiology

Electrophysiological analyses were performed by Dr. Kun-Han Lin in the Max-Planck Institute for Biophysical Chemistry. Patch-clamp recordings were obtained from differentiated cells using an EPC-10 amplifier controlled by Pulse software (HEKA Elektronik, Lambrecht/Pfalz, Germany). Cells were visualized by differential interference contrast microscopy through a 60x water-immersion objective (NA 1.0, Olympus, Hamburg, Germany) using an Axioskop FS microscope (Zeiss, Oberkochen, Germany). All experiments were performed at room temperature.

Patch pipettes were made from borosilicate glass (Science Products GmbH, Hofheim, Germany). Pipette resistance was 4–6 MΩ. Access resistance (Rs) values were ≤20MΩ for recordings. Rs was compensated 60–70% during voltage-clamp experiments. For measuring sodium ($I_{Na}(V)$), potassium currents ($I_{Ka}(V)$), and action potentials (APs), pipettes were filled with K-gluconate based solution (Lin, Oleskevich, & Taschenberger, 2011).

2.1.3.2 Carbonyl cyanide m-chlorophenyl hydrazine (CCCP) Treatments

The mitochondrial stress experiments were carried out by Dr. Susann Kummer in the Department of NanoBiophotonics, Max-Planck Institute for Biophysical Chemistry. The cells were exposed to CCCP (Fluka BioChemika, 21855), which integrates into the inner membrane of mitochondria leading to an uncoupling of the proton gradient, and thus, to cellular ATP depletion and cell death. Incubation of hiPSC-derived neurons with 100–200 µM CCCP for 45 min at 37°C, was followed by fixation using 4% paraformaldehyde, blocking of

unspecific bindings using 5% BSA, and cell membrane permeabilization using 0.1 % Triton X-100. (Incubation was at room temperature for 5 min for each step). Cells subjected to microscopic imaging were treated with specific antibodies in a double staining procedure. Immunostaining was performed using the antibody combinations summarized in table 2.2 & 2.4 for 1 h at room temperature to visualize mitochondria and dopaminergic neurons. The fluorescent images were acquired by using Leica DM6000 widefield microscope.

2.1.3.3 Intracellular ROS Assay

The cell-permeant 2', 7'-dichlorodihydrofluorescein diacetate (H2-DCFDA) is known as a general oxidative stress indicator for detection of intracellular ROS (Reactive Oxygen Species). The acetate groups of DCFDA are cleaved by intracellular esterases and oxidation, and fluorescent fluorophore, DCF, is yielded. Therefore, the level of ROS can be measured by the intensity of fluorescent DCF.

The hiPSC-derived neurons were exposed 100 mM H_2O_2 for 1 h at 37°C and followed by incubation with 10 µM DCFDA for additional 20 min. Afterwards, cells were harvested and suspended in HEPES buffer. The fluorescence of living cells was monitored using a flow cytometer (BD FACSCanto II). The excitation and emission wavelengths used for the dyes are λex/λem = 475/525 nm for DCF. The data was analyzed using flowing software (http://www.flowingsoftware.com).

2.2 Material

2.2.1 Medium & Reagents

2.2.1.1 Culture Medium

MEF Medium/ hFB Medium/ 293T Medium

High D-MEM (Invitrogen, 41965-039)

10% FCS (Fetal Calf Serum)

1x P/S (Penicillin-Streptomycin, Liquid)(Invitrogen, 15140-122)

hPSC Medium

Knockout D-MEM (Invitrogen, 10829-018)

20% Knockout Serum Replacement (KSR) (Invitrogen, 10828-028)

1x NEAA (Non-Essential Amino Acids Solution 10 mM, 100x) (Invitrogen, 11140-050)

2 mM L-Glutamine (Invitrogen, 25030-024)

0.1 mM β-Mercaptoethanol (Sigma, M3148)

1x P/S

Differentiation Medium

Knockout D-MEM (KO-DMEM)

20% FCS

1x NEAA

1x P/S

2 mM L-Glutamine

0.1 mM β-Mercaptoethanol

Neural Induction Medium

Knockout D-MEM

15% Knockout Serum Replacement

1x NEAA

1x P/S

2 mM L-Glutamine

0.1 mM β-Mercaptoethanol

Neural Precursor Medium (NP Medium)

Neurobasal Medium (Invitrogen, 21103-049)

1x NEAA

1x P/S

2 mM L-Glutamine

1x N2 (Invitrogen, 17502-048)

1x B27 Minus Vitamin A (Invitrogen, 12587-010)

0.2 mM Ascorbic Acid (Sigma, A4403)

Neuronal Differentiation Medium

Neurobasal Medium

1x NEAA

1x P/S

2 mM L-Glutamine

1x B27 Minus Vitamin A

0.2 mM Ascorbic Acid

PA6 Medium

MEM α medium, Nucleosides (Invitrogen, 12571-063)

10% FCS

1x P/S

FP Induction Medium

50% Knockout D-MEM

50% Neurobasal Medium

1x NEAA

1x P/S

2 mM L-Glutamine

1x N2

1x B27 Minus Vitamin A

2.2.1.2 Growth Factors, Recombinant Protein & Small molecules

bFGF (PeproTech, 100-18B)

Y27632 (TOCRIS, 1254)

Noggin (R&D SYSTEMS, 344-NG)

EGF (PeproTech, AF-100-15)

Dorsomorphin (Sigma, P5499)

FGF8 (PeproTech, 100-25)

Shh (PeproTech, 100-45)

BDNF (PeproTech, 450-02)

GDNF (PeproTech, 450-10)

TGF-β3 (R&D SYSTEMS, 243-B3-002)

dbcAMP (Sigma, D0627)

DAPT (TOCRIS, 2634)

SB431542 (TOCRIS, 1614)

LDN193189 (STEMGENT, 04-0074)

Shh C24II (R&D SYSTEMS, 1845-SH)

FGF20 (PeproTech, 100-41)

purmorphamine (Cayman Chemical, 10009634)

CHIR 99021 (STEMGENT, 04-0004)

Poly-D-Lysine (Sigma, P6407)

Laminin (Sigma, L2020)

Fibronectin (R&D SYSTEMS, 1030-FN)

H2-DCFDA (Sigma, D6883)

2.2.1.3 Buffers & Reagents

NTMT Solution

100 mM NaCl

100 mM Tris-HCl pH 9.5

50 mM MgCl2

1% Tween 20

DNA Lysis Buffer

100 mM Tris-HCl pH 8.0

5 mM EDTA

0.2% SDS

200 mM NaCl

1X Neutralization Buffer

1.5 M NaCl

0.5 M Tris-HCl pH 7.5

1X Denaturation Buffer

0.5 M NaOH

1.5 M NaCl

20X SSC Buffer

3 M NaCl

0.3 M Na Citrate

Hybrid Mix

500 mM Sodium Phosphate Buffer, PH 7.2

7% SDS

1 mM EDTA

HEPES Buffer

5 mM KCl

140 mM NaCl

2 mM $CaCl_2$

1 mM $MgCl_2$

10 mM Glucose

5 mM Hepes

2.2.2 Plasmids

Table 2.1: List of Plasmids used

Function	Plasmids	Source
Virus Production	pMD2.G	Addgene, 12259
Virus Production	psPAX2	Addgene, 12260
Reprogramming	pHAGE2 EF1aL-hSTEMCCA-W-loxP	Gift from Kotton Lab
Cre Excision	pHAGE2-Cre-IRES-PuroR	Gift from Kotton Lab
Bisulfite sequencing	pTZ57R/T Cloning Vector	Fermentas, K1214

Kotton Lab: Pulmonary Center, Boston University School of Medicine
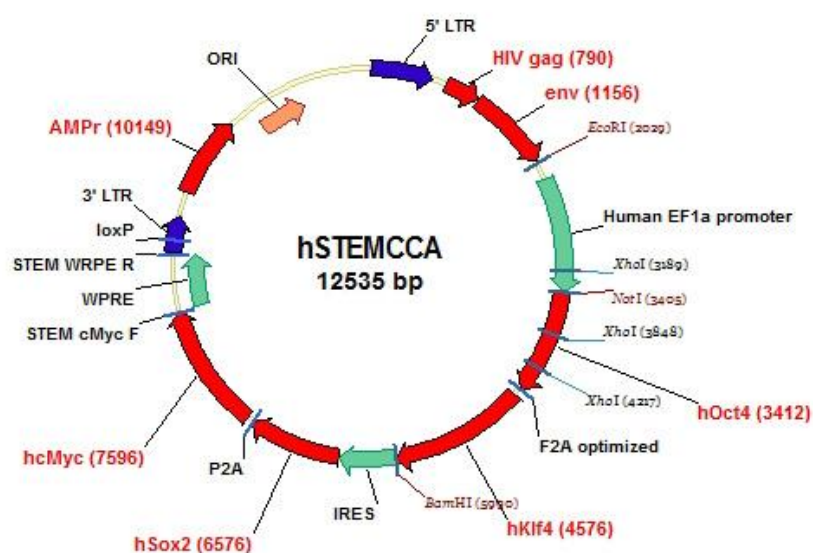
Figure 2.1: The Map of Lentiviral Vector hSTEMCCA.

(pHAGE2 EF1aL-hSTEMCCA-W-loxP)

2.2.3 Primary Antibodies

Table 2.2: List of Primary Antibodies used

Antibody	Species	Dilution	Source
Oct4	Rabbit Polyclonal	1: 500	Abcam, ab19857
Sox2	Rabbit Polyclonal	1: 400	Abcam, ab15830
Nanog	Rabbit Polyclonal	1: 100	Abcam, ab21624
Nanog	Goat Polyclonal	1: 100	R&D Systems, AF1997

Lin28	Rabbit Polyclonal	1: 750	Abcam, ab63740
TRA-1-60	Mouse Monoclonal	1: 100	Abcam, ab16288
SSEA4	Mouse Monoclonal	1: 100	Abcam, ab16287
Sox17	Goat Polyclonal	1: 100	R&D Systems, AF1924
Brachyury	Goat Polyclonal	1: 100	R&D Systems, AF2085
α-Fetoprotein/AFP	Mouse Monoclonal	1: 100	R&D Systems, MAB1368
Tyrosine Hydroxylase/TH	Rabbit Polyclonal	1: 300	Millipore, AB152
β-tubulin III/Tuj1	Mouse Monoclonal	1: 1000	Covance, MMS-435P
Nestin	Mouse Monoclonal	1: 750	R&D Systems, MAB1259
Msi1	Rabbit Polyclonal	1: 200	Abcam, 21628
Pax6	Rabbit Polyclonal	1: 300	Covance, PRB278P
FoxA2	Goat Polyclonal	1: 100	Santa Cruz, sc-6554
Lmx1A	Rabbit Polyclonal	1: 2000	Millipore, AB10533
EN1	Mouse Monoclonal	1: 50	DSHB, 4G11
TOM20	Mouse Monoclonal	1: 100	BD Bioscience, 612278

DSHB: Developmental Studies Hybridoma Bank

2.2.4 Secondary Antibodies

Table 2.3: List of Secondary Antibodies used

Conjugate	Host species	Reactivity	Dilution	Source
Alexa 488	Donkey	Rabbit	1: 750	Invitrogen, A-21206
Alexa 488	Goat	Rabbit	1: 750	Invitrogen, A-11008
Alexa 488	Goat	Rabbit	1: 100	Molecularprobes, A11034
Alexa 488	Chicken	Goat	1: 750	Invitrogen, A-21467
Alexa 488	Goat	Mouse	1: 750	Invitrogen, A-11001
Alexa 594	Chicken	Goat	1: 750	Invitrogen, A-21468
Alexa 594	Donkey	Rabbit	1: 750	Invitrogen, A-21207
Alexa 594	Goat	Rabbit	1: 750	Invitrogen, A-11012
Alexa 594	Donkey	Mouse	1: 750	Invitrogen, A-21203
Alexa 594	Goat	Mouse	1: 750	Invitrogen, A-11005
Rhodamine	Sheep	Mouse	1: 100	Dianova

Rhodamine labeling anti-mouse KK114 was made in the Department of NanoBiophotonics (Kolmakov et al., 2010).

2.2.5 PCR Primers used for Cre Excision

Table 2.4: List of PCR Primers for Cre Excision

Gene/ Oligos	Primer sequence 5'-3'
STEM_SPM_F	GCCGCCCCCAGCAGACTTCA
STEM_SPM_R	GGGGTGGGCAGCAGCTCGAA
WPRE_F	CGTAAGTCGATAGATCCTAATCAAC
WPRE_R	TTAAAGGTACCAGGCGGGGAG

2.2.6 PCR Primers used for Fingerprinting

Table 2.5: List of PCR Primers for Fingerprinting

Gene/ Oligos	Primer sequence 5'-3'
D21S2055_F	AACAGAACCAATAGGCTATCTATC
D21S2055_R	TACAGTAAATCACTTGGTAGGAGA
DS17S1290_F	GCAACAGAGCAAGACTGTC
DS17S1290_R	GGAAACAGTTAAATGGCCAA
D7S796_F	TTTTGGTATTGGCCATCCTA
D7S796_R	GAAAGGAACAGAGAGACAGGG
D10S1214_F	ATTGCCCCAAAACTTTTTTG
D10S1214_R	TTGAAGACCAGTCTGGGAAG

2.2.7 PCR Primers used for Pluripotency

Table 2.6: List of PCR Primers for Pluriopotency

Gene/ Oligos	Primer sequence 5'-3'
OCT4_F	CAGTGCCCGAAACCCACAC
OCT4_R	GGAGACCCAGCAGCCTCAAA
SOX2_F	TTACCTCTTCCTCCCACTCCAG
SOX2_R	GGGTTTTCTCCATGCTGTTTCT

NANOG_F	CCTGAAGACGTGTGAAGATGAG
NANOG_R	GCTGATTAGGCTCCAACCATAC
TERT_F	GTGAACAGCCTCCAGACGGT
TERT_R	GCGTTCTTGGCTTTCAGGAT
FOXD3_F	AAGCCCAAGAACAGCCTAGTGA
FOXD3_R	GGGTCCAGGGTCCAGTAGTTG
TDGF1_F	TACCTGGCCTTCAGAGATGACA
TDGF1_R	CCAGCATTTACACAGGGAACAC
GAPDH_F	TGACATCAAGAAGGTGGTGAAGC
GAPDH_R	CCCTGTTGCTGTAGCCGTATTC

2.2.8 PCR Primers used for Bisulfite OCT4 Promoter

Table 2.7: List of PCR Primers for Bisulfite OCT4 Promoter

Gene/ Oligos	Primer sequence 5'-3'
hOCT4P-4_F	GGATGTTATTAAGATGAAGATAGTTGG
hOCT4P-4_R	CCTAAACTCCCCTTCAAAATCTATT

2.2.9 PCR Primers used for QRT-PCR

Table 2.8: List of PCR Primers for QRT-PCR

Gene/ Oligos	Primer sequence 5'-3'
GAPDH_F	TGACATCAAGAAGGTGGTGAAGC
GAPDH_R	CCCTGTTGCTGTAGCCGTATTC
FGF20_F	GACCACAGCCTCTTCGGTAT
FGF20_R	CTGCTCCCTAAAGATGCATTCG

3 Results

3.1 Recruitment of PD Patients

In collaboration with Prof. Dr. Claudia Trenkwalder in Paracelsus-Elena-Klinik, Kassel, Germany, and following German ethical regulations, PD patients were recruited with the purpose of establishment of PD patient specific hiPSC model and investigation of the PD pathogenesis. At the start, 6 PD patients who developed obvious PD symptoms at the age of 38~54 years were enlisted and agreed to perform skin punch biopsy. However, only 4 PD patients' dermal fibroblasts could be isolated and derived from the skin biopsies. Together with 2 controls contributed by healthy persons, 3 PD patients' fibroblasts were further used for generation of hiPSC model and direct differentiation of dopaminergic neurons. The clinical information of 3 PD patients was listed in Table 3.1.

Table 3.1: Clinical Information of PD Patients

PD Patient	Kas01	Kas02	Kas05
Gender	female	male	female
Age of Onset	35	44	41
Age of Skin Biopsy	38	47	48
Family History	N/A	N/A	mother and maternal grandfather with PD
Features	pronounced dyskinesias	pronounced dyskinesias, DBS	
Clicical Symptoms	freezing, rigid, dysarthria,dystonia,left-sided hypokineseia , severe fluctuations	tremor and left-sided hypokinesia, motor fluctuations	rigid, dystonia, RLS, right-sided hypokinesia, fluctuations
UPDRS III	22/46	37/77	10/35
Levodopa Response	yes	yes	yes
Present Treatments	Amantsdin, Apomorphin, levodopa	DBS, Levodopa, Entacapon, Rasagilin, Ropinirol	Levodopa, Ropinirol, entacapon, amantadin

Note: UPDRS III (Unified Parkinson's Disease Rating Scale-motor examination), RLS (Restless legs syndrome), DBS (Deep Brain Stimulation), N/A (Not Available)

3.2 Generation of PD Patient Specific Induced Pluripotent Stem Cells

3.2.1 Reprogramming of PD patients' Fibroblasts to Pluripotent States

To generate human iPSCs, the protocol used in this study was adopted from Kotton and Mostoslavsky's published article. (Somers et al., 2010) They generated a humanized version of lentiviral Stem Cell Cassette (hSTEMCCA) (Figure 3.1.A) containing four defined factors (Oct4, Klf4, Sox2, and c-Myc). In addition, this lentiviral vector is flanked by a loxP site on 3' long terminal repeat (LTR) region. Upon proviral replication, the loxP site in the 3'LTR is duplicated into the 5'LTR, resulting in an integrated transgene flanked by loxP sites on both LTRs. The transgene would be then removed using the technology of Cre/loxP recombination.

Human dermal fibroblasts (Figure 3.2.a & d) used for reprogramming were within passage 4. (Figure 3.1.B) One day before transduction (day 0), 1x105 human fibroblasts were plated in hFB medium. The next day (day 1), the cells were infected with hSTEMCCA lentivirus. After 24 h of transduction (day 2), the virus remaining in the medium was removed, and the cells were fed with fresh hFB medium for 2 days. On day 5, the transduced fibroblasts were passaged onto inactive mouse embryonic fibroblast (MEF) feeder layers. Acting as normal human embryonic stem (hES) cell culture, the cells were fed with hPS medium supplemented with bFGF. In the first week (day 5-12), the cells were treated with sodium butyrate (Na butyrate) additionally. It has been reported that Na butyrate, as a Histone deacetylase inhibitor, greatly enhances the efficiency of hiPSC derivation (Mali et al., 2010). Afterwards, the cells were kept growing on the hPS medium. About day 20-25, some small human ES-like colonies, started to appear in the dish. Following one month of transduction, hiPSC colonies with the appropriate size for propagation in culture were passaged. These hiPSC colonies were isolated and picked up mechanically under the stereomicroscope in the laminar flow hood. Isolated colonies were transferred to a fresh MEF feeder plate respectively and propagated under standard hES cell culture condition. Unlike parental fibroblasts, fully reprogrammed colonies were easily distinguishable by their similarity to hESC colonies and their tightly packed morphology. All selected clones had high nuclei to cytoplasm ratio, well defined borders, densely packed colonies, and were indistinguishable from human ESCs. (Figure 3.2.b & e) In addition, those hiPSC clones showed the enzyme activity of alkaline phosphatase (ALP), one of the characteristics of hESC. (Figure 3.2 c & f)

For each sample, up to 30 hiPSC clones were picked primarily. 1-3 clones per sample were continuously passaged; the rest of them were frozen in the liquid nitrogen tank.

3.2.2 Excision of Transgene from Host Genome of Human ES-like Clones by Cre/loxP Recombination

The previous reports have shown that presences of transgenic reprogramming factors would interfere with cellular activities of iPSCs. For example, constitutive expression of reprogramming transgenes interrupts the ability of mouse iPSC differentiation into different germ layers. (Sommer et al., 2010) The remaining integrated transgenic factors could also cause tumor formation and affect the global genetic network (Okita, Ichisaka, & Yamanaka, 2007) (Soldner et al., 2009). Therefore, it is imperative for developing an improved method for generating human iPSC free of transgene integration. The lentiviral hSTEMCCA used in this work is a multicistronic vector flanked with a loxP site next to the transgenes. Use of this single vector allows deriving human iPSC with a single excisable viral integration, and further efficiently generating factor-free hiPSCs followed by Cre-mediated excision.

In order to excise the transgenic hSTEMCCA from the generated hiPSC clones, the plasmid pHAGE2-Cre-IRES-PuroR, ectopic expression of Cre recombinase and puromycin resistant plasmid, was delivered into the hiPSC clones for transient expression of Cre recombinase within cells. Besides, the cells were exposed to puromycin antibiotic selection for 2 days. Afterwards, the cells would recover and grow for 1-2 weeks till new surviving colonies mature for pick-up. Those pick-up subclones were cultivated, expanded, and then examined for transgene excision by PCR primarily. For each hiPSC clone, at least 7 subclones were picked. Deletion of hSTEMCCA vector was nearly 100% successful in these screened subclones. (Figure 3.3.A) Furthermore, the absence of integrated hSTEMCCA or Cre plasmid was evident using the technology of Southern blot probed with the same element (WPRE) in both vectors. (Figure 3.3.B)

In summary, human dermal fibroblasts isolated from 2 controls (wt & Hess) and 3 PD patients (Kas01, Kas02 & Kas05) were dedicated to generating hiPSCs using the single lentiviral vector hSTEMCCA. Beyond the excision of transgene, 2 hiPSC clones for each control (wt 1, wt 7 & Hess 6, Hess 9) and PD (Kas01 19, Kas01 21 & Kas02 14, Kas02 23 &

Kas05 5, Kas05 29) samples were employed for the characterization of hiPSC and directed differentiation of neural precursor and dopaminergic neurons.
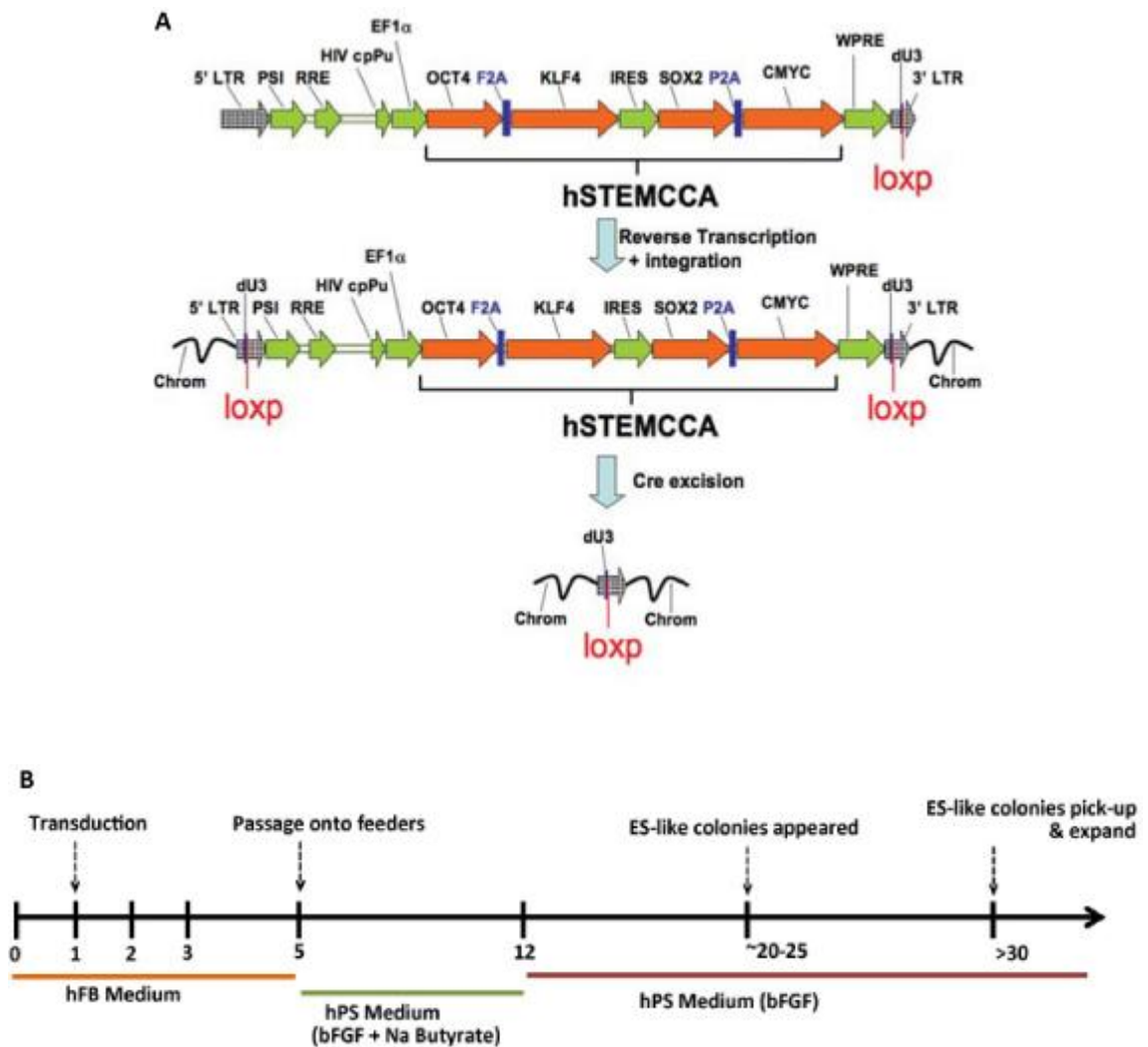

Figure 3.1 Generation of Human iPSC by a Lentiviral hSTEMCCA Vector.

(A) Human fibroblasts were reprogrammed by lentiviral hSTEMCCA-loxP vector encoding 4 defined factors (Oct4, Klf4, Sox, and c-Myc). The integrated transgene could be excised from the host genome by Cre/loxP recombination. The picture was adopted from (Somers, et al., 2010). (B) Time flow of reprogramming in this study.
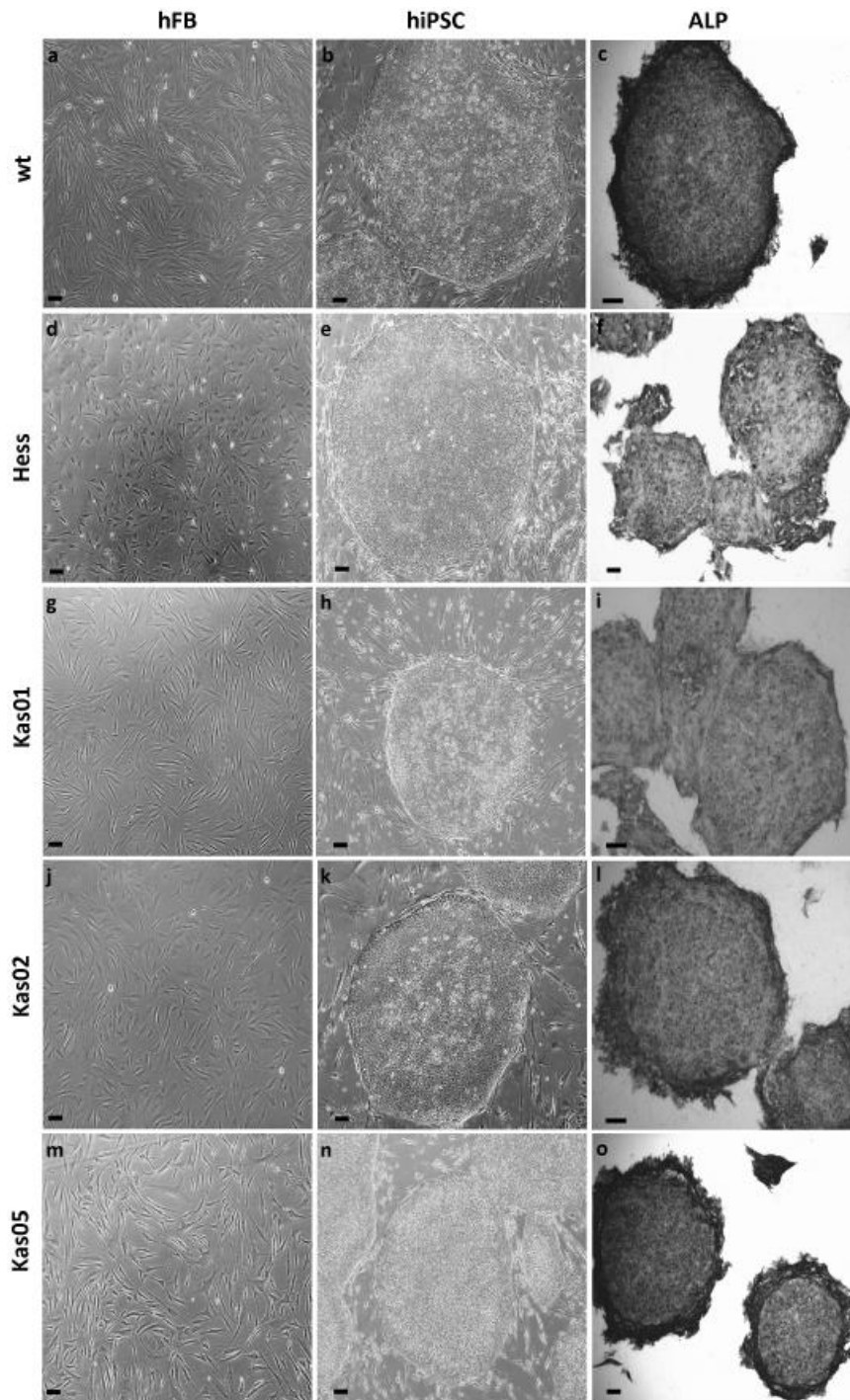
Figure 3.2: Cell Morphology of Human Skin Fibroblasts and Generated hiPSC Clones.

Cell morphologies of primary human fibroblasts were control wt (a) & Hess (d) and PD patient Kas01 (g), Kas02 (j) & Kas05 (m). (b), (e), (h), (k) & (n) were hiPSC clones derived from control and PD patients grown on feeder layers, respectively. Alkaline phosphatase (ALP) activity was examined for derived hiPSC clones (c, f, I, j & o). Black bar represents 100 μm.
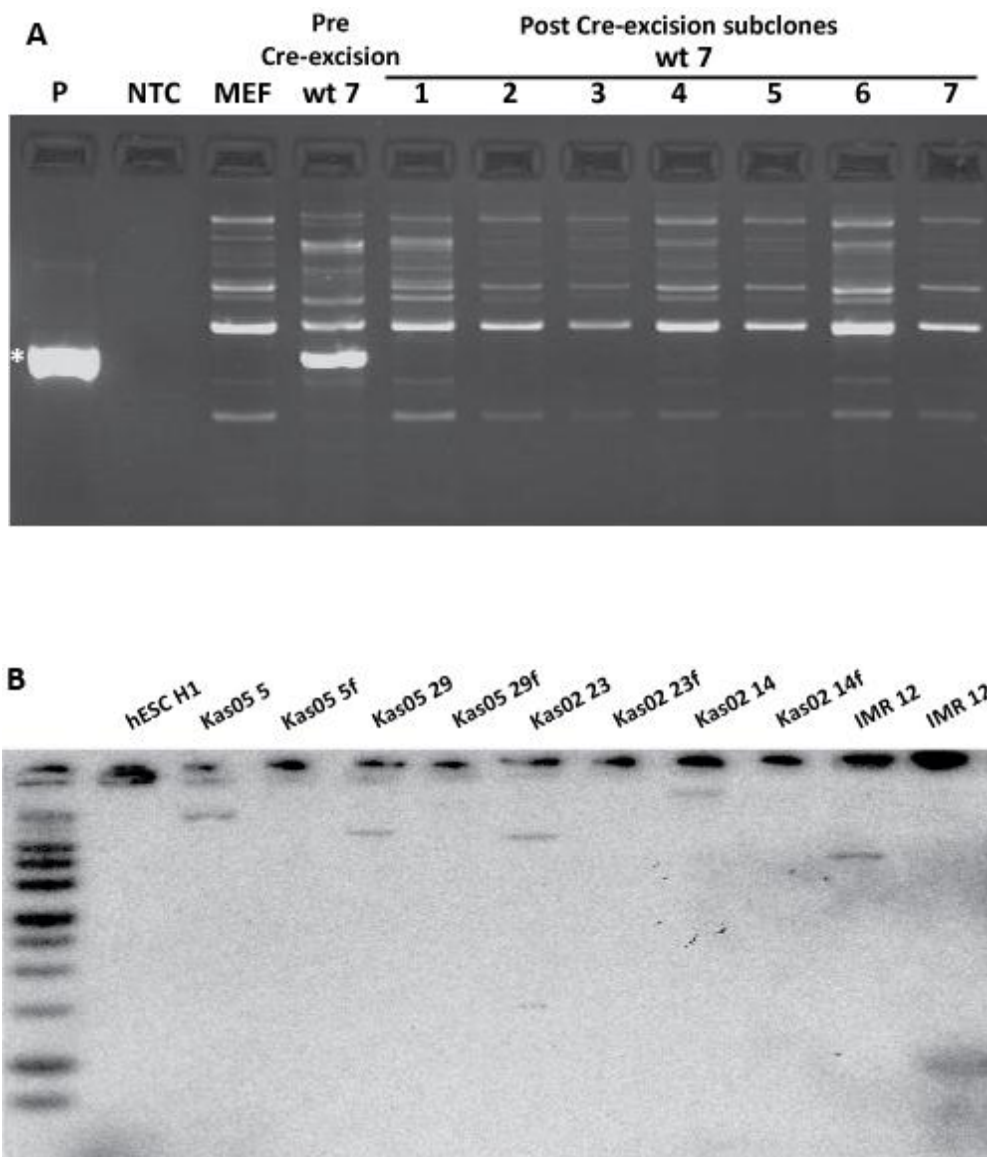
Figure 3.3: Screen of Transgene-free hiPSC Clones by PCR and Southern Blot.

(A) Preliminary screens were done by PCR using the plasmid specific primer set (SPM). P was diluted plasmid as positive control. 1~7 were post-excision subclones picked from hiPSC wt 7 clones. Note: MEF (feeder cells), NTC (non template control).

(B) Southern blot further confirmed that clone kas05 5f, Kas05 29f, kas02 23f, Kas02 14f & IMR 12f were transgenic-free excised form clone Kas05 5, Kas05 29, Kas02 23, Kas02 14 & IMR 12, respectively. hESC H1 cell line was negative control.

3.2.3 Characterization of PD Patient Specific hiPSC Lines

Overexpression of pluripotency-associated transcription factors, like Oct4, Sox2, Klf4, c-Myc, and/or Nanog & Lin28, convert human somatic cells (e.g. fibroblast or keratinocyte) to the undifferentiated state, termed human induced pluripotent stem cells (hiPSCs). hiPSC is not only indistinguishable from hESC in morphology but also exhibits the specific characteristics of hESC. Besides the demonstration of their genetic origin from the parental cell, hiPSC is supposed to meet several criteria: (1) unlimited proliferation; (2) expression of pluripotency markers and surface antigen of hESC, such as Oct4, Nanog & SSEA4, Tra-1-60; (3) potential of differentiation *in vitro* to three germ layers (ectoderm, mesoderm, and endoderm); (4) competence of teratoma formation *in vivo* when injected into immune-compromised mice. Higher standards for pluripotency are that pluripotent stem cells (PSCs) are competent for chimera contribution, germline transmission, and tetraploid complementation, routinely examined in murine iPSCs (Chen & Liu, 2009). However, due to ethical restriction, these stringent tests cannot be applied to the assessment of human pluripotent stem cells. In this work, a series of pluripotency tests would be examined in the generated PD patient specific hiPSCs (PD-hiPSCs).

DNA Fingerprinting

In order to verify the origins of control/ PD-hiPSCs, the PCR-based fingerprinting analysis was set up. The genomic DNA was isolated from respective parental fibroblasts and derived hiPSCs, and the genomic regions containing highly variable tetra-nucleotide repeats (VTNR) were amplified by designed PCR primers. Four different genomic loci were examined: D21S2055, repeat (GATA)n, average heterozygosity 0.88; D7S796, repeat (GATA)n, average heterozygosity 0.95; D10S1214, repeat (GGAA)n, average heterozygosity 0.97; and D17S1290, repeat (GATA)n, average heterozygosity 0.84 (Park, Arora, et al., 2008). The PCR amplified products were separated by agarose gel electrophoresis and shown the specific patterns among different parental fibroblasts and hiPSCs. By the combination of various sets of primers, the genetic relevance of derived hiPSC to the parental fibroblast was approved. Besides, the uncertainty of contamination of hESC cell line (e.g. H1) was excluded. (Figure 3.4)

Expression of hESC Specific Markers

Control/PD-hiPSCs were further evaluated for the specific features of human pluripotent stem cells (hPSCs) molecular signature. Previously, it was shown that the derived hiPSCs resemble hESC in terms of morphology and alkaline phosphatase activity. (Figure 3.1) Moreover, the pluripotency associated markers, including Oct4, Sox2, Nanog, and Lin28, were detected in Control/PD-hiPSCs using immunocytochemistry. The hES cell-specific surface antigens, like SSEA4 and tumor-related antigen (TRA)-1-60, were assessed as well. (Figure 3.5.I) In addition, RT-PCR analysis showed that hiPSCs expressed a set of undifferentiated ES cell-marker genes at RNA level. Control/PD-hiPSC expressed endogenous OCT4, SOX2 & NANOG with similar levels as seen in hESC cell line (H9). Besides, the presence of mRNA transcripts of reduced expression 1 (REX1), teratocarcinoma-derived growth factor 1 (TDGF1), and telomerase reverse transcriptase (hTERT) in control/PD-hiPSCs demonstrated the qualities of pluripotency regardless of the genetic condition represented within the parental fibroblasts. (Figure 3.5.II)
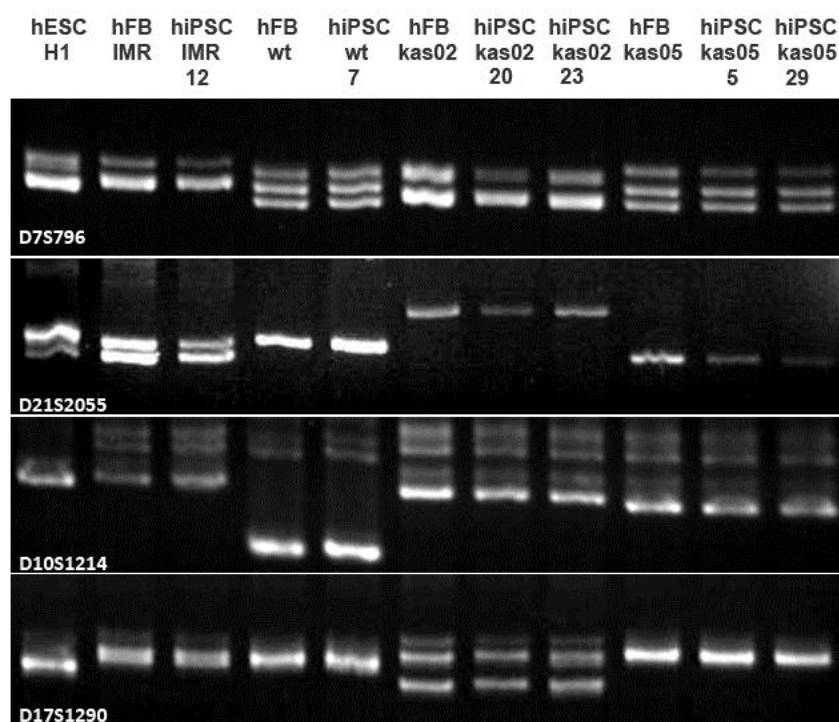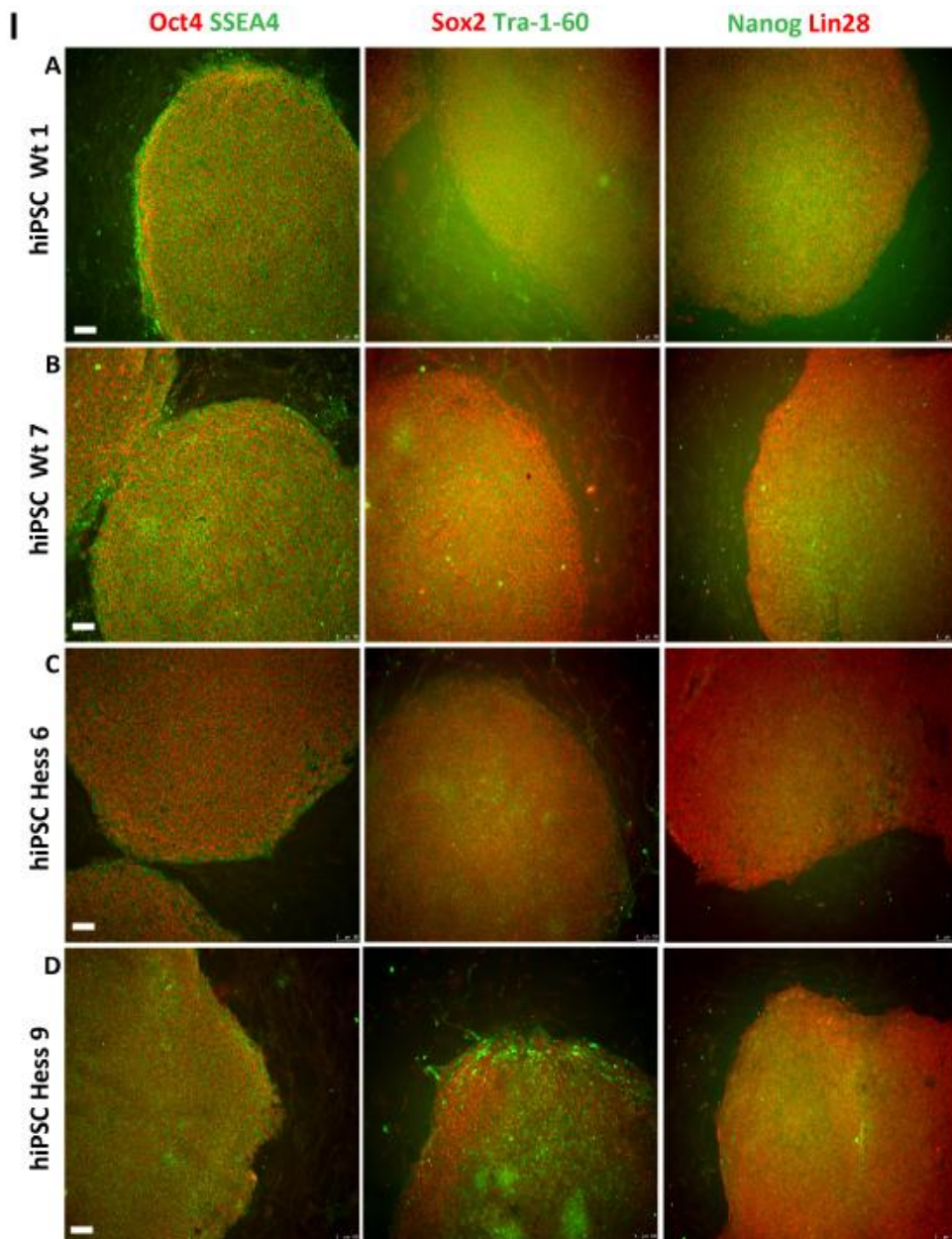

Figure 3.4: DNA Fingerprinting Analysis.

Genomic DNAs were prepared from hESC H9, IMR, control (wt) and PD patients (Kas02 & Kas05) fibroblasts, and derived hiPSCs. DNA fingerprinting was analyzed by genomic PCR

using designed primer sets (D7S796, D10S1214, D17S1290, and D21S2055). PCR products were subjected to 2.5% agarose gel electrophoresis.

Oct4 SSEA4   **Sox2** Tra-1-60   Nanog **Lin28**

E hiPSC Kas01 19

F hiPSC Kas01 21

G hiPSC Kas02 14

H hiPSC Kas02 23

I hiPSC Kas05 5

J hiPSC Kas05 29
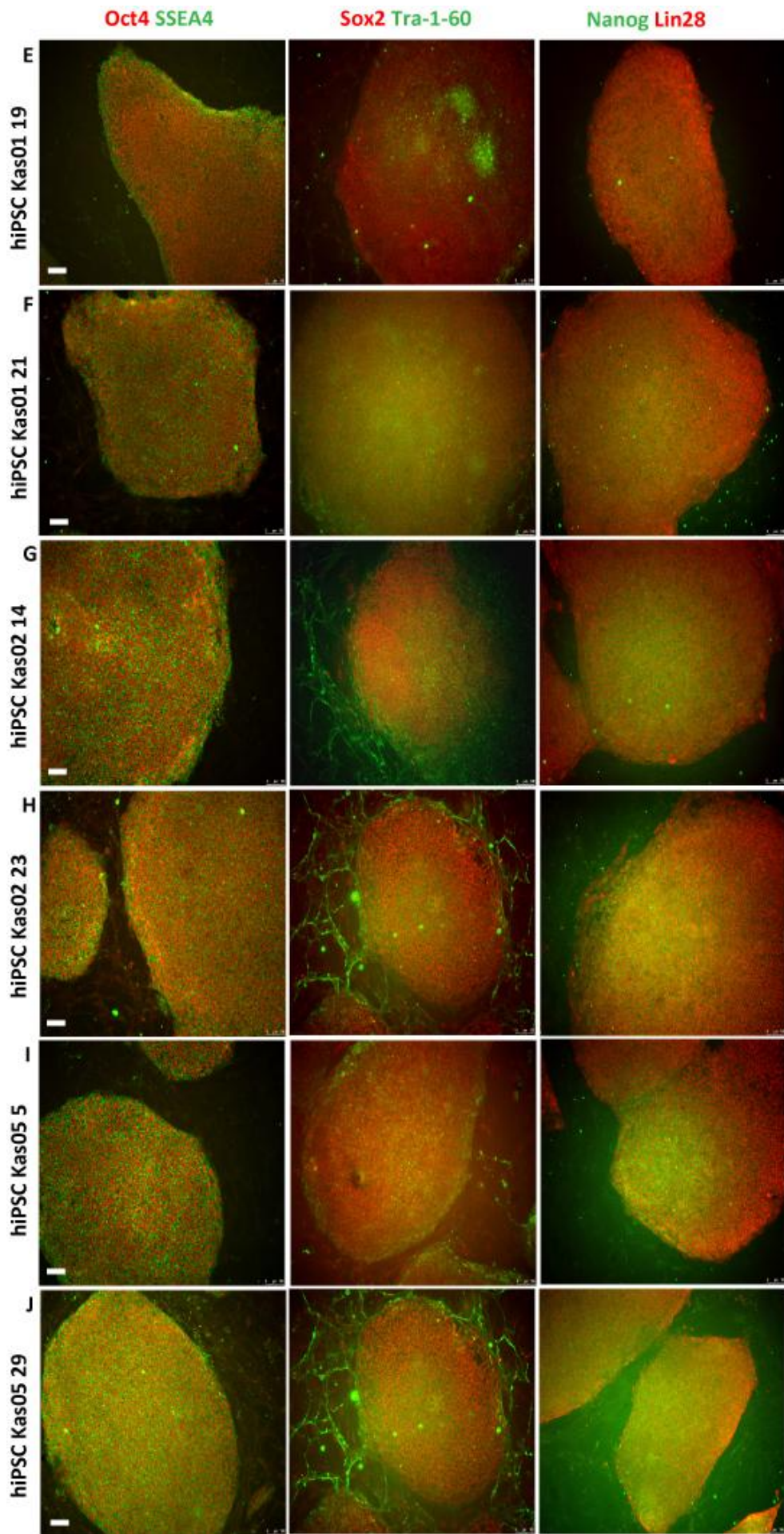
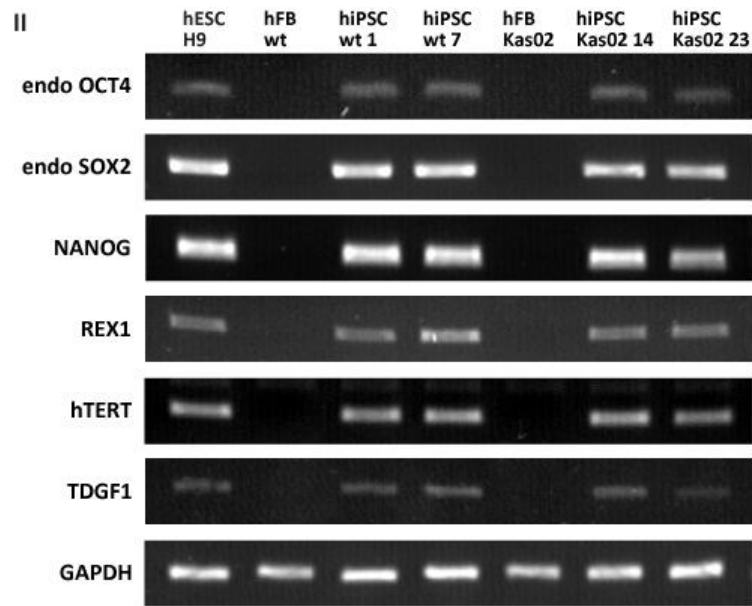**Figure 3.5: Detection of human ESC Markers in hiPSCs.**

(I) Control (wt 1 (A), 7 (B) & Hess 6(C), 9 (D)) and PD (Kas01 19 (E), 21 (F) & Kas02 14 (G), 23 (H) & Kas05 5(I), 29 (J)) hiPSC clones were examined for their pluripotency by immunostaining of Oct4, Sox2, Nanog & Lin28, respectively. hES surface antigens, SSEA4 & TRA-1-60, were present in those hiPSC cell lines as well. White bar represents 100 μm. (II) hES-related gene expressions (OCT4, SOX2, NANOG, REX1, hTERT, and TDGF1) were examined by RT-PCR. hESC H9 cell line was positive control, and hFB wt & hFB Kas02 were negative controls. wt 1& 7 and PD Kas02 14 & 23 hiPSC clone displayed these pluripotent genes' expression.

Methylation Analysis of the OCT4 Promoter Region

It is believed that the iPSC generation involves the modifications of the epigenome during conversion of somatic cell to the pluripotent state. DNA methylation controls the genomic epigenetic state that regulates gene expression. Methylation (-CH$_3$) in a cytosine-phosphate-guanosine (CpG) dinucleotide is a genetic alteration that favors genomic integrity, guarantees proper regulation of gene expression, and is required for long-term gene silencing. The reprogramming process has been shown to be associated with epigenetic changes (e.g. DNA hypomethylation) mostly on pluripotency-related gene promoters. Thus, the endogenous OCT4 and NANOG pluripotent genes may become reactivated in somatic cells undergoing faithful reprogramming. (Freberg, et al., 2007)

To assess stable reprogramming of the epigenetic state of the OCT4 promoter in Control/PD-hiPSCs, the degree of DNA methylation of 5 CpG dinucleotides in the OCT4 promoter (-2126~ -1891 bp from the transcriptional start site TSS)) was examined. This was followed by bisulfite conversion of genomic DNA, and PCR amplification of the evaluated OCT4 promoter region. The amplified PCR product was cloned into the vector and sequenced. Sequences of at least 3 bacterial clones per genomic region examined are represented as rows of circles, with each circle symbolizing the methylation state of one CpG dinucleotide. (Figure 3.6) The results revealed that hiPSCs were highly unmethylated while CpG dinucleotides of the evaluated region were highly methylated in parental fibroblasts, indicating that the OCT4 promoter is active in hiPS cells.
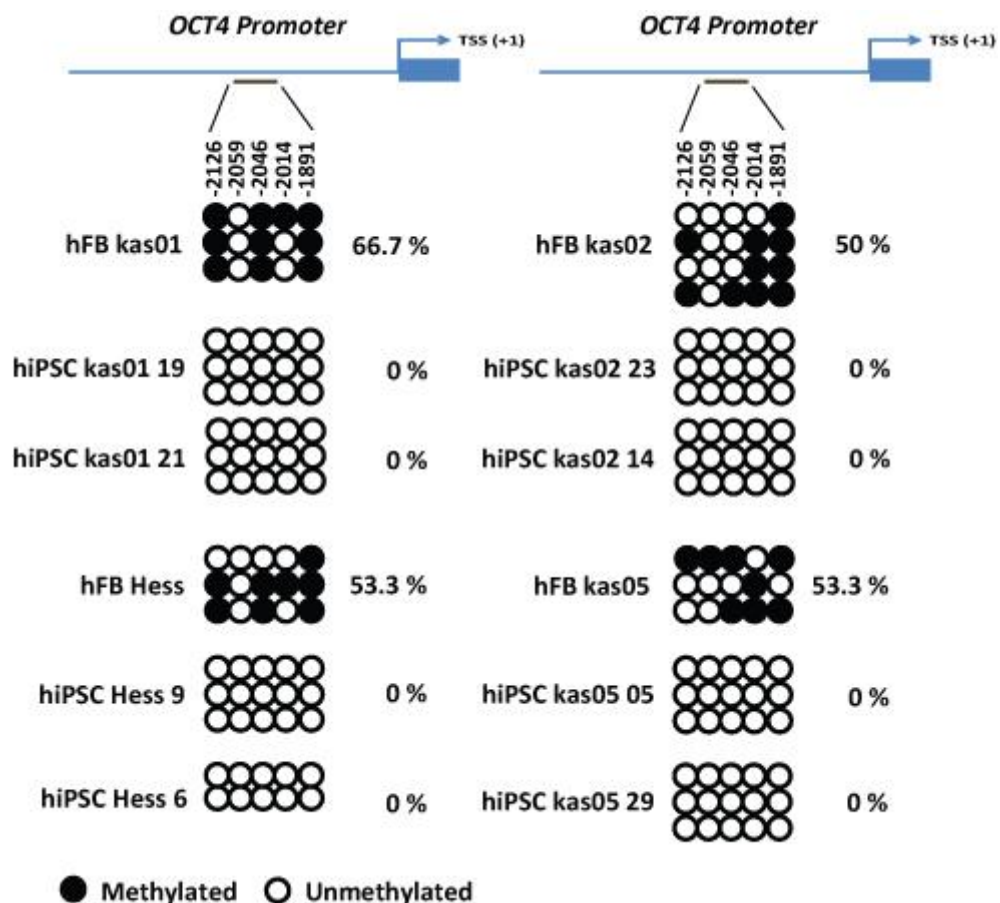

Figure 3.6: Methylation Status of OCT4 Promoter.

The CpG dinucleotides in the OCT4 promoter (-2126~ -1891 bp from the TSS) were examined for the methylation status. Open circles represent unmethylated CpG dinucleotides; closed circles represent methylated CpG dinucleotides. The cell line is indicated to the left of each
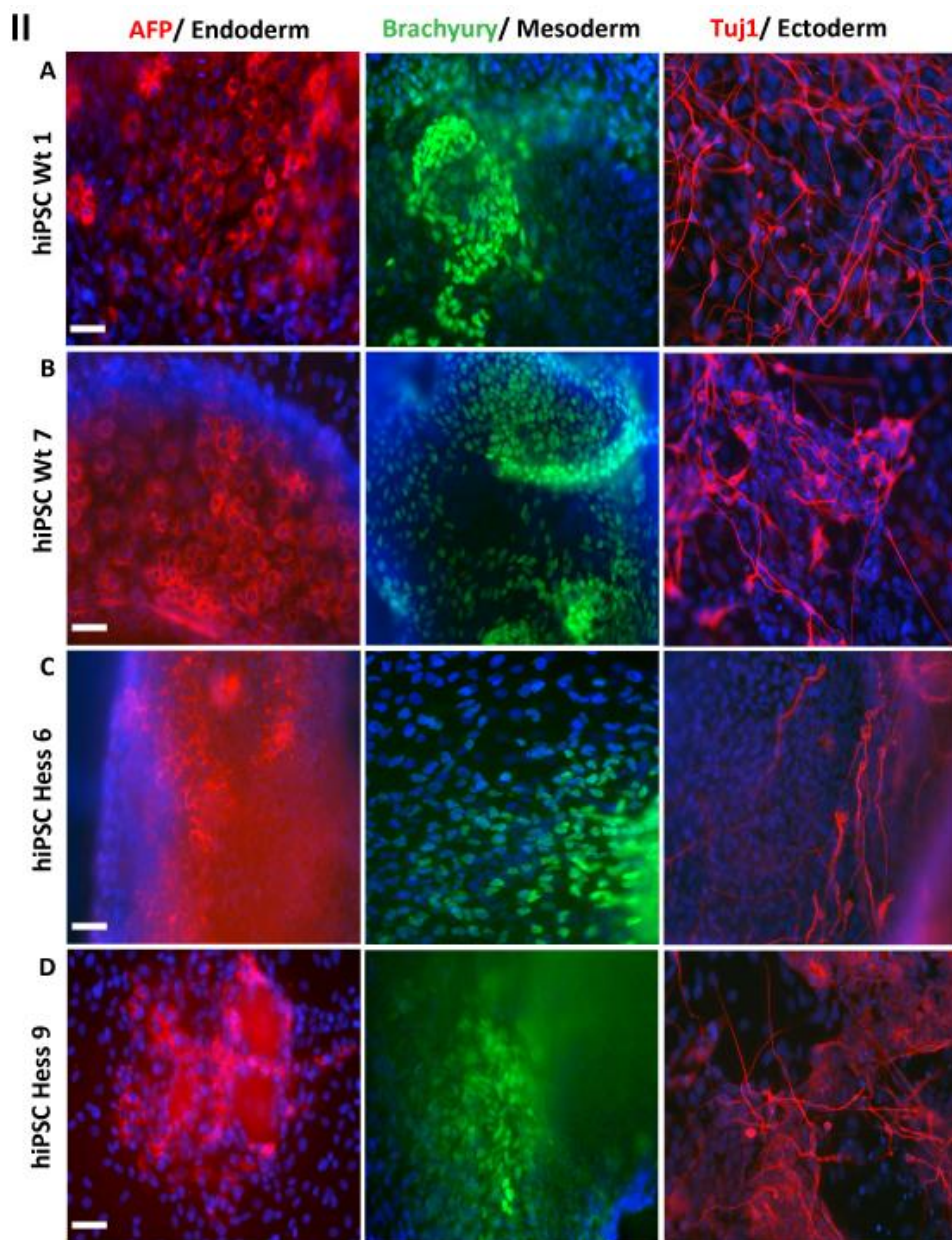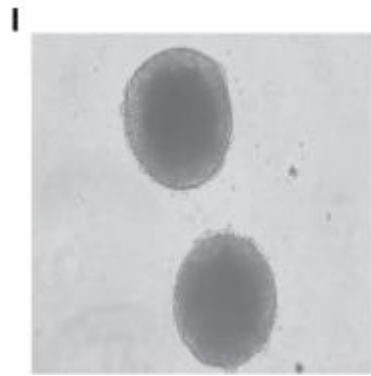
cluster. The percentage of all methylated CpGs for each promoter per cell line is noted to the right of each panel.
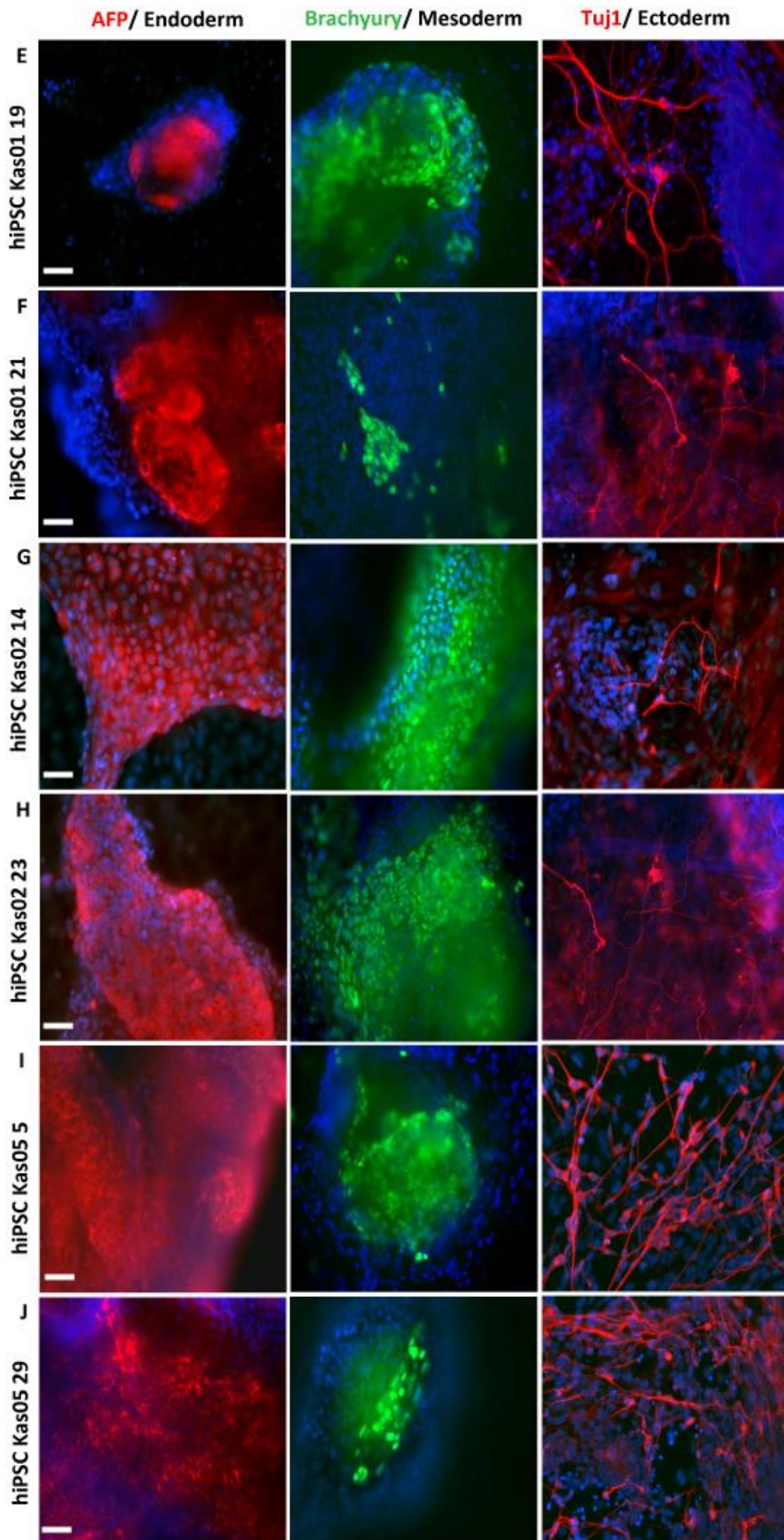
in vitro and *in vivo* Differentiation

The competence to differentiate into almost all cell types is the specific feature of human pluripotent stem cells (hPSCs). Embryoid bodies (EBs) formation is an *in vitro* test for PSCs. EB recapitulates many aspects of cell differentiation during early embryogenesis, and shows the ability of ES cells to differentiate into a variety of cell types *in vitro*. (Kurosawa, 2007) Another tool to monitor the capability of differentiation in stem cell research, also known as "gold standard" for assessing pluripotency, is teratoma formation *in vivo*. Teratomas are benign tumors composed of tissue or organ components from all three germ layers (endoderm, ectoderm, and mesoderm). When PSCs were injected into immune-deficient mice, PSCs develop into teratomas typically by remodeling their microenvironment to support their growth and generating blood vessels for nutrients (W. Y. Zhang, de Almeida, & Wu, 2008).

To verify the ability of differentiation *in vitro*, the Control/PD-hiPSC floating culture was set up to form embryoid bodies (EBs) (Figure 3.7.I). After one week of suspension culture, the resulting cell aggregates (EBs) were plated on the gelatinized coverslips and kept growing in differentiation medium without bFGF growth factor. The outgrowth of differentiated cells from EBs presented different population of cell lineages: Endoderm (α-Foetoprotein), Mesoderm (Brachyury), and Ectoderm (Neuron-specific class III beta-tubulin) as documented by immunohistochemistry (Figure 3.7.II).

Transplantation of Control/PD-hiPSCs into immunodeficient mice conducted the test for teratoma formation *in vivo*. If the tumor formation were observed, tumors would collect for histological analysis. Histological structures representing endoderm, mesoderm and ectoderm lineages showed that the derived hiPSCs have pluripotent potential (Figure 3.7.III).

I

II

AFP/ Endoderm	Brachyury/ Mesoderm	Tuj1/ Ectoderm

A hiPSC Wt 1

B hiPSC Wt 7

C hiPSC Hess 6

D hiPSC Hess 9

AFP/ Endoderm   Brachyury/ Mesoderm   Tuj1/ Ectoderm

E   hiPSC Kas01 19

F   hiPSC Kas01 21

G   hiPSC Kas02 14

H   hiPSC Kas02 23

I   hiPSC Kas05 5

J   hiPSC Kas05 29

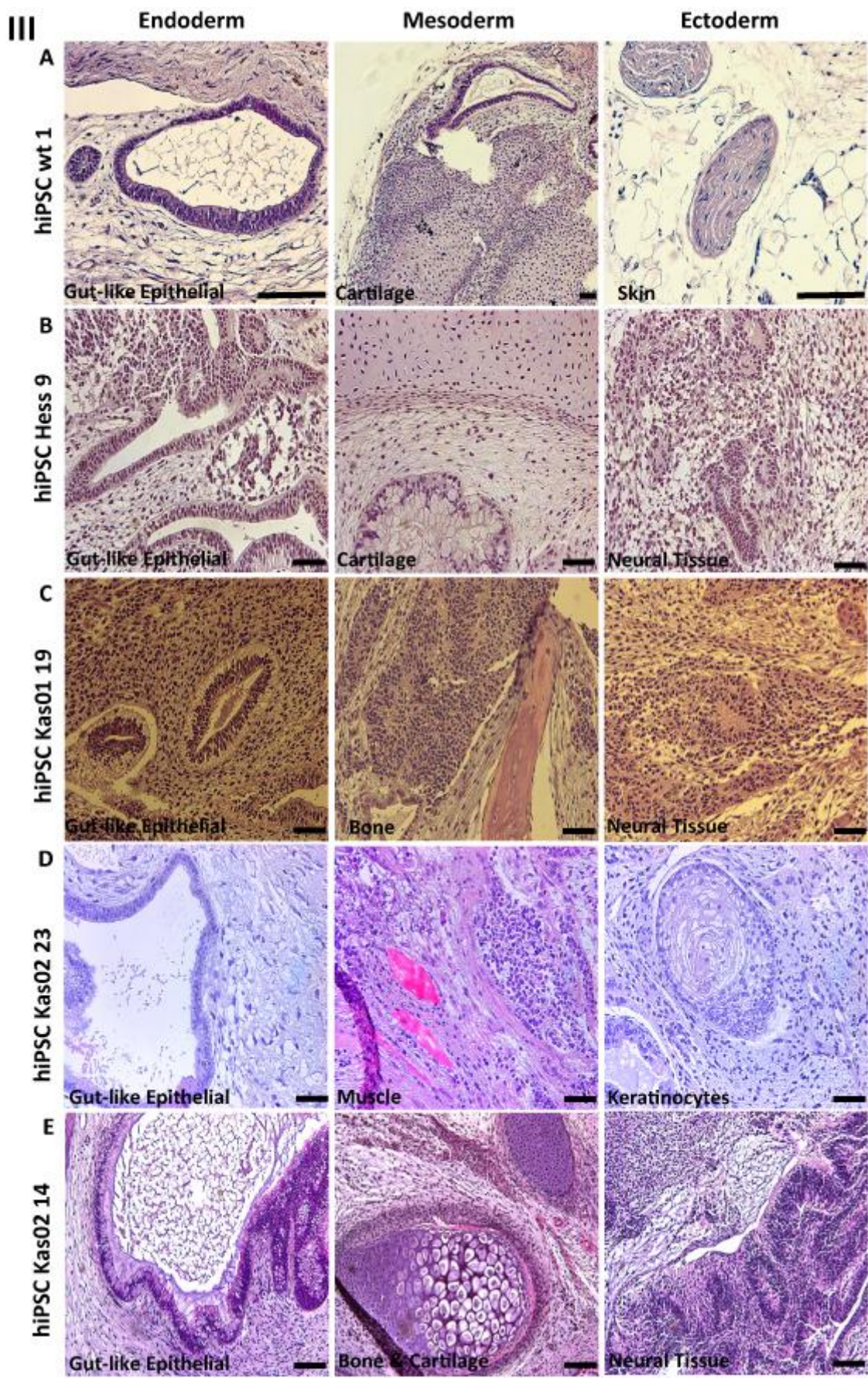|	Endoderm	Mesoderm	Ectoderm
hiPSC wt 1 (A)	Gut-like Epithelial	Cartilage	Skin
hiPSC Hess 9 (B)	Gut-like Epithelial	Cartilage	Neural Tissue
hiPSC Kas01 19 (C)	Gut-like Epithelial	Bone	Neural Tissue
hiPSC Kas02 23 (D)	Gut-like Epithelial	Muscle	Keratinocytes
hiPSC Kas02 14 (E)	Gut-like Epithelial	Bone & Cartilage	Neural Tissue

III

Figure 3.7: *in vitro* and *in vivo* Differentiation of hiPSCs.

(I) Embryoid body (EB) formation was carried in suspension culture of hiPSCs. (II) The outgrowth of adherent EBs derived from Control (wt 1 (A), 7 (B) & Hess 6(C), 9 (D)) and PD (Kas01 19 (E), 21 (F) & Kas02 14 (G), 23 (H) & Kas05 5(I), 29 (J)) hiPSC were analyzed by immunostaining of different lineage markers. AFP (α-Foetoprotein): Endoderm; Brachyury: Mesoderm; Tuj1 (Neuronal Class III β-Tubulin): Ectoderm. White bar represents 50 μm. (III) hiPSC were injected into Immunodeficient mouse recipients. Resulting teratomas from control hiPSCs (wt 1 (A), Hess 9 (B)) and PD hiPSCs (Kas01 19 (C), Kas02 23 (D) & Kas02 14 (E)) were histologically examined by HE staining. Gut-epithelial, cartilage & muscle & bone, skin & keratinocyte & neural tissue correspond to endo-, meso-, and ectodermal lineages, respectively. Black bar represents 50 μm.

3.3 Derivation of Neural Precursors from Control/PD-hiPSCs

3.3.1 Direct Differentiation of Neural Precursors form Control and PD hiPSCs

Current developed protocols for neural induction of human pluripotent stem cells (hPSCs) rely on embryoid body (EB) formation (S. C. Zhang, et al., 2001) or stromal feeder co-culture (Kawasaki, et al., 2000). In addition, it is evident that inhibition of SMAD signaling improves the efficiency of neural induction. Therefore, some identified BMP inhibitors, like Noggin (Smith & Harland, 1992) and Dorsomoprhin, have been used as neural inducing factors in several PSC neural differentiation protocols (Morizane, Doi, Kikuchi, Nishimura, & Takahashi, 2011) (S. M. Chambers, et al., 2009). For neuron differentiation in hPSCs, it is often carried out on co-culture with stromal feeders with respect to the elicited stromal cell derived inducing activity (SDIA) observed in mouse ESC efficient neuronal differentiation. However, the effect is relatively less in human ESC, suggesting that additional treatments of BMP inhibitors accelerate and improve the neural induction. In this study, the combination of stromal feeder co-culture and BMP inhibitor treatment was set up to commit control/PD-hiPSCs to neuroectodermal lineage, generate multipotent neural precursors, and then further differentiate to dopaminergic neurons.

The day before starting neural induction, hiPSCs were clonal passaged onto inactive PA6 cells (stromal cell line derived from mouse skull bone marrow). Then the hiPSCs were co-cultured on PA6 feeders and treated with BMP inhibitors (either recombinant Noggin protein or small molecule Dorsomorphin). (Figure 3.8) After one week of neural induction, neural rosette structures (Figure 3.9.C) started to appear on the neural induced hiPSC colonies. By this time point, the expression of the neuroepithelial cell marker-Pax6 (Figure 3.9.A) as well as the neural stem/progenitor cell marker-Nestin (Figure 3.9.B) was present in neural induced cells. The neural rosettes were isolated mechanically and plated on poly-D-Lysine (PDL) coated dishes separately. Meanwhile, the neural rosettes were fed with Neural Precursor (NP) medium (serum free N2B27 defined medium) containing bFGF and EGF growth factors. In the presence of bFGF and EGF, hES-derived rosettes are able to proliferate and maintain the expressions of neural stem cell markers, Sox1, Sox2, and nestin (Elkabetz et al., 2008). After some days, the cell outgrowth of neural rosettes was observed. Following Accutase treatments, the neural rosettes were dissociated into single cells and replated onto new dishes. Those emerging neural precursors display the bipolar morphology maintaining the

characteristics of neural rosette (Figure 3.9.D). The neural precursors grew as monolayers on the PDL coated dishes and were expansible with Accutase. When derived neural precursors were grown in suspension, they were able to form the neurospheres (Figure 3.9.E).

The generated transgene-free control/PD-hiPSCs were employed to derive multipotent neural precursors through this combination of BMP inhibitor treatments and co-culture on PA6 stromal feeders. Those control/PD-hiPSC derived neural precursors displayed the neural epithelial cell morphology and expressed neural precursor specific markers, e.g. Msi1, Sox1, Sox2, Nestin, and Pax6 (Figure 3.10). To date, control/PD-hiPSC derived neural precursors can be maintained up to passage 25.
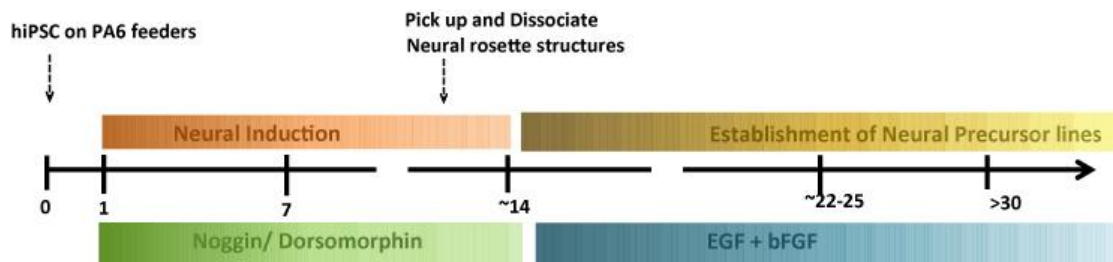

Figure 3.8: Flow Chart of Derivation of Neural Precursors.
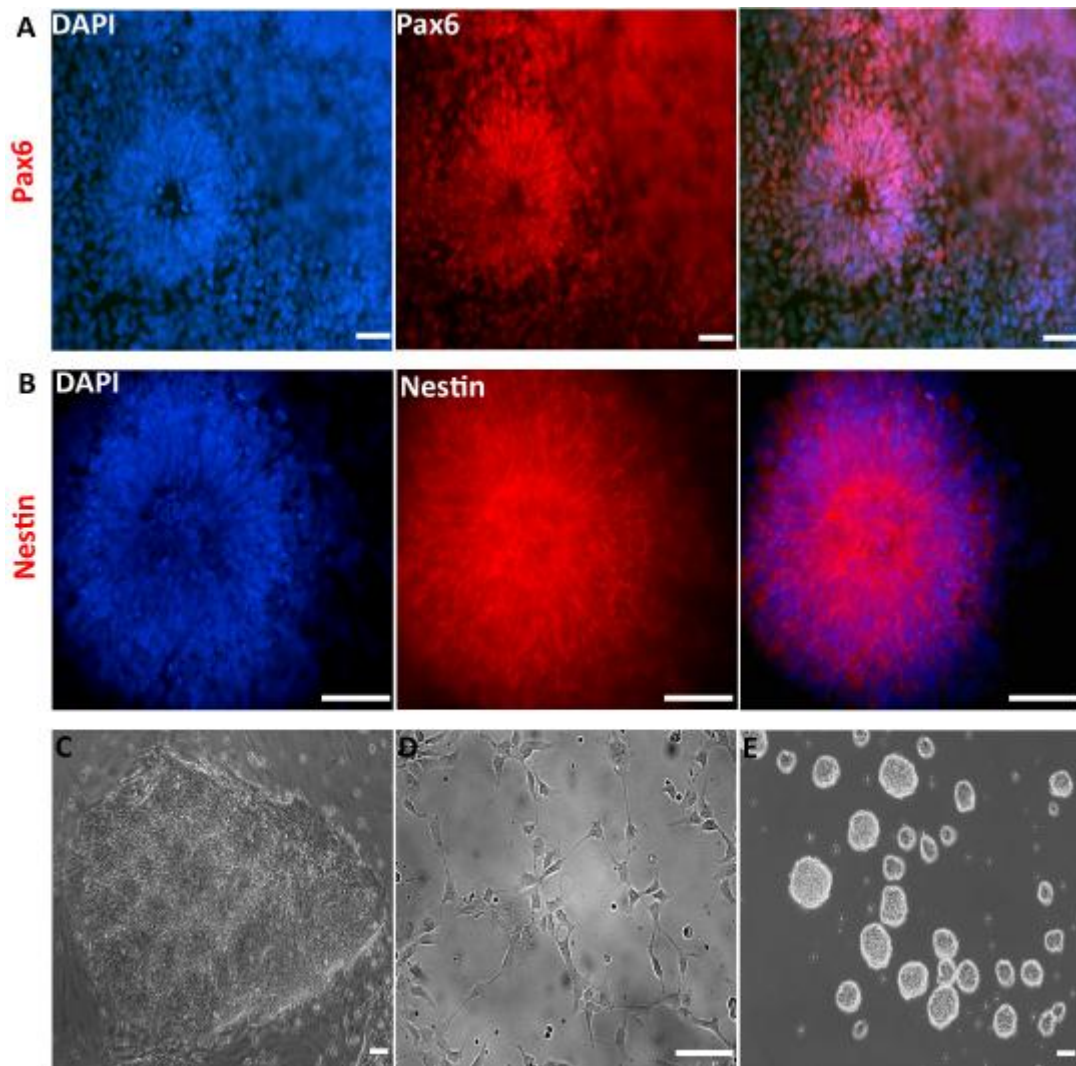
Figure 3.9: Neural Rosettes Structures in Neural Inductions.

Neural epithelial markers, Pax6 (A) & nestin (B), were observed in neural rosettes during neural inductions. Nuclei were counterstained with DAPI (blue). The morphology of neural rosettes (C) was present in a neural induced hiPSC clone. Neural precursors displayed bipolar neural epithelial morphology (D). Neural precursors were able to form neurospheres (E). White scale bar corresponds to 100 μm.
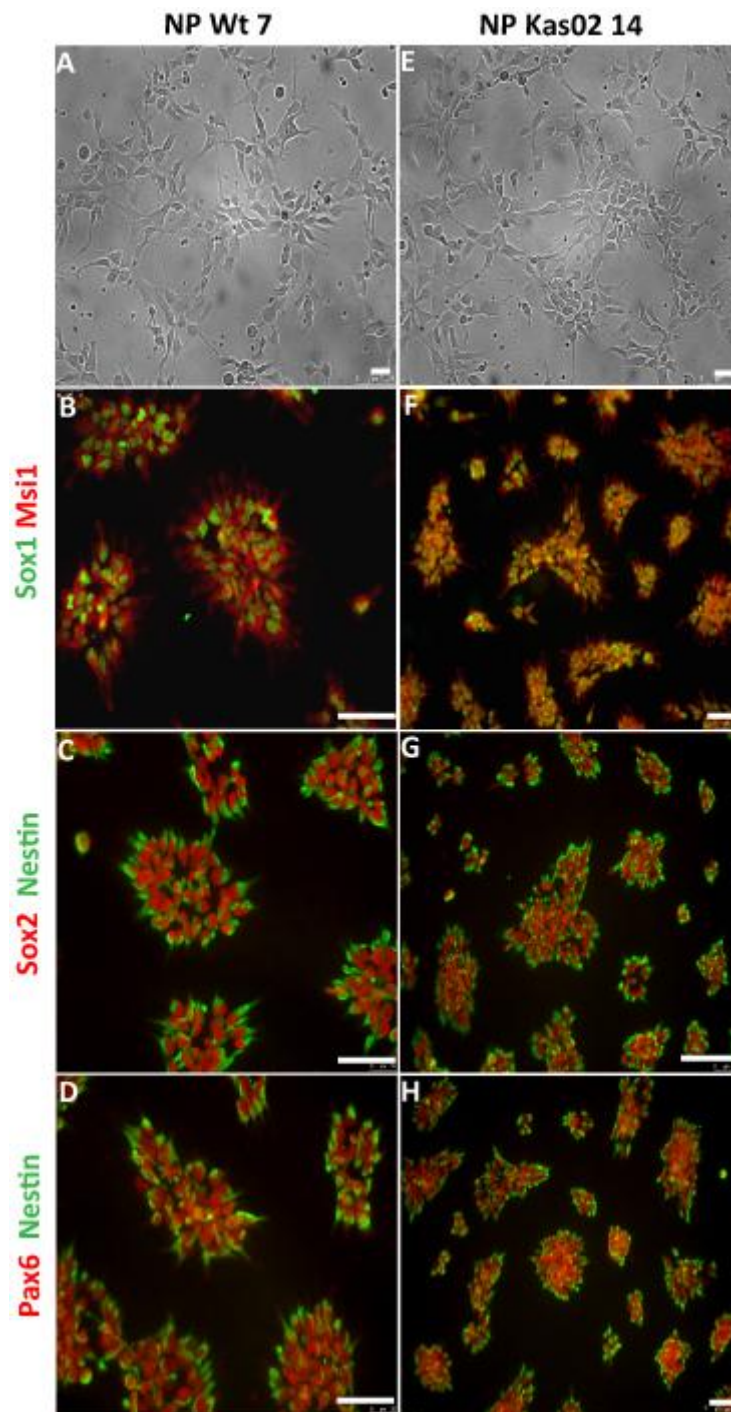
Figure 3.10: Derivation of Neural Precursors from Control/PD-hiPSCs Neural Inductions.

(A & E) cell morphology of control & PD hiPSCs derived neural precursors. These neural precursors expressed neural epithelial markers, Sox1 & Msi1, Sox2, Pax6, and Nestin (B-D & F-H). White scale bar corresponds to 50 μm

3.3.2 Generation of dopaminergic neurons from Control/PD-hiPSC derived Neural Precursors

After the establishment of PD patient specific neural precursor cell lines from the pluripotent state, further differentiation was required to demonstrate the ability of conversion into terminally differentiated neurons. To enrich for dopaminergic neurons, PD relevant cell type, neural precursors were exposed to Shh and FGF8 growth factors to mediate the cell fates of dorsal-ventral patterning for two weeks. Afterwards, the differentiated cells were maintained in the neural differentiation medium containing BDNF, GDNF, dbcAMP, Ascorbic acid, and TGF-β3 for maturation of dopaminergic neurons and to prevent cell death.

After 30 days of final dopaminergic maturation, control/PD-hiPSC derived neural precursors were able to differentiate into neuronal cells. They showed the expression of Neuronal Class III β-Tubulin (Tuj1), a pan neuronal marker (Figure 3.11). More importantly, the expression of Tyrosine hydroxylase (TH), the marker for dopaminergic neurons, was observed in differentiated neurons as well.

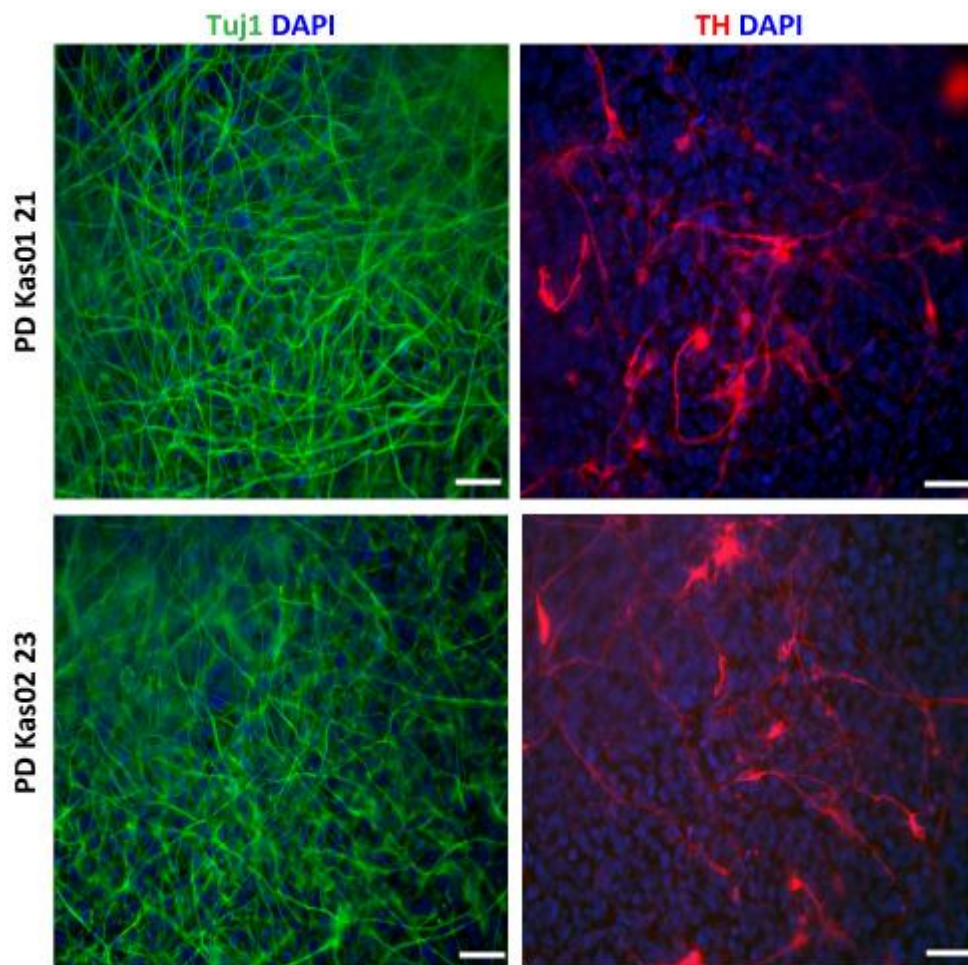**Figure 3.11: Dopamine Neuron Differentiation from PD-hiPSC derived Neural Precursors.**

Immunofluorescent images of differentiated neurons following dopaminergic neuron patterning and maturations. Tuj1 (Neuronal Class III β-Tubulin) (green) represented as pan neuron marker while TH (Tyrosine Hydroxylase) (red) indicated dopamine neurons. Nuclei were counterstained with DAPI (blue). White scale bar corresponds to 100 μm.

3.3.3 Transcriptome Analysis of Control/PD-hiPSC Derived Neural Precursors

On account of the increased knowledge of human genome, the technology of gene microarray has provided a rapid and parallel assay of gene expression patterns. The plenty of obtained data from the microarray platform can be used to assign a comprehensive understanding of genetic networks. Thus, it is a mighty technique to evaluate the global gene expression changes correlated with differential treatments of the samples and to demonstrate the correlation among various samples. Furthermore, it is possible to discover the new regulatory networks by the differential gene expression patterns.

To reveal novel molecular players involved in the PD pathogenesis, the control/PD-hiPSC derived neural precursors were used for transcriptome analysis using RNA microarray. 4 control neural precursors (wt 1, wt 7 & Hess 6, Hess 9) were derived from 2 healthy persons' hiPSCs and 6 PD neural precursors (Kas01 19, Kas01 21 & Kas02 14, Kas02 23 & Kas05 5, Kas05 29) were derived from 3 individual PD patients' hiPSCs, respectively. The RNA microarray of control/PD-hiPSC derived neural precursors and initial data processing were carried out by the "Transkriptomanalyselabor (TAL)" at the University of Göttingen. The hierarchical correlation among the corresponding control and PD neural precursors was presented by the heatmap (Figure 3.12). The slight discrepancy between clones of the same sample can be observed, and might be due to the process of derivation of neural precursors. On account of individual samples with diverse genetic backgrounds, the global transcriptomes of respective samples' neural precursors were not similar to each other. Using the platform "GeneSifter®" (PerkinElmer Inc.), the differential gene expressions of respective neural precursors were computed by Dr. Patrick Collombat, Institut de Biologie Valrose, Nice, France. To be considered differentially expressed between PD neural precursors versus control ones (PD-Control), genes had to be at least 1.5 folds up- or down-regulated and the corresponding p-value should be less than or equal to 0.05. The number of resulting up- and down-regulated genes among PD-Control was 485 and 332, respectively.

To comprehensively understand the role of differentially expressed genes and their involved signaling pathways, total 817 genes (up- and down-regulated) were upload to the DAVID Bioinformatics Resources 6.7 (http://david.abcc.ncifcrf.gov/) for functional annotation and enrichment analyses. Based on the functional clustering, 13 pathways (p-value less than or

equal to 0.05) were depicted by KEGG pathways (Figure 3.13.A). Among them, the pathway of axon guidance was most significant and might be associated with PD (Lesnick et al., 2007) (J. M. Kim et al., 2011). The fold changes (PD versus Control) of 14 genes involved in axon guidance were presented on Figure 3.13.B and S1. Besides, the genes counted in Gene Ontology (GO) term for neuron differentiation (GO0030182) were picked up and displayed the fold changes (PD versus Control) in Table 3.2. Of note, EPHA4 gene was significantly increased (3.5 fold) in the pool of PD-hiPSC derived neural precursors and annotated in both of axon guidance and neuron differentiation. Besides, FGF20 was attributed to the scope of GO term: neuron differentiation (Table3.2) and remarkably reduced (4 fold) in PD-hiPSC derived neural precursors among genes of susceptibility to Parkinson disease (e.g. GAK (Cyclin G associated kinase), DGKQ (Diacylglycerol kinase, theta 110kDa), and FGF20 (Fibroblast Growth Factor 20)) (Pankratz et al., 2009) (Lill et al., 2012) (van der Walt et al., 2004) in this transcriptome analysis (Figure 3.14.A). Besides, the genetic variability of FGF20 has long been considered as a risk factor of PD (van der Walt, et al., 2004). Furthermore, the decreased expression level of FGF20 was verified among respective clones of PD-hiPSC derived neural precursors by QRT-PCR.
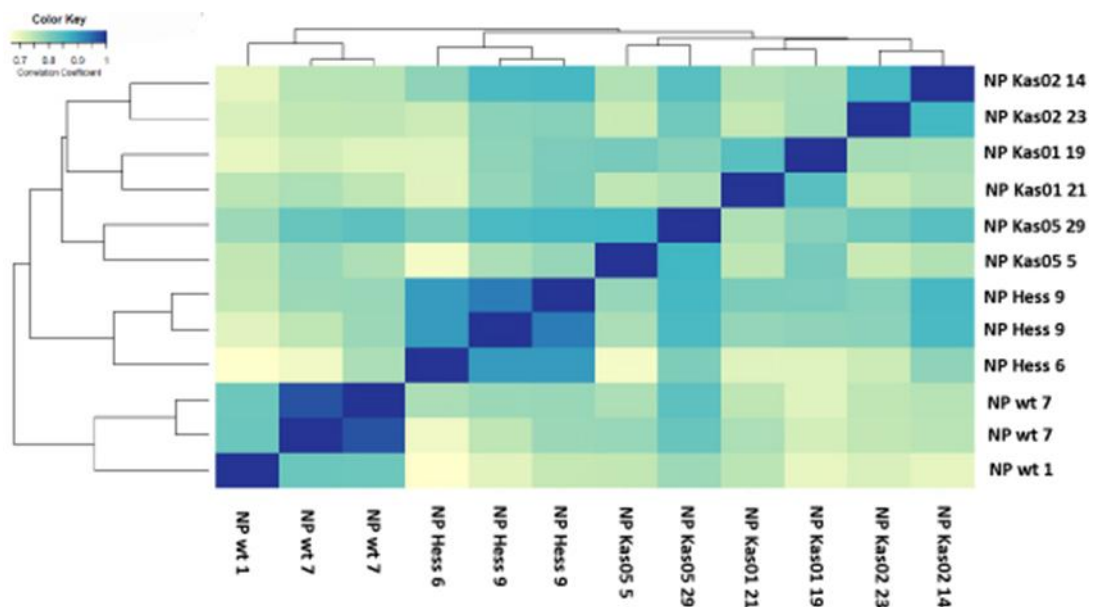
Figure 3.12: Comparative Transcriptome Analysis of Control/PD-hiPSC derived Neural Precursors.

This heatmap showed the correlation among controls (wt & Hess) and PD (Kas01, Kas02 & Kas05) samples. For each sample (Control and PD), 2 clones of neural precursors derived

from 2 individual hiPSC clones were used as duplicate for analysis of RNA microarray. For the reason of fitting the experimental samples to the Aglient chip, NP wt 7 and NP Hess 9 were applied one more time.

A.
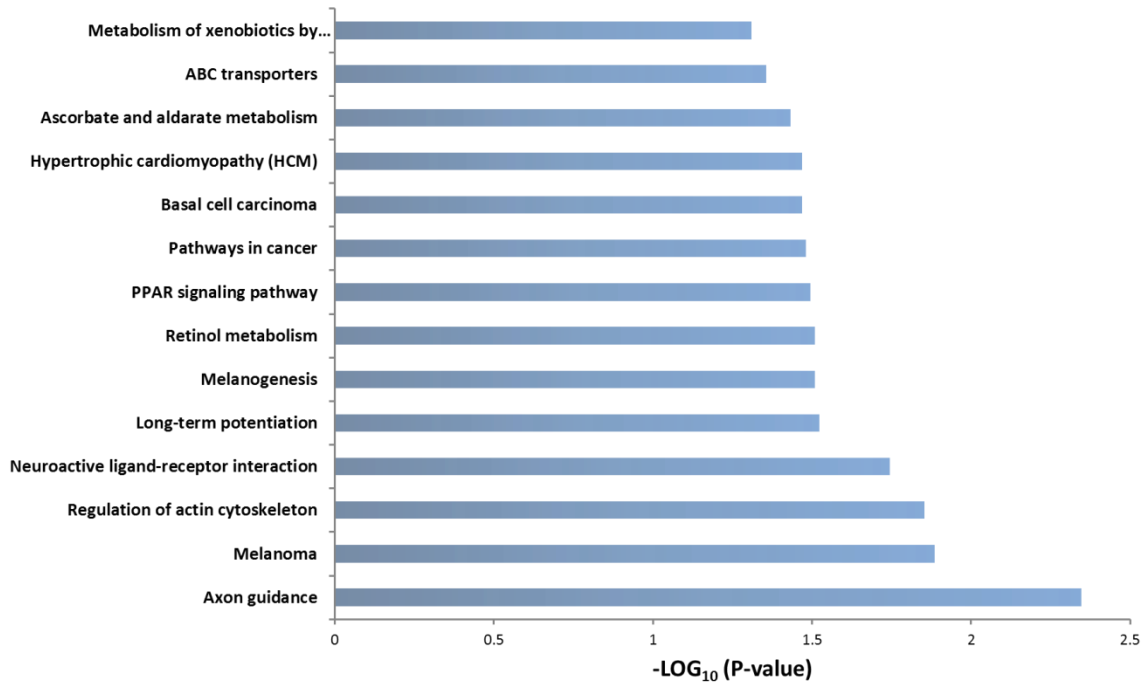
B.

Figure 3.13: Functional Annotation Clustering by KEGG pathway.

(A) showed the significance of enriched pathways clustered by total differential expressed genes. (B) presented the fold change (PD versus Control) of various genes in the pathway of axon guidance.

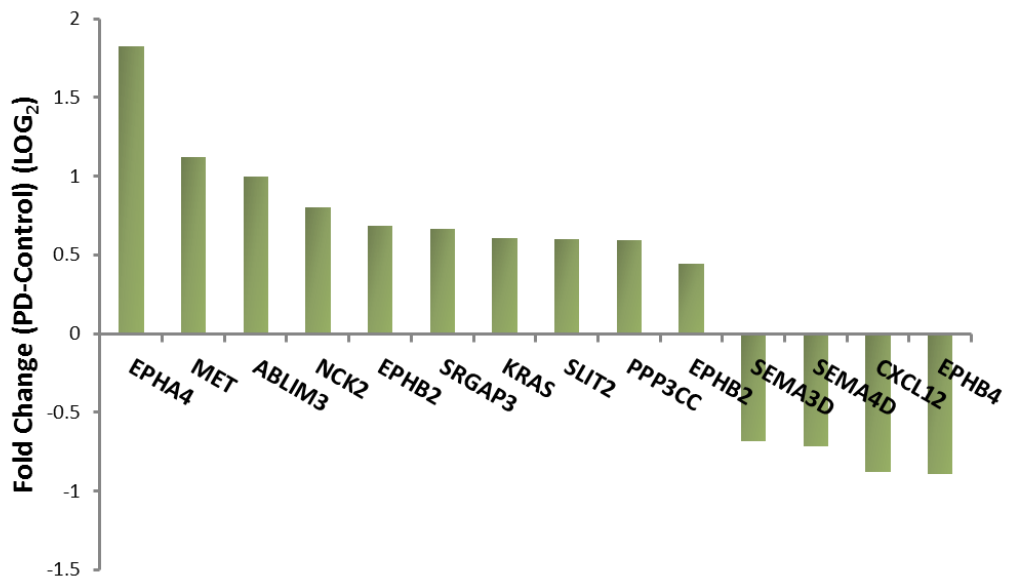**Table 3.2: Gene Ontology Analysis of Differential Gene Expression of Neuronal Precursors Annotated with the GO Term: Neuron Differentiation.**

REFSEQ_MRNA	Fold Change (PD-Control)	GENE SYMBOL	GENE NAME
NM_001101	2.75	ACTB	actin, beta
NM_004438	1.82	EPHA4	EPH receptor A4
NM_000555	1.74	DCX	doublecortin
NM_001018065	1.67	NTRK2	neurotrophic tyrosine kinase, receptor, type 2
NM_004496	1.52	FOXA1	forkhead box A1
NM_201264	1.49	NRP2	neuropilin 2
NM_021955	1.49	GNGT1	G protein, gamma transducing activity polypeptide 1
NM_004796	1.25	NRXN3	neurexin 3
NM_001145661	1.11	GATA2	GATA binding protein 2
NM_153487	1.04	MDGA1	MAM domain containing glycosylphosphatidylinositol anchor 1
NM_002487	0.97	NDN	necdin homolog (mouse)
NM_005986	0.91	SOX1	SRY (sex determining region Y)-box 1
NM_000280	0.86	PAX6	paired box 6
NM_002167	0.86	ID3	inhibitor of DNA binding 3
NM_000052	0.82	ATP7A	ATPase, Cu++ transporting, alpha polypeptide
NM_171999	0.80	SALL3	sal-like 3 (Drosophila)
NM_005964	0.77	MYH10	myosin, heavy chain 10, non-muscle
NM_022363	0.69	LHX5	LIM homeobox 5
NM_000675	0.65	ADORA2A	adenosine A2a receptor
NM_001719	0.62	BMP7	bone morphogenetic protein 7
NM_004787	0.60	SLIT2	slit homolog 2 (Drosophila)
NM_004442	0.45	EPHB2	EPH receptor B2
NM_001982	-0.66	ERBB3	v-erb-b2 erythroblastic leukemia viral oncogene homolog 3 (avian)
NM_001033886	-0.88	CXCL12	chemokine (C-X-C motif) ligand 12
NM_032109	-0.92	OTP	orthopedia homeobox
NM_002507	-0.99	NGFR	nerve growth factor receptor
NM_014624	-1.20	S100A6	S100 calcium binding protein A6
NM_000230	-1.40	LEP	leptin
NM_005172	-1.60	ATOH1	atonal homolog 1 (Drosophila)
NM_001426	-1.92	EN1	engrailed homeobox 1
NM_019851	-2.01	FGF20	fibroblast growth factor 20

Note: Fold Change (PD-Control) LOG_2

A.
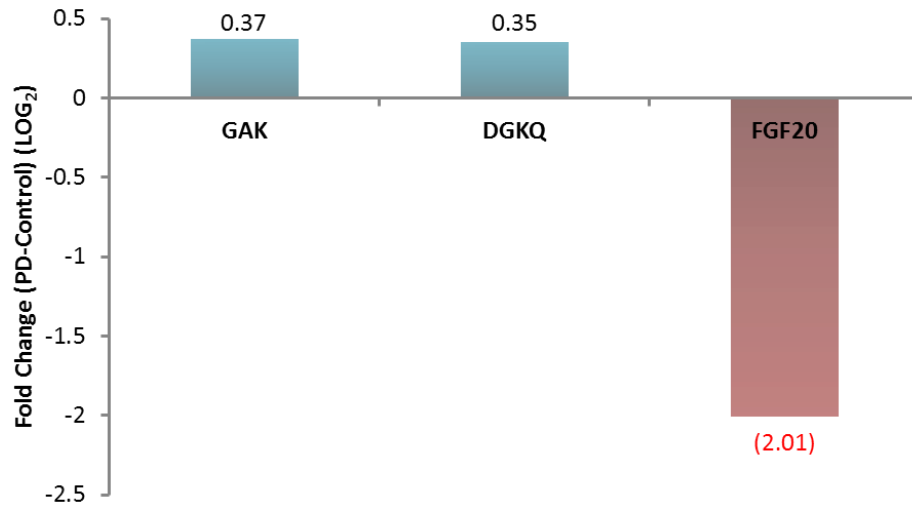
B.

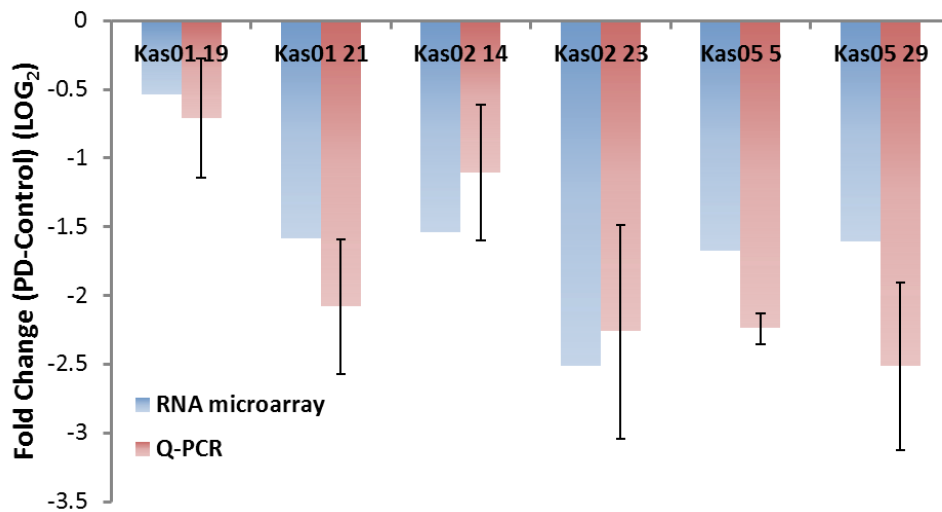**Figure 3.14: Expression Level of Genes of Susceptibility to Parkinson Disease.**

(A) In the transcriptome analysis of control/PD-hiPSC derived neural precursors, 3 genes (GAK, DGFQ, and FGF20) associated with the susceptibility to PD were differential expressed. (B) showed the expression changes of FGF20 (PD-Control) for each clone of PD-hiPSC derived neural precursors in both of RNA microarray and Q-PCR.

3.4 Derivation of Floor Plated-based Differentiated mDA Neurons from Conrtol/PD-hiPSCs

3.4.1 Direct Differentiation of midbrain Dopaminergic Neurons from Control/PD-hiPSCs

In order to increase the number of midbrain dopaminergic neurons from control/PD-hiPSCs for functional and phenotype assays, the alternative strategy of differentiation, floor plate (FP)-based dopamine neuron differentiation, was conducted in this study. Since 2012, several protocols have been adopted for hPSCs, including hPSC monolayer culture, EB suspension culture, or hPSC co-culture with feeders (Kriks, et al., 2011) (Xi, et al., 2012) (Denham, et al., 2012). The general features are early activation of Shh and wnt signaling during neural induction of hPSC by inhibition of dual SMAD signaling. The essential transcription factor, also known as the marker of FP, FoxA2 would mark FP-based induced cells due to the activation of Shh. Through the induction of wnt signaling, Lmx1a would be co-expressed on FoxA2 positive cells, then midbrain FP DA precursors emerged. Midbrain DA Neurons would appear to follow further differentiation and maturation of midbrain FP DA progenitors.

In this study, the differentiation of FP-based dopamine neurons was adopted and modified from (Xi, et al., 2012). (Figure 3.14) One day before differentiation, hiPSCs were clonal passaged onto inactive PA6 feeder layers. The next day, hiPSCs were fed with FP induction medium in the presence of SB431542 (SB) and LDN193189 (LDN) for neural induction. In the meantime, purmorphamine (pur) (an activator of Shh) and CHIR99021 (CHIR) (an activator of wnt) were added to the hiPSC to drive Shh-FoxA2 and Wnt1-Lmx1a regulatory loops. After 9 days of neural induction, dual SMAD inhibitors were removed, but the cells were still exposed to pur and CHIR for continuous activation of Shh and wnt signaling till day 13. At this time, the induced hiPSCs were prepared to examine the co-expression of FoxA2 and Lmx1a, the markers of midbrain FP precursors (Figure 3.15.A). Then the cells were fed with neuronal differentiated medium supplemented with a set of neurotrophic factors (BDNF, GDNF), growth factor (TGF-β3), and small molecules (Ascorbic acid, cAMP, and DAPT) for preventing cell death and promoting maturation of midbrain DA neurons. After 30 days of differentiation, the expressions of Tuj1 and TH were observed in a large proportion of cells

(Figure 3.15.B). More importantly, the specific markers of midbrain DA neurons, Lmx1a and engrailed 1 (EN1), were present in TH positive cell as well (Figure 3.15.C & D).

3.4.2 Electrophysiological Analysis of FP-based Control/PD-hiPSC Derived mDA Neurons

Neurons are cells specialized to processes and transmit information through electrical and chemical events (neurotransmitters). It is believed that neurons communicate with each other as well as with other terminal tissues through electrical activity. Therefore, the electrophysiological analysis of neurons is capable of showing hugh discernment into the function of neuronal elements.

hiPSC derived mDA neurons were used for the technique of whole cell patch clamp after 40 days of differentiation. From the result, it appeared that the differentiated cells (Figure 3.16.A) exhibited characteristics of neurons: Action potentials were triggered by injection of current (Figure 3.16.B); both inward Na+ and outward K+ currents were observed in these cells by voltage clamp (Figure 3.16.C & D); the spontaneous excitatory postsynaptic current (ESPC) was observed (Figure 3.16.E). The results from the electrophysiological recordings demonstrated that the hiPSC derived mDA neurons presented neuronal functional properties, and were capable of synaptic transmission.

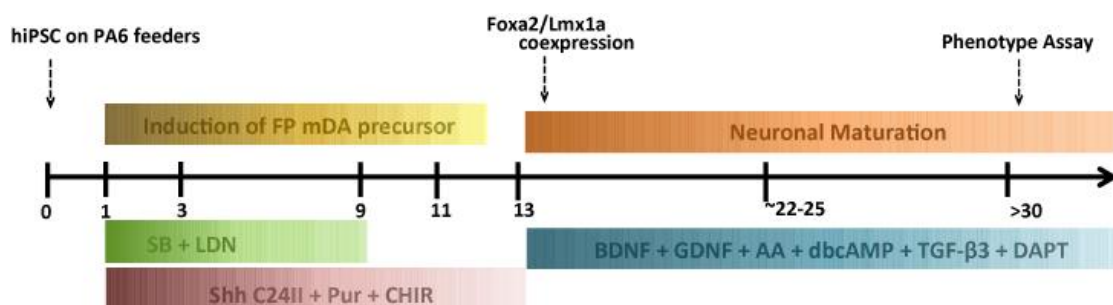**Figure 3.15: Flow Chart of FP-based Differentiation of Midbrain Dopaminergic Neurons.**
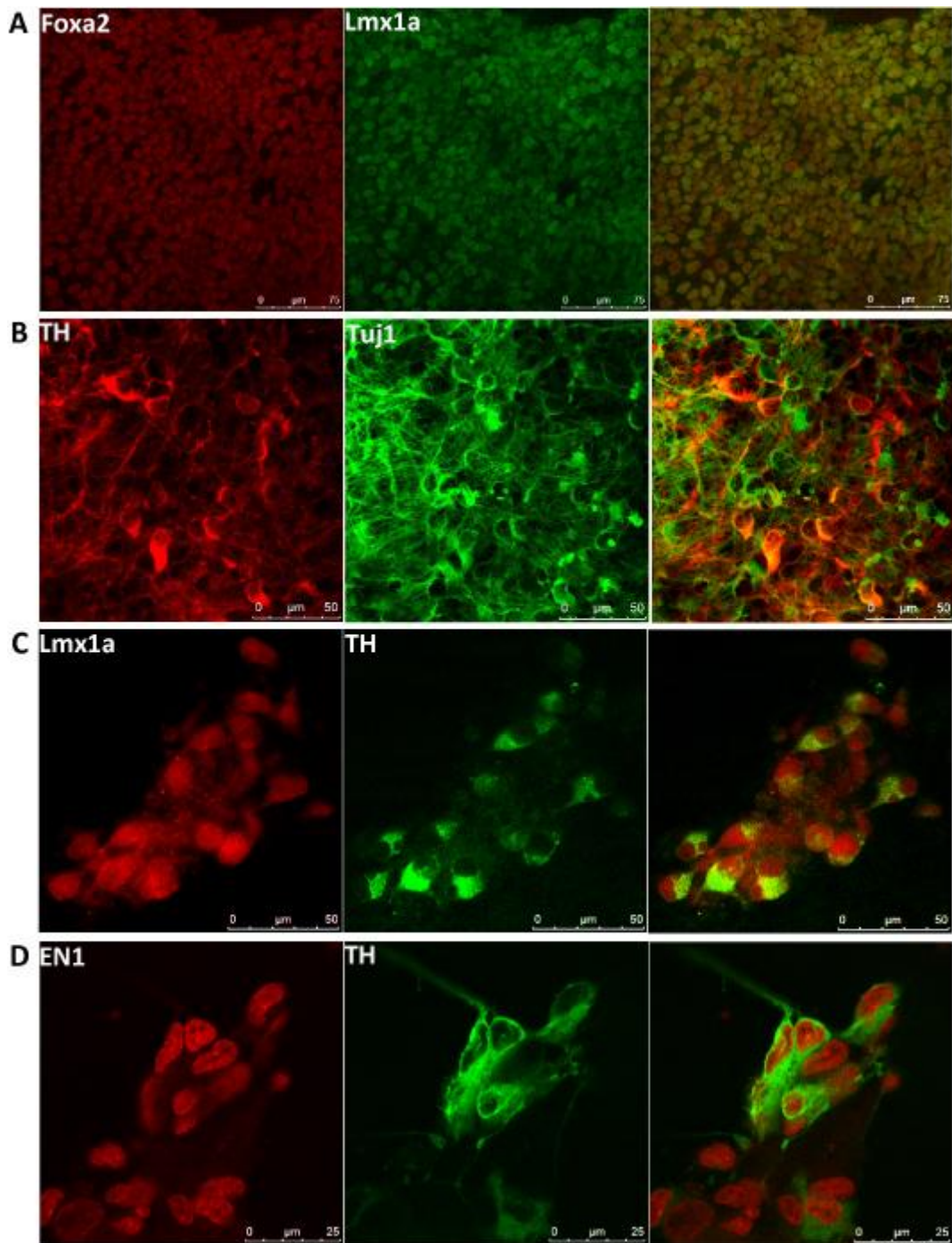
Figure 3.16: Induction and Maturation of hiPSC derived mDA neurons.

(A) Immunostaining showed colocalization of Foxa2 and Lmx1a in induced hiPSC at day13. (B) After one month of differentiation, Tuj1$^+$/TH$^+$ cell populations were observed. (C) Lmx1a and (D) EN1, mDA neuron specific markers, were coexpressed in TH positive cells.
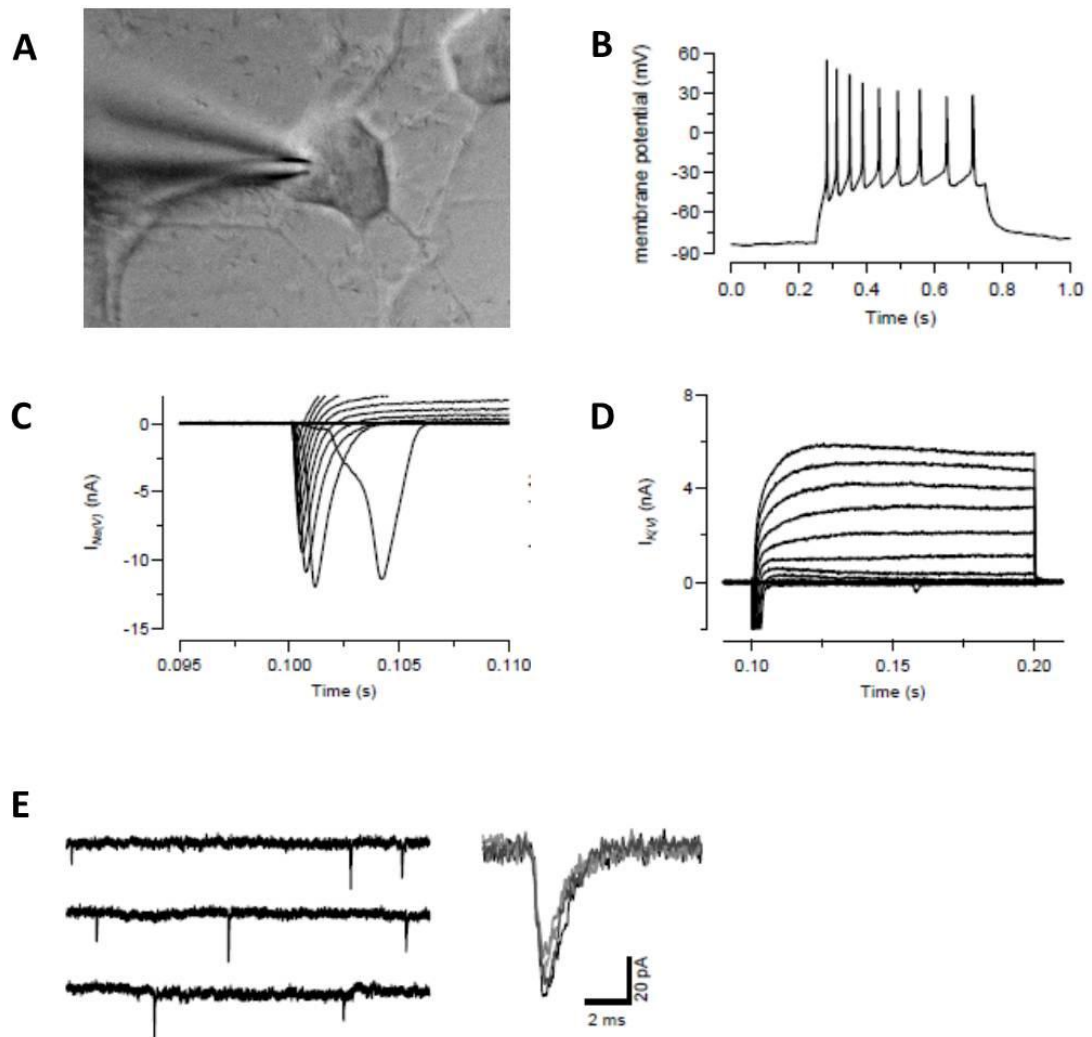
Figure 3.17: Electrophysiological Analyses of hiPSC Derived mDA Neurons.

(A) Phase contrast image of the patched cell with typical neuronal morphology was taken under the 60x water-immersion objective. (B) Action Potential (AP) elicited by a sustained (500 ms, 75 pA) current injection recorded in the current-clamp mode. (C) $I_{Na(V)}$ and (D) $I_{Ka(V)}$ were evoked by voltage step pulses (50 ms and 100 ms) from a holding potential of −70 mV, starting at −70 mV with 10 mV increments up to +60 mV. *Left* is the representative traces and *right* is its I-V curve. (E) Baseline recording shows individual miniature EPSCs (mEPSCs) from hiPSC-derived cells. These spontaneously occurring events have amplitudes of ~60 pA.

3.4.3 PD-hiPSC Derived mDA Neurons were Sensitive to CCCP-induced Mitochondrial Damage

Parkinson's disease (PD) has long been proposed to be probably induced by the interaction of genetic predisposition and environmental factors. Some genetic defects (e.g. PINK1, Parkin & LRRK2) associated with familial PD have linked to mitochondrial deficits (J. Y. Lee, Nagano, Taylor, Lim, & Yao, 2010) (Matsuda, et al., 2010) (Nguyen et al., 2011). In particular, mitochondrial dysfunction and oxidative damage have been implicated in PD pathogenesis. Therefore, it is critical to examine the effects of mitochondrial dysfunction in PD-hiPSC derived DA neurons.

To evaluate the impact of mitochondrial malfunction in mDA neurons derived from hiPSCs, exogenous stress (e.g. mitochondrial toxin) was applied for phenotypic assay. After 30 days of FP-based dopamine neuron differentiation, the control/PD-hiPSC derived mDA neurons were treated with a high concentration of carbonyl cyanide m-chlorophenylhydrazone (CCCP) for 1 h to dissipate mitochondrial membrane potential (MMP) resulting in mitochondrial damage and cell death. It was followed by the immunohistochemical staining for TOM20, translocase of outer mitochondrial membrane, which indicated the localization of mitochondria in the TH positive DA neurons (Figure 3.17.A). Upon CCCP treatment fewer cells were alive in PD-hiPSC derived mDA neurons. Moreover, the expression of TOM20 was found to be reduced by the quantitative analysis of integrated density of TOM20 in PD-hiPSC derived mDA neurons (Kas01 19, Kas02 23) (Figure 3.4. C, D & E) indicating that the mitochondrial network was disturbed. In comparison to mDA neurons derived from healthy control, PD-hiPSC derived mDA neurons showed stronger mitochondrial damage which might be caused by an enhanced sensitivity towards CCCP.
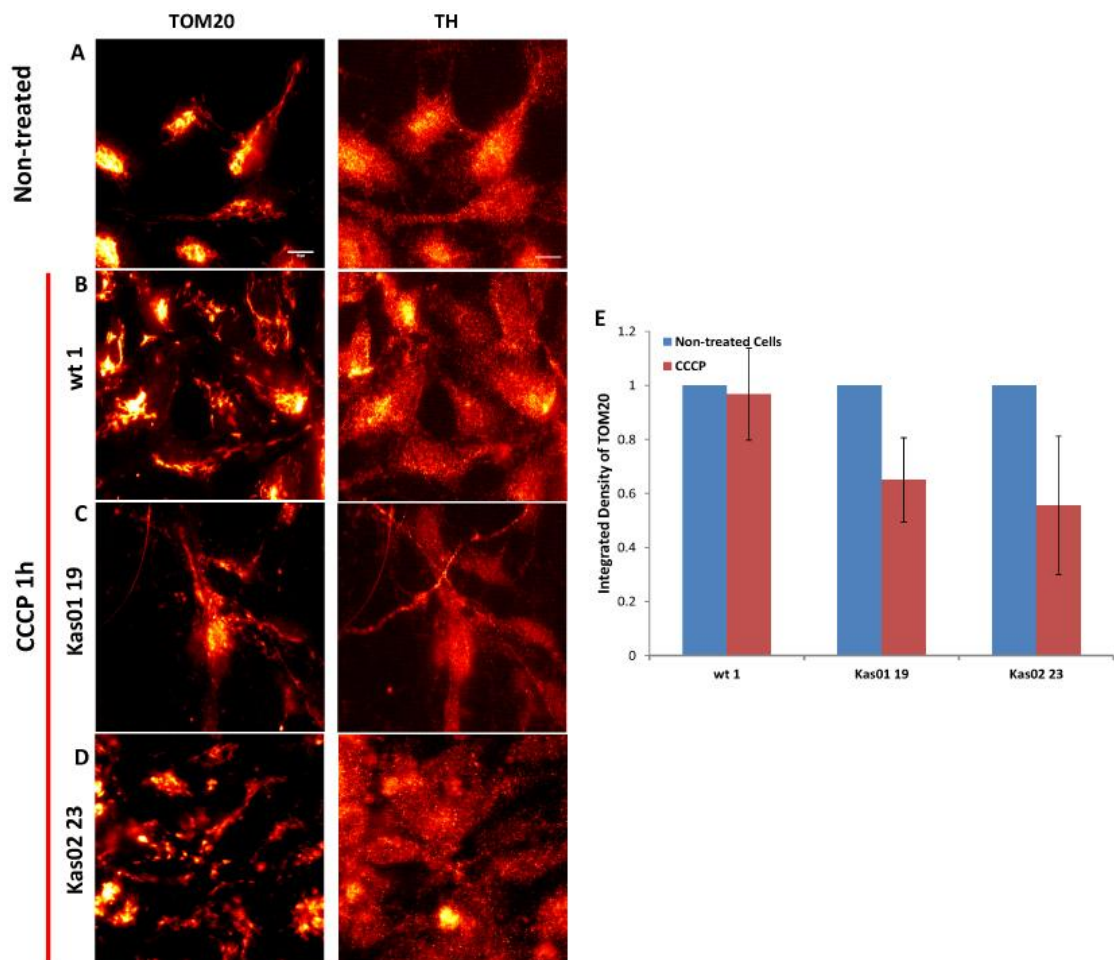
Figure 3.18: CCCP induced Mitochondrial Damage in hiPSC derived mDA Neurons.

After 30 days of FP-based mDA neuron differentiation, control/PD-hiPSC derived mDA neurons were treated with 100 μM CCCP for 1 h at 37°C. Immunostaining of TOM20 and TH were used to mark the the mitochondrial outer membrane protein and the DA neurons. (A) Non-treated Cells, (B) control (wt), and (C)~(D) PD (Kas01 & Kas02) mDA neurons, respectively. White scale bar corresponds to 10 μm. Image acquisition was performed by Dr. Susann Kummer. (E) Quantification of integrated density TOM20 in mDA neurons. 2-5 cells per image were chosen to quantify the average integrated density of TOM20. Bars indicate the mean of two independent images ± the standard error of the mean (SEM).

3.4.4 FGF20 Might Counteract the Mitochondrial Damage Induced by CCCP

From the current results of transcriptome analysis, the expression of FGF20 was significantly down-regulated in PD-hiPSC derived neural precursors (Figure 3.13). FGF20 is part of the fibroblast growth factor (FGF) family with diverse functions in development and metabolism. In the brain, FGF20 is preferentially expressed in the region of substantia Nigra pars compacta (SNpc) (Ohmachi et al., 2000), and has been suggested to boost the development of dopaminergic neurons (Shimada, Yoshimura, Tsuji, & Kunisada, 2009). Besides, FGF20 has been shown to protect mouse dopaminergic neurons against toxins in vitro and to restore some degree of motor function in a 6-OHDA-lesioned rodent PD model (Sleeman, Boshoff, & Duty, 2012). Thus, FGF20 might elicit the restorative effect to counteract neurodegeneration of PD.

In order to examine the neuroprotective effect of FGF20 on PD-hiPSC derived mDA neurons, FGF20 was added to the differentiated control/PD-hiPSC derived mDA neurons 1 day prior to CCCP treatment. Consistent with the previous results, CCCP treated PD-hiPSC derived mDA neurons showed a disruption of the mitochondrial network (Figure 3.18.E, H & K) that denoted mitochondrial damage due to uncoupling of the proton gradient and thus, loss of membrane potential resulting in the breakdown of the respiratory chain. Of note, if the cells were pretreated with FGF20 (100 ng/ml) for 24 h, mitochondrial damage was reduced, which indirectly demonstrated the neuroprotective effect of FGF20 on hiPSC derived PD mDA neurons (Figure 3.18.F, I & L).

	Non-treated Cell	CCCP 1h	FGF20 24h + CCCP 1h

wt 1
A TH / TOM20 — B TH / TOM20 — C TH / TOM20

Kas01 19
D TH / TOM20 — E TH / TOM20 — F TH / TOM20

Kas02 23
G TH / TOM20 — H TH / TOM20 — I TH / TOM20

Kas05 29
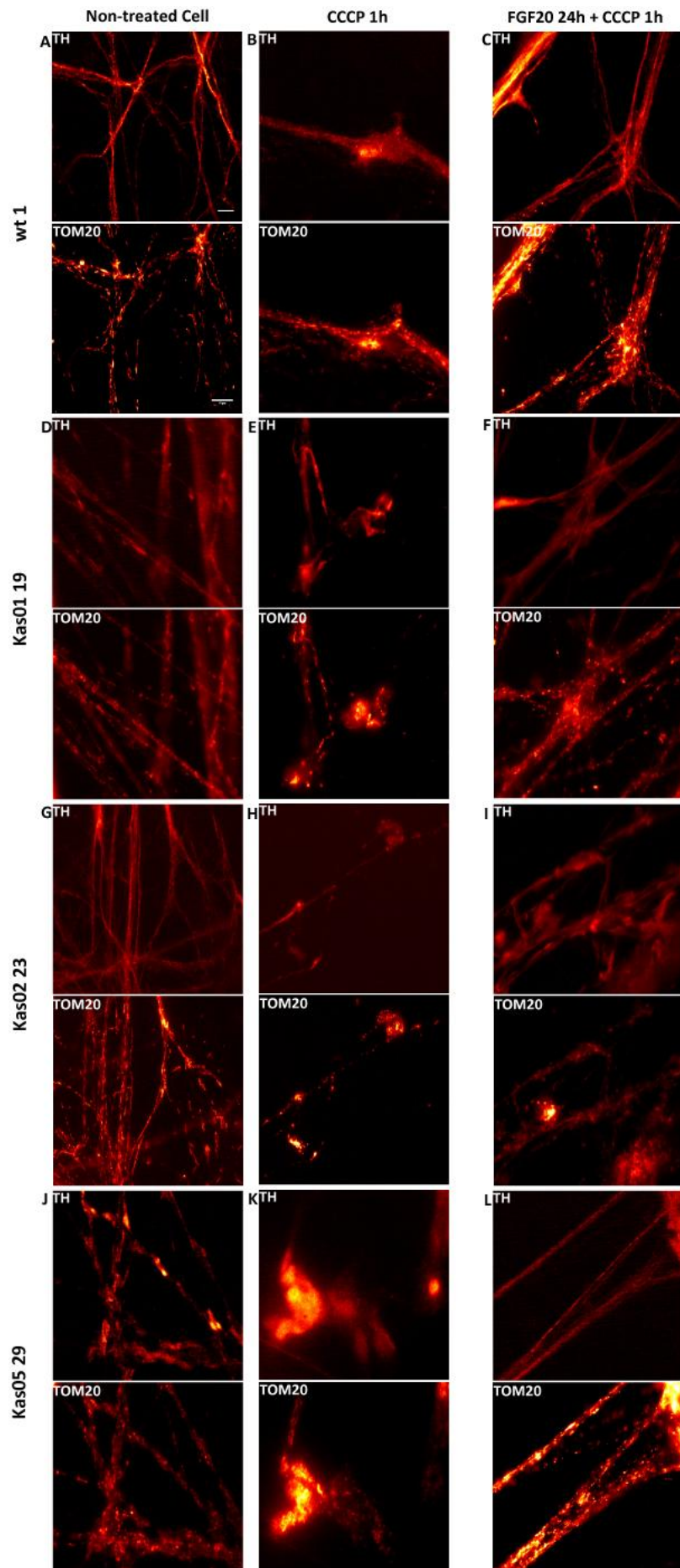J TH / TOM20 — K TH / TOM20 — L TH / TOM20

Figure 3.19: Effect of FGF20 on CCCP Triggered Mitochondrial Damage in hiPSC-derived mDA Neurons.

100 ng/ml FGF20 was added to the control/PD-hiPSC derived mDA neurons one day before 100 µM CCCP treatment. Immunostaining of TOM20 and TH marked the mitochondrial outer membrane protein and the DA neurons, respectively. (A), (D), (G), (J) non-treated cells, (B), (E), (H), (K) CCCP treated cells, (C), (F), (I), (L) cells pretreated with FGF20 followed by CCCP treatment. (A)~(C), (D)~(F), and (G)~(I) presented control (wt) and PD (Kas01, Kas02 & Kas05) hiPSC derived mDA neurons, respectively. Image acquisition was performed by Dr. Susann Kummer.

3.4.5 FGF20 Might Reduce the Excess Intracellular Reactive Oxygen Species (ROS)

To examine the neuroprotective effect of FGF20 on oxidative damage in PD patient hiPSC derived mDA neurons, H_2O_2-mediated oxidative stress was employed. FGF20 was added to the differentiated control/PD-hiPSC derived mDA neurons 1 day before the cells were exposed to a high concentration of H_2O_2. Afterwards, the H_2O_2 remaining in the medium was removed and the cells were incubated with the cell-permeable 2', 7'-dichlorodihydrofluorescein diacetate (H2-DCFDA), a general oxidative stress indicator for detection of intracellular ROS. Upon the cleavage by the intracellular oxidation, the non-fluorescent H2-DCFDA is converted to fluorescent DCF. Using flow cytometer, the fluorescence of living cells was monitored to correspond to the amount of intracellular ROS (Figure 3.19.A). High concentration of H_2O_2 induced an acute increase in ROS within the control/PD-hiPSC derived mDA neurons. It was noted that pretreatments of FGF20 could reduce some degree of excess intracellular ROS. Although the results were not significant, the tendency of decrease of ROS level upon FGF20 pretreatments could be observed (Figure 3.19.B). Similar to the effect seen in CCCP treatments, it suggested that FGF20 indirectly counteracted the dysfunction of mDA neurons caused by either mitochondrial damage or oxidative stress.

A.
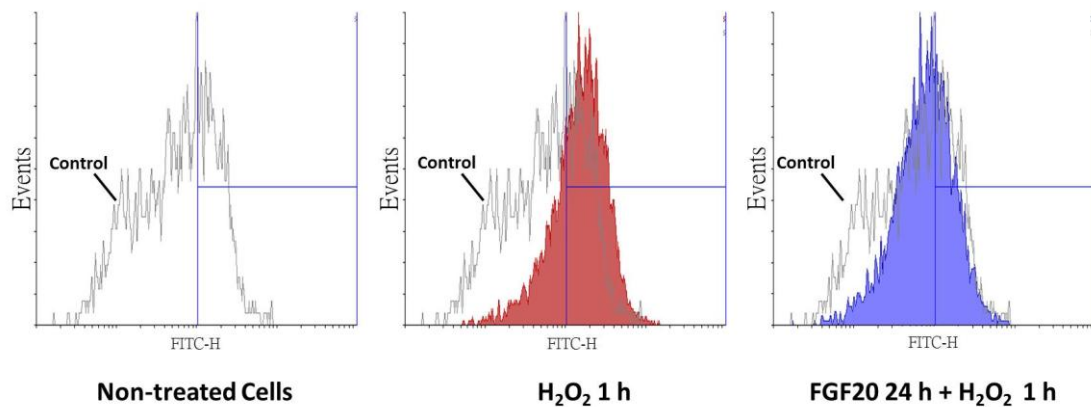
B.
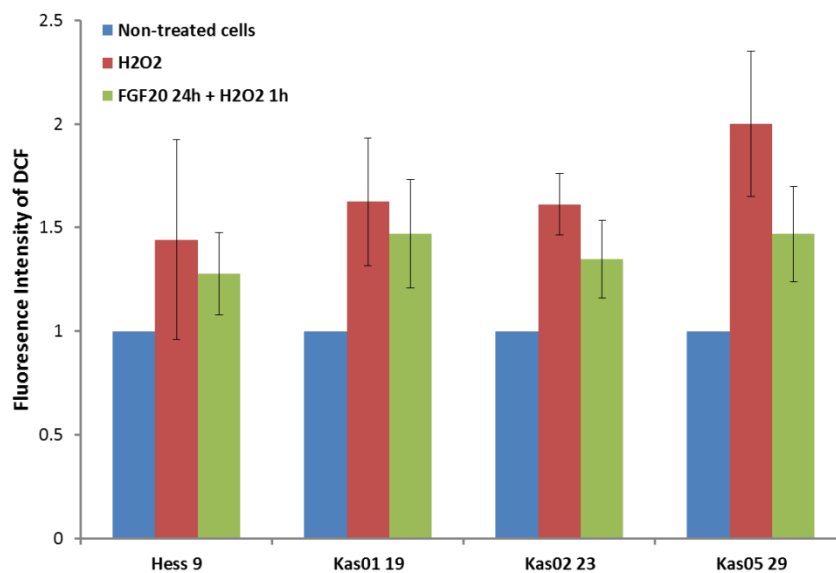
Figure 3.20: Effects of FGF20 on H$_2$O$_2$-induced Generation of Reactive Oxygen Species (ROS) in hiPSC-derived mDA Neurons.

The cells were preteated with FGF20 100 ng/ml for 24 h followed by treatment with 100 µM H$_2$O$_2$. The ROS production was measured by the fluorescence of DCF using flow cytometry as described in Methods. (A) The representative plots of the analyses (B) Quantitative analysis of ROS production. Bars indicate the mean of three independent experiments ± the standard error of the mean (SEM).

4 Discussion

In this study, 3 individual PD patients' dermal fibroblasts, together with 2 healthy persons, were converted to induced pluripotent stem cells (hiPSC) using a lentiviral polycistronic vector (hSTEMCCA). After conducting a series of tests to confirm the pluripotency, control/PD-hiPSCs were used to derive neural precursors and midbrain dopaminergic neurons with the purpose of investigation of PD pathogenesis. In an attempt to molecularly characterize iPSC that were generated from PD patients, we examined iPSC derived neural precursors using transcriptome analysis. From the result of transcriptome analysis of control/PD-hiPSC derived neural precursors, it is suggested that axon guidance pathway might be implicated in PD etiology and/or progression. Besides, the expression of FGF20, the gene associated with the risk of PD, was significantly reduced in PD-hiPSC derived neural precursors. Based on the phenotypic assay of control/PD-hiPSC derived mDA neurons, PD-hiPSC derived mDA neurons were more prone to the CCCP-induced mitochondrial damage. When the cells were exposed to FGF20 prior to external stress (e.g. CCCP or H2O2) treatments, the cellular damage was attenuated, suggesting that FGF20 elicit the neuroprotective effects on PD-hiPSC derived mDA neurons.

4.1 Generation of Transgene free PD patient specific hiPSCs

Over decades' studies of PD, the second prevalent neurodegenerative disorder, were primarily relied on the analysis of post mortem of PD brains and mouse models due to the inaccessibility to the live PD patient's brain tissues. To date, it is possible to generate and study the PD relevant cell types in culture by virtue of advanced development of iPSC technology. In the last few years, various monogenic PD hiPS cell lines have been generated (Table 1.2), and provided insights into mechanisms contributing to PD progression, like mitochondrial dysfunction and oxidative stress. However, all of these PD-hiPS cell lines were established using retroviral delivery of reprogramming transgenes. There are several drawbacks for the use of integrating retroviral vectors to generate hiPSCs: multiple random insertions of transgenes into the host genomes would disturb the genomic integrity; exogenous reprogramming genes might not be completely silenced and interfere with the further use during differentiation or therapeutic purpose (Hartfield, Fernandes, Vowles, Cowley, & Wade-Martins, 2012).

In this work, a polycistronic lentiviral vector (hSTEMCCA) encoding 4 defined factors (Oct4, Sox2, Klf4, and c-Myc) and flanked one loxP site on 3'UTR (Somers, et al., 2010) was employed to convert PD patients' dermal fibroblasts to pluripotent states, and subsequently excised following reprogramming. In consequence of lentiviral based delivery, the efficiency of hiPSC generation (0.1~1.5%) is greatly higher than retroviral based methods (0.01~0.25%) (Table 1.1). Additionally, Na butyrate was applied to the cells in the first week of reprogramming. As reported (Mali, et al., 2010), Na butyrate, as a Histone deacetylase inhibitor, largely enhanced the efficiency of hiPSC generation (Figure S2). For each sample, up to 30 hiPSC clones could be picked for propagation primarily. Consistent with previous reports of generation of PD patient specific hiPSCs (Park, Zhao, et al., 2008) (Soldner, et al., 2009) (Sanchez-Danes et al., 2012), the reprogramming efficiency varied among different individuals, but not due to the context of PD or donor age (data not shown).

The advantages of the use of a polycistronic hSTEMCCA for hiPSC generation are that it would lead to one insertion site on the host genome, and transgene can be excised via Cre-loxP recombination. Thus, Cre-mediated excision of transgenes was carried out among the generated control/PD-hiPSCs. It was successful to cut off the transgenes from the host genome as confirmed by PCR and southern blotting. In this way, transgene free control/PD-hiPSCs were obtained, characterized for the pluripotency. Moreover, they were further differentiated to PD relevant cell type, midbrain dopaminergic neurons, for study of PD pathogenesis.

Although the risk of exo-transgenic insertion was minimized via Cre excision, it should be noticed that one small DNA fragment (~200 bp) of an inactive viral LTR remains in the host genome. The incomplete elimination might give rise to insertional mutagenesis. Although the possibility of single integration which induced the interruption of gene regulations is statistically minimal, the risk can be reduced by targeting the hSTEMCCA into a safe locus on the genome (Somers, et al., 2010) (Stadtfeld, Maherali, Borkent, & Hochedlinger, 2010). Furthermore, the non-integrating approach, like RNA based method (Warren et al., 2010), can be applied for reprogramming. However the low efficiency of hiPSC generation is a problem and might be might be improved by additional combinations of treatments with small molecules, like Valproic acid (Shi et al., 2008) or Na butyrate (Mali, et al., 2010).

4.2 Derivation of Control/PD-hiPSC Neural Precursors and Transcriptome Analysis

To get more insights into the putative molecular players involved in PD etiology and progression, neural precursors were derived from control/PD-hiPSCs and subjected to transcriptome analysis. Neural precursors are multipotent cells, which are able to differentiate further into astrocytes, oligodendrocytes, and neurons. Besides, neural precursors are a homogeneous cell population instead of mixed heterogeneous differentiated neuronal cells. Therefore, it is applicable to perform transcriptome analysis using control/PD-hiPSC derived neural precursors to reduce noise backgrounds, and more importantly to reveal the possible regulatory networks at the very early stage of PD progression.

Herein, derivation of control/PD-hiPSC neural precursors was set up for the combination of stromal feeder co-culture and BMP inhibitor treatment. Following one week of neural induction, it was possible to observe the neural rosette structures. Neural rosette cell is a novel neural stem cell type which holds broad potential toward CNS and PNS lineage differentiation and capability of in vivo functional engraftment in rodent models (Elkabetz, et al., 2008). Therefore, neural rosette structures were manually picked up and expanded to establish the neural precursor cell (NPC) lines. Isolated neural precursors showed the homogeneous population, the proliferative property, and expressed these neural specific markers: Sox1, Pax6, Msi1 and Nestin. Afterwards, a collection of control/PD-hiPSC derived neural precursors were used for profiling of gene expression. According to the heatmap of hierarchical correlation, the discrepancy between clones of the same sample was possible to be observed, and might be due to either clonal variations from the parental hiPSC clone or the process of derivation of neural precursors. However, a recent report has shown that there is a risk of some undifferentiated Oct4 positive cells remaining in the NPC culture (Mak et al., 2012). They suggested that use of magnetic bead sorting with a neural cell adhesion molecule antibody against polysialic acid neural cell adhesion molecule (PSA-NCAM) to enrich more specific and pure population of neural precursors (Mak, et al., 2012). In another study, neural induction of hESC/hiPSC using monolayer culture with treatments of dual SMAD inhibition was developed and showed high efficiency of neural conversion (S. M.

Chambers, et al., 2009). Both of these studies could reduce the uncertain effects from co-culture with stromal factors and enrich the population of neural precursors.

Through the profiling of gene expression for each derived neural precursor from control and PD-hiPSCs, the transcriptome analysis was set up for comparison of controls vs. PDs. Although a set of differential gene expressions was perceived, the overall gene enrichment groups were diverse (Figure 3.12.A), and differences of gene expression between controls and PDs were not significant. It is probably due to either the variable genetic backgrounds from different individuals or the number of samples (controls or PDs) that was not statistically representative for the major PD population. However, a class of genes involved in axon guidance pathway was noticed. The axon guidance pathway (Figure S1), which regulates the formation of neuronal network by driving axons towards their synaptic targets, has been implicated to predispose to the development of PD. The studies of genetic variability (Single-nucleotide polymorphisms (SNPs)) in the axon guidance pathway associated with the PD have been reported (J. M. Kim, et al., 2011) (Bossers et al., 2009) (Srinivasan et al., 2009). Relying on whole-genome association study of SNPs in PD patients and controls from unaffected siblings, one research group used a bioinformatics approach to discover joint actions of common gene variants within axon guidance pathway that were predictive of PD susceptibility (Lesnick, et al., 2007). Besides, the gene expression analysis in post-mortem brains of 23 PD patients and 23 healthy donors also showed that genes associated with axon-guidance were differentially expressed in the PD-affected brain tissues (Papapetropoulos et al., 2006), further suggesting the relevance of axon guidance pathway in PD. Therefore, as appeared in the transcriptome analysis, some differentially expressed genes (Figure 3.12.B) in the axon guidance pathway might play roles in PD progression. Of note, EPHA4 gene expression was significantly increased (3.5 fold) in affected PD population. EPHA4 has been shown to display high expression level in the degenerated motor neurons in amyotrophic lateral sclerosis (ALS). Inhibition of EPHA4 could rescue neurodegeneration in ALS (Van Hoecke et al., 2012). Thus, EPHA4, or even other candidate genes within axon guidance pathway, might be the target for further investigation of PD pathogenesis.

The here performed transcriptome analysis revealed that 3 genes which were susceptible to Parkinson disease (e.g. GAK, DGKQ, and FGF20) displayed an altered transcription in PD-hiPSC derived neural precursors. Nevertheless, only for FGF20 it is noticed that gene expression was reduced remarkably (~4 fold) in affected PD population, which was further

verified by QRT-PCR analysis. FGF20 has been suggested to promote the differentiation of dopaminergic neurons (Correia, Anisimov, Roybon, Li, & Brundin, 2007) (Shimada, et al., 2009) and prevent the cell death of dopaminergic neurons (Ohmachi, Mikami, Konishi, Miyake, & Itoh, 2003). More importantly, genetic variability (SNPs) of FGF20 is strongly correlated with the risk of PD (van der Walt, et al., 2004) (Mizuta et al., 2008) (Pan et al., 2012).

Through the transcriptome analysis of control/PD-hiPSC derived neural precursors, the correlation might be established among gene expression profiling of affected PD derived neural precursors and genomic variants studies of PD patients. The previous reports about the risks of genetic variability associated with PD might find out the supportive evidence and even the downstream regulatory networks via gene expression analysis in PD-hiPSC derived neural precursors. Thus, our analysis clearly points to the potential impact of hiPSCs in getting novel insights into the molecular pathways controlling disease mechanisms. The derivation of basically any tissue of the three germ layers from patient's hiPS cells provides useful material for molecular analysis.

4.3 Direct differentiation of midbrain Dopaminergic (mDA) Neurons from Control/PD-hiPSCs and Phenotypic Assays

It has long been thought that neurodegeneration in PD reflects the cooperation of genetic susceptibility and environmental vulnerability. In particular, mitochondrial dysfunction and oxidative stress have been implicated in the cell death of mDA neurons in PD. To evaluate the effect of mitochondrial damage and oxidative stress on PD affected neurons, control/PD-hiPSCs were committed to conversion of mDA neurons using floor plate (FP)-based dopaminergic neuron differentiation. The advantage of FP-based approach is the highly increased amount of differentiated cells displaying a midbrain dopaminergic fate and faithful representation of the PD relevant cell types.

By conducting treatment of CCCP, which interrupts mitochondrial membrane potential (MMP), the expression of mitochondrial protein (TOM20) was monitored and found reduced in PD-hiPSC derived mDA neurons, indicating that mitochondrial activity was attenuated. It showed that PD-hiPSC derived neurons were sensitive to CCCP-induced mitochondrial damage. Besides, examination of CCCP-induced loss of MMP resulting in the mitochondrial

dysfunction, in the future, it would be necessary to develop more extensive assessments of cellular stress on PD-hiPSC derived mDA neurons, like the various external stimulations described in (Cooper et al., 2012) (Figure 4.1). Thus, it could specify the exact mechanism leading to PD and provide a platform for screening the potential therapeutic targets for PD.
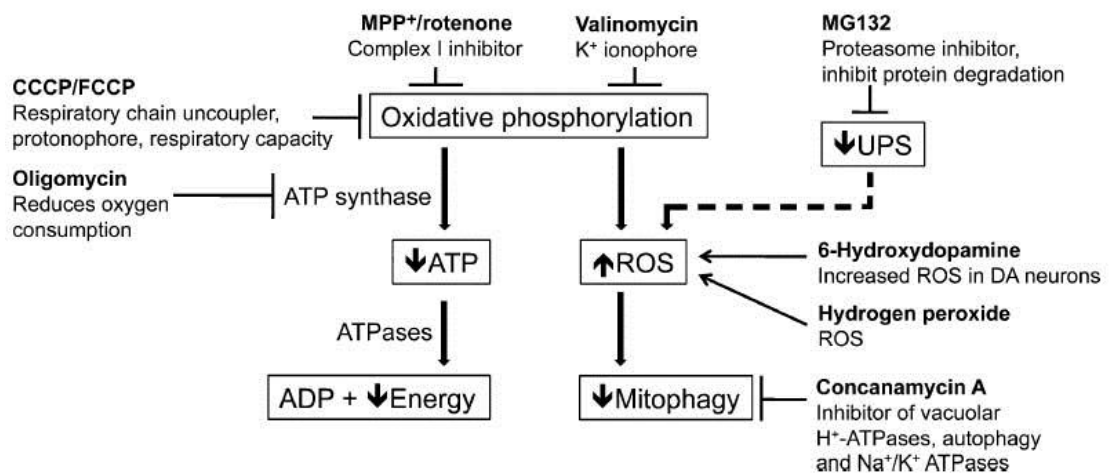

Figure 4.1: Various Cellular Stress Treatments on PD-hiPSC derived neural cells.

Oliver Cooper's group applied different toxins to measure mitochondrial responses, including ROS production, loss of MPP, and depletion of ATP (energy), on PD-hiPSC derived neural cells and their parental fibroblasts. They showed that neural cells were more vulnerable for cell stress as compared to fibroblasts (Cooper, et al., 2012).

4.4 The Role of FGF20 in PD

FGF20 is a paracrine growth factor, preferentially expressed in the substantia nigra pars compacta (SNpc) (Itoh & Ornitz, 2011). FGF20 signaling is mediated through phosphorylation of FGFR1c that is a receptor tyrosine kinase and activates the downstream MAPK pathway (Figure 4.2). Since both of FGF20 and FGFR1c are expressed in most mDA neurons, FGF20 might act in an autocrine/paracrine manner to regulate the differentiation and cell survival of mDA neurons (Itoh & Ohta, 2013). With neurotrophic activity, FGF20 prevents cell death and thus promotes cell survival of dopaminergic neurons in 6-OHDA injured rodent model (Sleeman, et al., 2012). From our current result of gene expression profiling, the expression of FGF20 was reduced in PD-hiPSC derived neural precursors. Therefore, it is expected that FGF20 might exert a neuroprotective effect on PD affected mDA neurons exposed to

external toxins. Indeed, pretreatment of PD-hiPSC derived mDA neurons with FGF20 counteracted the cellular stress following either CCCP induced mitochondrial damage (Figure 3.18) or H_2O_2 induced excess reactive oxygen species (ROS) (Figure 3.19), which indirectly confirmed that restorative effect of FGF20 in neurodegeneration of PD. In connection with the results of reduced expression in PD-hiPSC derived neural precursors and elicited neuroprotective effect, FGF20 plays a critical role of maintaining normal function of mDA dopaminergic neurons.
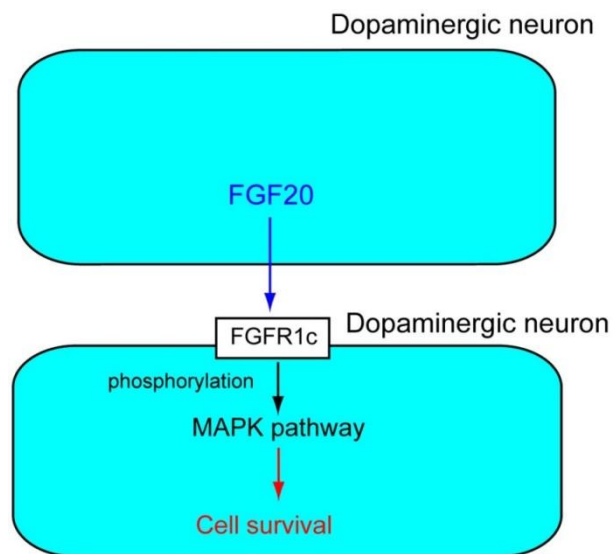

Figure 4.2: The action of FGF20 on dopaminergic neurons.

Acting in a paracrine/autocrine manner, FGF20 binds to FGFR1c and phosphorylates the cytoplasmic tyrosine residues to trigger the activation of the downstream MAPK pathway for enhancement of survival of DA neurons. The picture was taken from (Itoh & Ohta, 2013).

5 Supplementary Figures
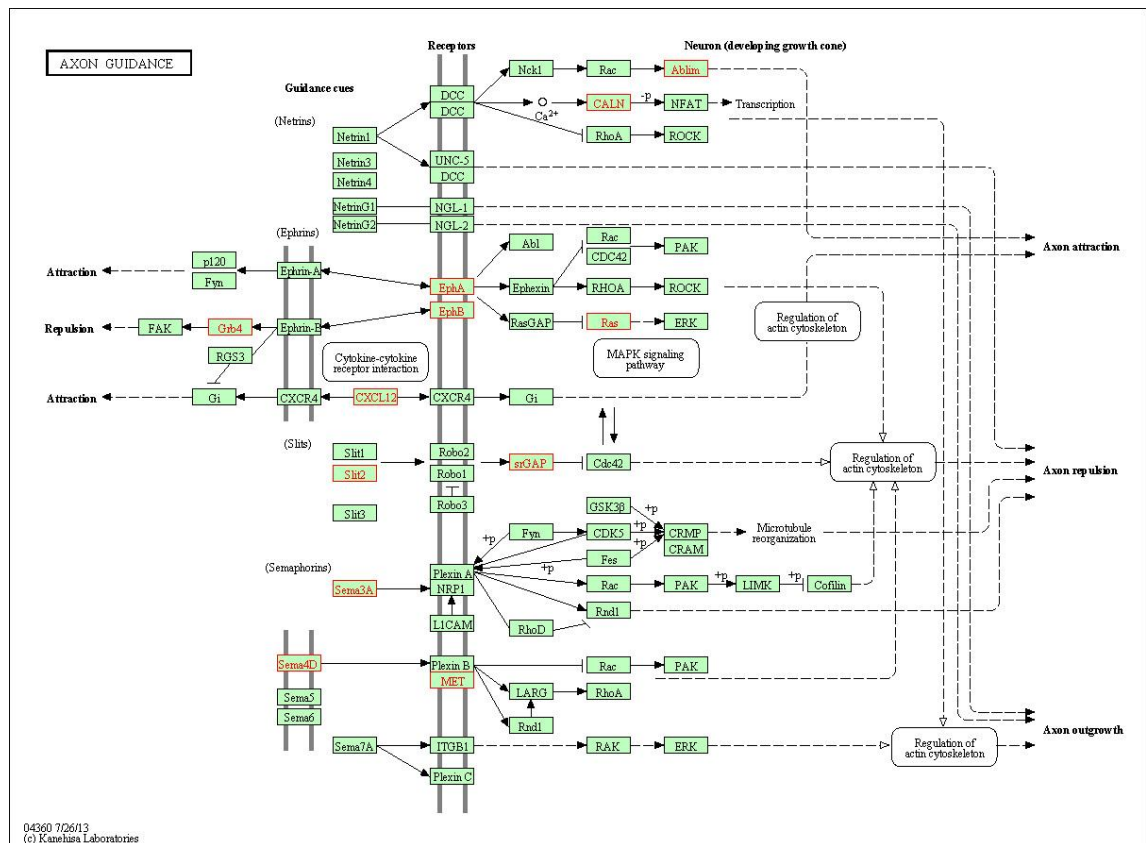
Figure S1: KEGG pathway enrichment analysis of Axon Guidance.

Axon guidance plays a critical role in the formation of neuronal network, concerning how neurons send out axons to reach the corresponding targets. There are four classical families of guidance cues: netrin, ephrin (EPH receptors), Slit, and semaphoring (neuropilins, plexins). Interactions of these signaling networks orientate the growth cone by alterations of cellular cytoskeletal organization.

The changes of gene expression level in the transcriptome analysis of control/PD-hiPSC derived neural precursors are highlighted in red. The picture is adopted from the database of KEGG: Kyoto Encyclopedia of Genes and Genomes (http://www.genome.jp/kegg/).

Figure S2: Alkaline Phosphatase (ALP) Staining of hiPSC Colonies.

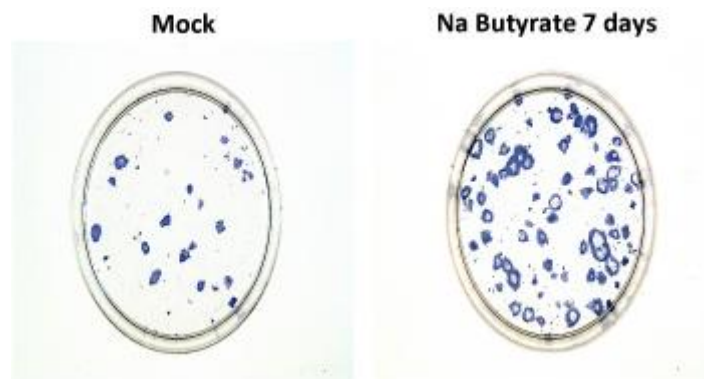Representative dishes of ALP staining of hiPSC colonies act in response to treatments of Na Butyrate during hiPSC generation.

6 References

Aasen, T., Raya, A., Barrero, M. J., Garreta, E., Consiglio, A., Gonzalez, F., et al. (2008). Efficient and rapid generation of induced pluripotent stem cells from human keratinocytes. *Nat Biotechnol, 26*(11), 1276-1284.

Andersson, E., Tryggvason, U., Deng, Q., Friling, S., Alekseenko, Z., Robert, B., et al. (2006). Identification of intrinsic determinants of midbrain dopamine neurons. *Cell, 124*(2), 393-405.

Avilion, A. A., Nicolis, S. K., Pevny, L. H., Perez, L., Vivian, N., & Lovell-Badge, R. (2003). Multipotent cell lineages in early mouse development depend on SOX2 function. *Genes Dev, 17*(1), 126-140.

Ban, H., Nishishita, N., Fusaki, N., Tabata, T., Saeki, K., Shikamura, M., et al. (2011). Efficient generation of transgene-free human induced pluripotent stem cells (iPSCs) by temperature-sensitive Sendai virus vectors. Proc Natl Acad Sci U S A, 108(34), 14234-14239.

Bekris, L. M., Mata, I. F., & Zabetian, C. P. (2010). The genetics of Parkinson disease. *J Geriatr Psychiatry Neurol, 23*(4), 228-242.

Bellin, M., Marchetto, M. C., Gage, F. H., & Mummery, C. L. (2012). Induced pluripotent stem cells: the new patient? *Nat Rev Mol Cell Biol, 13*(11), 713-726.

Bennett, M. C., Bishop, J. F., Leng, Y., Chock, P. B., Chase, T. N., & Mouradian, M. M. (1999). Degradation of alpha-synuclein by proteasome. *J Biol Chem, 274*(48), 33855-33858.

Blandini, F., & Armentero, M. T. (2012). Animal models of Parkinson's disease. *FEBS J, 279*(7), 1156-1166.

Bossers, K., Meerhoff, G., Balesar, R., van Dongen, J. W., Kruse, C. G., Swaab, D. F., et al. (2009). Analysis of gene expression in Parkinson's disease: possible involvement of neurotrophic support and axon guidance in dopaminergic cell death. *Brain Pathol, 19*(1), 91-107.

Boyer, L. A., Lee, T. I., Cole, M. F., Johnstone, S. E., Levine, S. S., Zucker, J. P., et al. (2005). Core transcriptional regulatory circuitry in human embryonic stem cells. *Cell, 122*(6), 947-956.

Braak, H., & Braak, E. (2000). Pathoanatomy of Parkinson's disease. *J Neurol, 247 Suppl 2*, II3-10.

Byers, B., Cord, B., Nguyen, H. N., Schule, B., Fenno, L., Lee, P. C., et al. (2011). SNCA triplication Parkinson's patient's iPSC-derived DA neurons accumulate alpha-synuclein and are susceptible to oxidative stress. *PLoS One, 6*(11), e26159.

Byrne, J. A., Pedersen, D. A., Clepper, L. L., Nelson, M., Sanger, W. G., Gokhale, S., et al. (2007). Producing primate embryonic stem cells by somatic cell nuclear transfer. *Nature, 450*(7169), 497-502.

Caiazzo, M., Dell'Anno, M. T., Dvoretskova, E., Lazarevic, D., Taverna, S., Leo, D., et al. (2011). Direct generation of functional dopaminergic neurons from mouse and human fibroblasts. *Nature, 476*(7359), 224-227.

Campbell, K. H., McWhir, J., Ritchie, W. A., & Wilmut, I. (1996). Sheep cloned by nuclear transfer from a cultured cell line. *Nature, 380*(6569), 64-66.

Chambers, I., Colby, D., Robertson, M., Nichols, J., Lee, S., Tweedie, S., et al. (2003). Functional expression cloning of Nanog, a pluripotency sustaining factor in embryonic stem cells. *Cell, 113*(5), 643-655.

Chambers, S. M., Fasano, C. A., Papapetrou, E. P., Tomishima, M., Sadelain, M., & Studer, L. (2009). Highly efficient neural conversion of human ES and iPS cells by dual inhibition of SMAD signaling. *Nat Biotechnol, 27*(3), 275-280.

Chen, L., & Liu, L. (2009). Current progress and prospects of induced pluripotent stem cells. *Sci China C Life Sci, 52*(7), 622-636.

Ciccone, S., Maiani, E., Bellusci, G., Diederich, M., & Gonfloni, S. (2013). Parkinson's disease: a complex interplay of mitochondrial DNA alterations and oxidative stress. *Int J Mol Sci, 14*(2), 2388-2409.

Cooper, O., Seo, H., Andrabi, S., Guardia-Laguarta, C., Graziotto, J., Sundberg, M., et al. (2012). Pharmacological rescue of mitochondrial deficits in iPSC-derived neural cells from patients with familial Parkinson's disease. *Sci Transl Med, 4*(141), 141ra190.

Correia, A. S., Anisimov, S. V., Roybon, L., Li, J. Y., & Brundin, P. (2007). Fibroblast growth factor-20 increases the yield of midbrain dopaminergic neurons derived from human embryonic stem cells. *Front Neuroanat, 1*, 4.

Corti, O., Lesage, S., & Brice, A. (2011). What genetics tells us about the causes and mechanisms of Parkinson's disease. *Physiol Rev, 91*(4), 1161-1218.

den Dunnen, W. F. (2013). Neuropathological diagnostic considerations in hyperkinetic movement disorders. *Front Neurol, 4*, 7.

Denham, M., Bye, C., Leung, J., Conley, B. J., Thompson, L. H., & Dottori, M. (2012). Glycogen synthase kinase 3beta and activin/nodal inhibition in human embryonic stem cells induces a pre-neuroepithelial state that is required for specification to a floor plate cell lineage. *Stem Cells, 30*(11), 2400-2411.

Devine, M. J., Ryten, M., Vodicka, P., Thomson, A. J., Burdon, T., Houlden, H., et al. (2011). Parkinson's disease induced pluripotent stem cells with triplication of the alpha-synuclein locus. Nat Commun, 2, 440.

Elkabetz, Y., Panagiotakos, G., Al Shamy, G., Socci, N. D., Tabar, V., & Studer, L. (2008). Human ES cell-derived neural rosettes reveal a functionally distinct early neural stem cell stage. *Genes Dev, 22*(2), 152-165.

Fasano, C. A., Chambers, S. M., Lee, G., Tomishima, M. J., & Studer, L. (2010). Efficient derivation of functional floor plate tissue from human embryonic stem cells. *Cell Stem Cell, 6*(4), 336-347.

Fearnley, J. M., & Lees, A. J. (1991). Ageing and Parkinson's disease: substantia nigra regional selectivity. *Brain, 114 (Pt 5)*, 2283-2301.

Ferrari, D., Sanchez-Pernaute, R., Lee, H., Studer, L., & Isacson, O. (2006). Transplanted dopamine neurons derived from primate ES cells preferentially innervate DARPP-32 striatal progenitors within the graft. *Eur J Neurosci, 24*(7), 1885-1896.

Freberg, C. T., Dahl, J. A., Timoskainen, S., & Collas, P. (2007). Epigenetic reprogramming of OCT4 and NANOG regulatory regions by embryonal carcinoma cell extract. *Mol Biol Cell, 18*(5), 1543-1553.

Freire, C., & Koifman, S. (2012). Pesticide exposure and Parkinson's disease: epidemiological evidence of association. *Neurotoxicology, 33*(5), 947-971.

Fukui, H., & Moraes, C. T. (2008). The mitochondrial impairment, oxidative stress and neurodegeneration connection: reality or just an attractive hypothesis? *Trends Neurosci, 31*(5), 251-256.

Gurdon, J. B. (1962). The developmental capacity of nuclei taken from intestinal epithelium cells of feeding tadpoles. *J Embryol Exp Morphol, 10*, 622-640.

Han, S. S., Williams, L. A., & Eggan, K. C. (2011). Constructing and deconstructing stem cell models of neurological disease. *Neuron, 70*(4), 626-644.

Hargus, G., Cooper, O., Deleidi, M., Levy, A., Lee, K., Marlow, E., et al. (2010). Differentiated Parkinson patient-derived induced pluripotent stem cells grow in the adult rodent brain and reduce motor asymmetry in Parkinsonian rats. *Proc Natl Acad Sci U S A, 107*(36), 15921-15926.

Hart, A. H., Hartley, L., Ibrahim, M., & Robb, L. (2004). Identification, cloning and expression analysis of the pluripotency promoting Nanog genes in mouse and human. *Dev Dyn, 230*(1), 187-198.

Hartfield, E. M., Fernandes, H. J., Vowles, J., Cowley, S. A., & Wade-Martins, R. (2012). Cellular reprogramming: a new approach to modelling Parkinson's disease. *Biochem Soc Trans, 40*(5), 1152-1157.

Hu, K., Yu, J., Suknuntha, K., Tian, S., Montgomery, K., Choi, K. D., et al. (2011). Efficient generation of transgene-free induced pluripotent stem cells from normal and neoplastic bone marrow and cord blood mononuclear cells. Blood, 117(14), e109-119.

Imaizumi, Y., Okada, Y., Akamatsu, W., Koike, M., Kuzumaki, N., Hayakawa, H., et al. (2012). Mitochondrial dysfunction associated with increased oxidative stress and alpha-synuclein accumulation in PARK2 iPSC-derived neurons and postmortem brain tissue. Mol Brain, 5, 35.

Itoh, N., & Ohta, H. (2013). Roles of FGF20 in dopaminergic neurons and Parkinson's disease. *Front Mol Neurosci, 6*, 15.

Itoh, N., & Ornitz, D. M. (2011). Fibroblast growth factors: from molecular evolution to roles in development, metabolism and disease. *J Biochem, 149*(2), 121-130.

Jackson-Lewis, V., & Przedborski, S. (2007). Protocol for the MPTP mouse model of Parkinson's disease. *Nat Protoc, 2*(1), 141-151.

Jankovic, J. (2008). Parkinson's disease: clinical features and diagnosis. *J Neurol Neurosurg Psychiatry, 79*(4), 368-376.

Jenner, P. (2003). Oxidative stress in Parkinson's disease. *Ann Neurol, 53 Suppl 3*, S26-36; discussion S36-28.

Jenner, P. (2007). Oxidative stress and Parkinson's disease. *Handb Clin Neurol, 83*, 507-520.

Jiang, H., Ren, Y., Yuen, E. Y., Zhong, P., Ghaedi, M., Hu, Z., et al. (2012). Parkin controls dopamine utilization in human midbrain dopaminergic neurons derived from induced pluripotent stem cells. Nat Commun, 3, 668.

Kadzik, R. S., & Morrisey, E. E. (2012). Directing lung endoderm differentiation in pluripotent stem cells. *Cell Stem Cell, 10*(4), 355-361.

Kaji, K., Norrby, K., Paca, A., Mileikovsky, M., Mohseni, P., & Woltjen, K. (2009). Virus-free induction of pluripotency and subsequent excision of reprogramming factors. Nature, 458(7239), 771-775.

Kalaitzakis, M. E., Graeber, M. B., Gentleman, S. M., & Pearce, R. K. (2008). The dorsal motor nucleus of the vagus is not an obligatory trigger site of Parkinson's disease: a critical analysis of alpha-synuclein staging. *Neuropathol Appl Neurobiol, 34*(3), 284-295.

Kawasaki, H., Mizuseki, K., Nishikawa, S., Kaneko, S., Kuwana, Y., Nakanishi, S., et al. (2000). Induction of midbrain dopaminergic neurons from ES cells by stromal cell-derived inducing activity. *Neuron, 28*(1), 31-40.

Kim, D., Kim, C. H., Moon, J. I., Chung, Y. G., Chang, M. Y., Han, B. S., et al. (2009). Generation of human induced pluripotent stem cells by direct delivery of reprogramming proteins. Cell Stem Cell, 4(6), 472-476.

Kim, H., Lee, G., Ganat, Y., Papapetrou, E. P., Lipchina, I., Socci, N. D., et al. (2011). miR-371-3 expression predicts neural differentiation propensity in human pluripotent stem cells. *Cell Stem Cell, 8*(6), 695-706.

Kim, J. H., Auerbach, J. M., Rodriguez-Gomez, J. A., Velasco, I., Gavin, D., Lumelsky, N., et al. (2002). Dopamine neurons derived from embryonic stem cells function in an animal model of Parkinson's disease. *Nature, 418*(6893), 50-56.

Kim, J. M., Park, S. K., Yang, J. J., Shin, E. S., Lee, J. Y., Yun, J. Y., et al. (2011). SNPs in axon guidance pathway genes and susceptibility for Parkinson's disease in the Korean population. *J Hum Genet, 56*(2), 125-129.

Kirkeby, A., Grealish, S., Wolf, D. A., Nelander, J., Wood, J., Lundblad, M., et al. (2012). Generation of regionally specified neural progenitors and functional neurons from human embryonic stem cells under defined conditions. *Cell Rep, 1*(6), 703-714.

Klein, C., & Schlossmacher, M. G. (2007). Parkinson disease, 10 years after its genetic revolution: multiple clues to a complex disorder. *Neurology, 69*(22), 2093-2104.

Kleiner-Fisman, G., Herzog, J., Fisman, D. N., Tamma, F., Lyons, K. E., Pahwa, R., et al. (2006). Subthalamic nucleus deep brain stimulation: summary and meta-analysis of outcomes. *Mov Disord, 21 Suppl 14*, S290-304.

Kolmakov, K., Belov, V. N., Bierwagen, J., Ringemann, C., Muller, V., Eggeling, C., et al. (2010). Red-emitting rhodamine dyes for fluorescence microscopy and nanoscopy. *Chemistry, 16*(1), 158-166.

Kriks, S., Shim, J. W., Piao, J., Ganat, Y. M., Wakeman, D. R., Xie, Z., et al. (2011). Dopamine neurons derived from human ES cells efficiently engraft in animal models of Parkinson's disease. *Nature, 480*(7378), 547-551.

Kurian, L., Sancho-Martinez, I., Nivet, E., Aguirre, A., Moon, K., Pendaries, C., et al. (2013). Conversion of human fibroblasts to angioblast-like progenitor cells. *Nat Methods, 10*(1), 77-83.

Kurosawa, H. (2007). Methods for inducing embryoid body formation: in vitro differentiation system of embryonic stem cells. *J Biosci Bioeng, 103*(5), 389-398.

Lang, A. E., & Lozano, A. M. (1998). Parkinson's disease. Second of two parts. *N Engl J Med, 339*(16), 1130-1143.

Langston, J. W., Ballard, P., Tetrud, J. W., & Irwin, I. (1983). Chronic Parkinsonism in humans due to a product of meperidine-analog synthesis. *Science, 219*(4587), 979-980.

Lee, J. Y., Nagano, Y., Taylor, J. P., Lim, K. L., & Yao, T. P. (2010). Disease-causing mutations in parkin impair mitochondrial ubiquitination, aggregation, and HDAC6-dependent mitophagy. *J Cell Biol, 189*(4), 671-679.

Lee, S. H., Lumelsky, N., Studer, L., Auerbach, J. M., & McKay, R. D. (2000). Efficient generation of midbrain and hindbrain neurons from mouse embryonic stem cells. *Nat Biotechnol, 18*(6), 675-679.

Lees, A. J. (2007). Unresolved issues relating to the shaking palsy on the celebration of James Parkinson's 250th birthday. *Mov Disord, 22 Suppl 17*, S327-334.

Lesnick, T. G., Papapetropoulos, S., Mash, D. C., Ffrench-Mullen, J., Shehadeh, L., de Andrade, M., et al. (2007). A genomic pathway approach to a complex disease: axon guidance and Parkinson disease. *PLoS Genet, 3*(6), e98.

Li, C., Zhou, J., Shi, G., Ma, Y., Yang, Y., Gu, J., et al. (2009). Pluripotency can be rapidly and efficiently induced in human amniotic fluid-derived cells. *Hum Mol Genet, 18*(22), 4340-4349.

Lill, C. M., Roehr, J. T., McQueen, M. B., Kavvoura, F. K., Bagade, S., Schjeide, B. M., et al. (2012). Comprehensive research synopsis and systematic meta-analyses in Parkinson's disease genetics: The PDGene database. *PLoS Genet, 8*(3), e1002548.

Lin, K. H., Oleskevich, S., & Taschenberger, H. (2011). Presynaptic Ca2+ influx and vesicle exocytosis at the mouse endbulb of Held: a comparison of two auditory nerve terminals. *J Physiol, 589*(Pt 17), 4301-4320.

Lindvall, O., & Bjorklund, A. (2004). Cell therapy in Parkinson's disease. *NeuroRx, 1*(4), 382-393.

Lotharius, J., & Brundin, P. (2002). Impaired dopamine storage resulting from alpha-synuclein mutations may contribute to the pathogenesis of Parkinson's disease. *Hum Mol Genet, 11*(20), 2395-2407.

Mak, S. K., Huang, Y. A., Iranmanesh, S., Vangipuram, M., Sundararajan, R., Nguyen, L., et al. (2012). Small molecules greatly improve conversion of human-induced pluripotent stem cells to the neuronal lineage. *Stem Cells Int, 2012*, 140427.

Mali, P., Chou, B. K., Yen, J., Ye, Z., Zou, J., Dowey, S., et al. (2010). Butyrate greatly enhances derivation of human induced pluripotent stem cells by promoting epigenetic remodeling and the expression of pluripotency-associated genes. *Stem Cells, 28*(4), 713-720.

Mansouri, A., Fukumitsu, H., Schindehuette, J., & Krieglstein, K. (2009). Differentiation of embryonic stem cells. *Curr Protoc Neurosci, Chapter 3*, Unit3 6.

Matsuda, N., Sato, S., Shiba, K., Okatsu, K., Saisho, K., Gautier, C. A., et al. (2010). PINK1 stabilized by mitochondrial depolarization recruits Parkin to damaged mitochondria and activates latent Parkin for mitophagy. *J Cell Biol, 189*(2), 211-221.

Mizuta, I., Tsunoda, T., Satake, W., Nakabayashi, Y., Watanabe, M., Takeda, A., et al. (2008). Calbindin 1, fibroblast growth factor 20, and alpha-synuclein in sporadic Parkinson's disease. *Hum Genet, 124*(1), 89-94.

Morizane, A., Doi, D., Kikuchi, T., Nishimura, K., & Takahashi, J. (2011). Small-molecule inhibitors of bone morphogenic protein and activin/nodal signals promote highly efficient neural induction from human pluripotent stem cells. *J Neurosci Res, 89*(2), 117-126.

Murry, C. E., & Keller, G. (2008). Differentiation of embryonic stem cells to clinically relevant populations: lessons from embryonic development. *Cell, 132*(4), 661-680.

Nakamura, K., Nemani, V. M., Azarbal, F., Skibinski, G., Levy, J. M., Egami, K., et al. (2011). Direct membrane association drives mitochondrial fission by the Parkinson disease-associated protein alpha-synuclein. *J Biol Chem, 286*(23), 20710-20726.

Narsinh, K. H., Jia, F., Robbins, R. C., Kay, M. A., Longaker, M. T., & Wu, J. C. (2011). Generation of adult human induced pluripotent stem cells using nonviral minicircle DNA vectors. Nat Protoc, 6(1), 78-88.

Nguyen, H. N., Byers, B., Cord, B., Shcheglovitov, A., Byrne, J., Gujar, P., et al. (2011). LRRK2 mutant iPSC-derived DA neurons demonstrate increased susceptibility to oxidative stress. *Cell Stem Cell, 8*(3), 267-280.

Nichols, J., Zevnik, B., Anastassiadis, K., Niwa, H., Klewe-Nebenius, D., Chambers, I., et al. (1998). Formation of pluripotent stem cells in the mammalian embryo depends on the POU transcription factor Oct4. *Cell, 95*(3), 379-391.

Obeso, J. A., Rodriguez-Oroz, M. C., Goetz, C. G., Marin, C., Kordower, J. H., Rodriguez, M., et al. (2010). Missing pieces in the Parkinson's disease puzzle. *Nat Med, 16*(6), 653-661.

Ohmachi, S., Mikami, T., Konishi, M., Miyake, A., & Itoh, N. (2003). Preferential neurotrophic activity of fibroblast growth factor-20 for dopaminergic neurons through fibroblast growth factor receptor-1c. *J Neurosci Res, 72*(4), 436-443.

Ohmachi, S., Watanabe, Y., Mikami, T., Kusu, N., Ibi, T., Akaike, A., et al. (2000). FGF-20, a novel neurotrophic factor, preferentially expressed in the substantia nigra pars compacta of rat brain. *Biochem Biophys Res Commun, 277*(2), 355-360.

Okita, K., Ichisaka, T., & Yamanaka, S. (2007). Generation of germline-competent induced pluripotent stem cells. *Nature, 448*(7151), 313-317.

Ossowska, K., Smialowska, M., Kuter, K., Wieronska, J., Zieba, B., Wardas, J., et al. (2006). Degeneration of dopaminergic mesocortical neurons and activation of compensatory processes induced by a long-term paraquat administration in rats: implications for Parkinson's disease. *Neuroscience, 141*(4), 2155-2165.

Pan, J., Li, H., Wang, Y., Ma, J. F., Zhang, J., Wang, G., et al. (2012). Fibroblast growth factor 20 (FGF20) polymorphism is a risk factor for Parkinson's disease in Chinese population. *Parkinsonism Relat Disord, 18*(5), 629-631.

Pankratz, N., Wilk, J. B., Latourelle, J. C., DeStefano, A. L., Halter, C., Pugh, E. W., et al. (2009). Genomewide association study for susceptibility genes contributing to familial Parkinson disease. *Hum Genet, 124*(6), 593-605.

Papapetropoulos, S., Ffrench-Mullen, J., McCorquodale, D., Qin, Y., Pablo, J., & Mash, D. C. (2006). Multiregional gene expression profiling identifies MRPS6 as a possible candidate gene for Parkinson's disease. *Gene Expr, 13*(3), 205-215.

Park, I. H., Arora, N., Huo, H., Maherali, N., Ahfeldt, T., Shimamura, A., et al. (2008). Disease-specific induced pluripotent stem cells. *Cell, 134*(5), 877-886.

Park, I. H., Zhao, R., West, J. A., Yabuuchi, A., Huo, H., Ince, T. A., et al. (2008). Reprogramming of human somatic cells to pluripotency with defined factors. *Nature, 451*(7175), 141-146.

Pawitan, J. A. (2011). Prospect of cell therapy for Parkinson's disease. *Anat Cell Biol, 44*(4), 256-264.

Poskanzer, D. C., & Schwab, R. S. (1963). Cohort Analysis of Parkinson's Syndrome: Evidence for a Single Etiology Related to Subclinical Infection About 1920. *J Chronic Dis, 16*, 961-973.

Pu, J., Jiang, H., Zhang, B., & Feng, J. (2012). Redefining Parkinson's disease research using induced pluripotent stem cells. *Curr Neurol Neurosci Rep, 12*(4), 392-398.

Rakovic, A., Shurkewitsch, K., Seibler, P., Grunewald, A., Zanon, A., Hagenah, J., et al. (2013). Phosphatase and tensin homolog (PTEN)-induced putative kinase 1 (PINK1)-dependent ubiquitination of endogenous Parkin attenuates mitophagy: study in human primary fibroblasts and induced pluripotent stem cell-derived neurons. J Biol Chem, 288(4), 2223-2237.

Reinhardt, P., Schmid, B., Burbulla, L. F., Schondorf, D. C., Wagner, L., Glatza, M., et al. (2013). Genetic correction of a LRRK2 mutation in human iPSCs links parkinsonian neurodegeneration to ERK-dependent changes in gene expression. *Cell Stem Cell, 12*(3), 354-367.

Samii, A., Nutt, J. G., & Ransom, B. R. (2004). Parkinson's disease. *Lancet, 363*(9423), 1783-1793.

Sanchez-Danes, A., Richaud-Patin, Y., Carballo-Carbajal, I., Jimenez-Delgado, S., Caig, C., Mora, S., et al. (2012). Disease-specific phenotypes in dopamine neurons from human iPS-based models of genetic and sporadic Parkinson's disease. *EMBO Mol Med, 4*(5), 380-395.

Schapira, A. H., & Jenner, P. (2011). Etiology and pathogenesis of Parkinson's disease. *Mov Disord, 26*(6), 1049-1055.

Seibler, P., Graziotto, J., Jeong, H., Simunovic, F., Klein, C., & Krainc, D. (2011). Mitochondrial Parkin recruitment is impaired in neurons derived from mutant PINK1 induced pluripotent stem cells. J Neurosci, 31(16), 5970-5976.

Seki, T., Yuasa, S., Oda, M., Egashira, T., Yae, K., Kusumoto, D., et al. (2010). Generation of induced pluripotent stem cells from human terminally differentiated circulating T cells. Cell Stem Cell, 7(1), 11-14.

Shi, Y., Do, J. T., Desponts, C., Hahm, H. S., Scholer, H. R., & Ding, S. (2008). A combined chemical and genetic approach for the generation of induced pluripotent stem cells. *Cell Stem Cell, 2*(6), 525-528.

Shimada, H., Yoshimura, N., Tsuji, A., & Kunisada, T. (2009). Differentiation of dopaminergic neurons from human embryonic stem cells: modulation of differentiation by FGF-20. *J Biosci Bioeng, 107*(4), 447-454.

Shimura, H., Hattori, N., Kubo, S., Mizuno, Y., Asakawa, S., Minoshima, S., et al. (2000). Familial Parkinson disease gene product, parkin, is a ubiquitin-protein ligase. *Nat Genet, 25*(3), 302-305.

Sleeman, I. J., Boshoff, E. L., & Duty, S. (2012). Fibroblast growth factor-20 protects against dopamine neuron loss in vitro and provides functional protection in the 6-hydroxydopamine-lesioned rat model of Parkinson's disease. *Neuropharmacology, 63*(7), 1268-1277.

Smith, W. C., & Harland, R. M. (1992). Expression cloning of noggin, a new dorsalizing factor localized to the Spemann organizer in Xenopus embryos. *Cell, 70*(5), 829-840.

Soldner, F., Hockemeyer, D., Beard, C., Gao, Q., Bell, G. W., Cook, E. G., et al. (2009). Parkinson's disease patient-derived induced pluripotent stem cells free of viral reprogramming factors. *Cell, 136*(5), 964-977.

Somers, A., Jean, J. C., Sommer, C. A., Omari, A., Ford, C. C., Mills, J. A., et al. (2010). Generation of transgene-free lung disease-specific human induced pluripotent stem cells using a single excisable lentiviral stem cell cassette. *Stem Cells, 28*(10), 1728-1740.

Sommer, C. A., Sommer, A. G., Longmire, T. A., Christodoulou, C., Thomas, D. D., Gostissa, M., et al. (2010). Excision of reprogramming transgenes improves the differentiation potential of iPS cells generated with a single excisable vector. *Stem Cells, 28*(1), 64-74.

Spence, J. R., Mayhew, C. N., Rankin, S. A., Kuhar, M. F., Vallance, J. E., Tolle, K., et al. (2011). Directed differentiation of human pluripotent stem cells into intestinal tissue in vitro. *Nature, 470*(7332), 105-109.

Spillantini, M. G., Schmidt, M. L., Lee, V. M., Trojanowski, J. Q., Jakes, R., & Goedert, M. (1997). Alpha-synuclein in Lewy bodies. *Nature, 388*(6645), 839-840.

Srinivasan, B. S., Doostzadeh, J., Absalan, F., Mohandessi, S., Jalili, R., Bigdeli, S., et al. (2009). Whole genome survey of coding SNPs reveals a reproducible pathway determinant of Parkinson disease. *Hum Mutat, 30*(2), 228-238.

Stadtfeld, M., Maherali, N., Borkent, M., & Hochedlinger, K. (2010). A reprogrammable mouse strain from gene-targeted embryonic stem cells. *Nat Methods, 7*(1), 53-55.

Studer, L., Psylla, M., Buhler, B., Evtouchenko, L., Vouga, C. M., Leenders, K. L., et al. (1996). Noninvasive dopamine determination by reversed phase HPLC in the medium of free-floating roller tube cultures of rat fetal ventral mesencephalon: a tool to assess dopaminergic tissue prior to grafting. *Brain Res Bull, 41*(3), 143-150.

Su, Y. C., & Qi, X. (2013). Inhibition of excessive mitochondrial fission reduced aberrant autophagy and neuronal damage caused by LRRK2 G2019S mutation. *Hum Mol Genet*.

Tachibana, M., Amato, P., Sparman, M., Gutierrez, N. M., Tippner-Hedges, R., Ma, H., et al. (2013). Human embryonic stem cells derived by somatic cell nuclear transfer. *Cell, 153*(6), 1228-1238.

Takahashi, K., Tanabe, K., Ohnuki, M., Narita, M., Ichisaka, T., Tomoda, K., et al. (2007). Induction of pluripotent stem cells from adult human fibroblasts by defined factors. *Cell, 131*(5), 861-872.

Takahashi, K., & Yamanaka, S. (2006). Induction of pluripotent stem cells from mouse embryonic and adult fibroblast cultures by defined factors. *Cell, 126*(4), 663-676.

Tamaoki, N., Takahashi, K., Tanaka, T., Ichisaka, T., Aoki, H., Takeda-Kawaguchi, T., et al. (2010). Dental pulp cells for induced pluripotent stem cell banking. *J Dent Res, 89*(8), 773-778.

Thomas, B., & Beal, M. F. (2007). Parkinson's disease. *Hum Mol Genet, 16 Spec No. 2*, R183-194.

Thomson, J. A., Itskovitz-Eldor, J., Shapiro, S. S., Waknitz, M. A., Swiergiel, J. J., Marshall, V. S., et al. (1998). Embryonic stem cell lines derived from human blastocysts. *Science, 282*(5391), 1145-1147.

Tofaris, G. K., Layfield, R., & Spillantini, M. G. (2001). alpha-synuclein metabolism and aggregation is linked to ubiquitin-independent degradation by the proteasome. *FEBS Lett, 509*(1), 22-26.

van der Walt, J. M., Noureddine, M. A., Kittappa, R., Hauser, M. A., Scott, W. K., McKay, R., et al. (2004). Fibroblast growth factor 20 polymorphisms and haplotypes strongly influence risk of Parkinson disease. *Am J Hum Genet, 74*(6), 1121-1127.

Van Hoecke, A., Schoonaert, L., Lemmens, R., Timmers, M., Staats, K. A., Laird, A. S., et al. (2012). EPHA4 is a disease modifier of amyotrophic lateral sclerosis in animal models and in humans. *Nat Med, 18*(9), 1418-1422.

Vazin, T., Chen, J., Lee, C. T., Amable, R., & Freed, W. J. (2008). Assessment of stromal-derived inducing activity in the generation of dopaminergic neurons from human embryonic stem cells. *Stem Cells, 26*(6), 1517-1525.

Warren, L., Manos, P. D., Ahfeldt, T., Loh, Y. H., Li, H., Lau, F., et al. (2010). Highly efficient reprogramming to pluripotency and directed differentiation of human cells with synthetic modified mRNA. *Cell Stem Cell, 7*(5), 618-630.

Woltjen, K., Michael, I. P., Mohseni, P., Desai, R., Mileikovsky, M., Hamalainen, R., et al. (2009). piggyBac transposition reprograms fibroblasts to induced pluripotent stem cells. Nature, 458(7239), 766-770.

Xi, J., Liu, Y., Liu, H., Chen, H., Emborg, M. E., & Zhang, S. C. (2012). Specification of midbrain dopamine neurons from primate pluripotent stem cells. *Stem Cells, 30*(8), 1655-1663.

Yu, J., Hu, K., Smuga-Otto, K., Tian, S., Stewart, R., Slukvin, II, et al. (2009). Human induced pluripotent stem cells free of vector and transgene sequences. Science, 324(5928), 797-801.

Yu, J., Vodyanik, M. A., Smuga-Otto, K., Antosiewicz-Bourget, J., Frane, J. L., Tian, S., et al. (2007). Induced pluripotent stem cell lines derived from human somatic cells. *Science, 318*(5858), 1917-1920.

Zhang, S. C., Wernig, M., Duncan, I. D., Brustle, O., & Thomson, J. A. (2001). In vitro differentiation of transplantable neural precursors from human embryonic stem cells. *Nat Biotechnol, 19*(12), 1129-1133.

Zhang, W. Y., de Almeida, P. E., & Wu, J. C. (2008). Teratoma formation: A tool for monitoring pluripotency in stem cell research *StemBook*. Cambridge (MA).

Zhou, T., Benda, C., Dunzinger, S., Huang, Y., Ho, J. C., Yang, J., et al. (2012). Generation of human induced pluripotent stem cells from urine samples. *Nat Protoc, 7*(12), 2080-2089.

Zhou, W., & Freed, C. R. (2009). Adenoviral gene delivery can reprogram human fibroblasts to induced pluripotent stem cells. Stem Cells, 27(11), 2667-2674.

Zhu, Z., & Huangfu, D. (2013). Human pluripotent stem cells: an emerging model in developmental biology. *Development, 140*(4), 705-717.